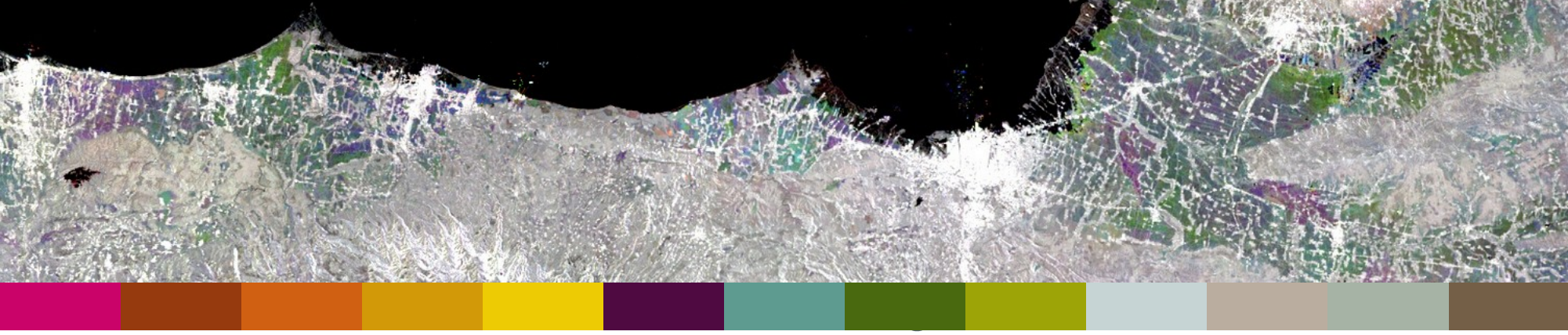

SAR and InSAR Application in Disaster Management

A Brief Introduction

Firman Hadi

Dept. of Geodesy Eng., UNDIP

firmanhadi21@lecturer.undip.ac.id

https://firmanhadi.github.io

@jalmiburung

Contents

Intro

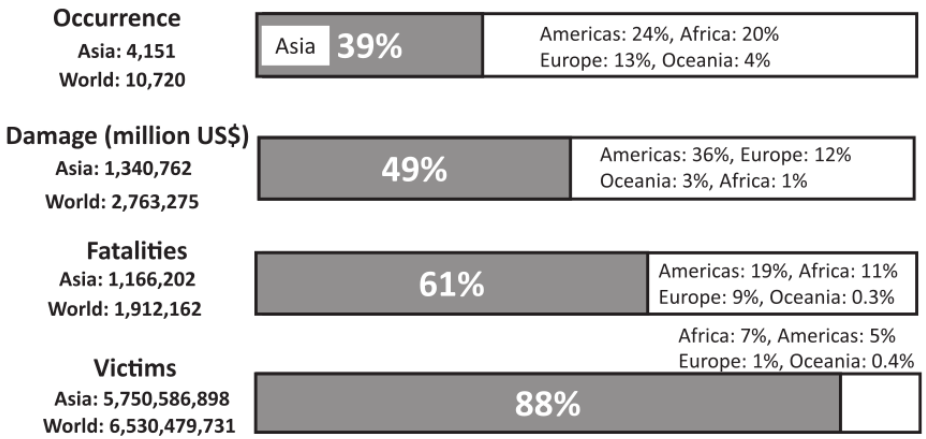

Fig. 2. Impacts of natural disasters by region, 1987–2016.
Source: ADRC-Natural Disasters Data Book 2016 [7].

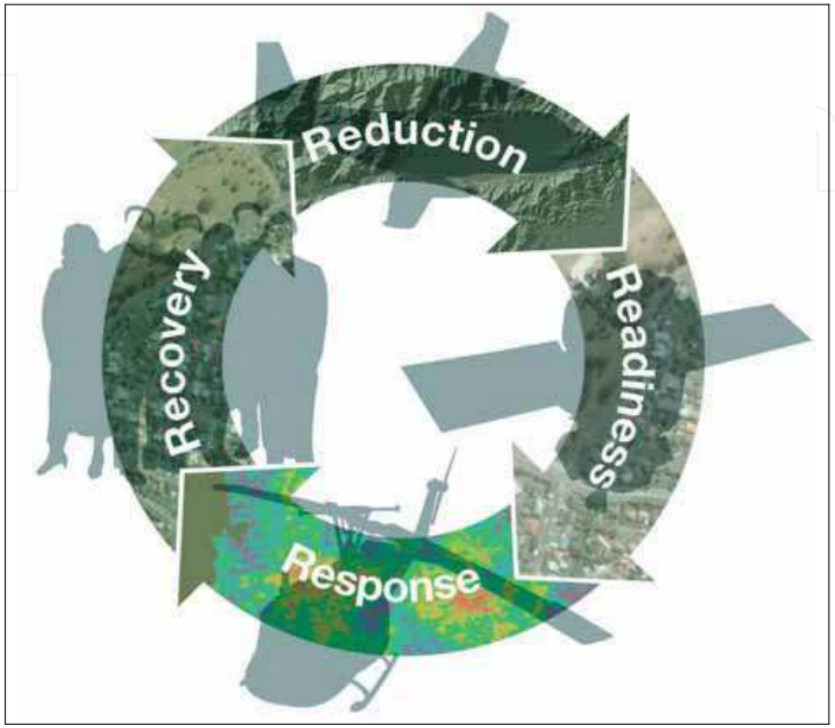

¶ ‖

¶ Kaku, 2019

‖ Joyce et al. 2009

Remote Sensing in Disaster Management

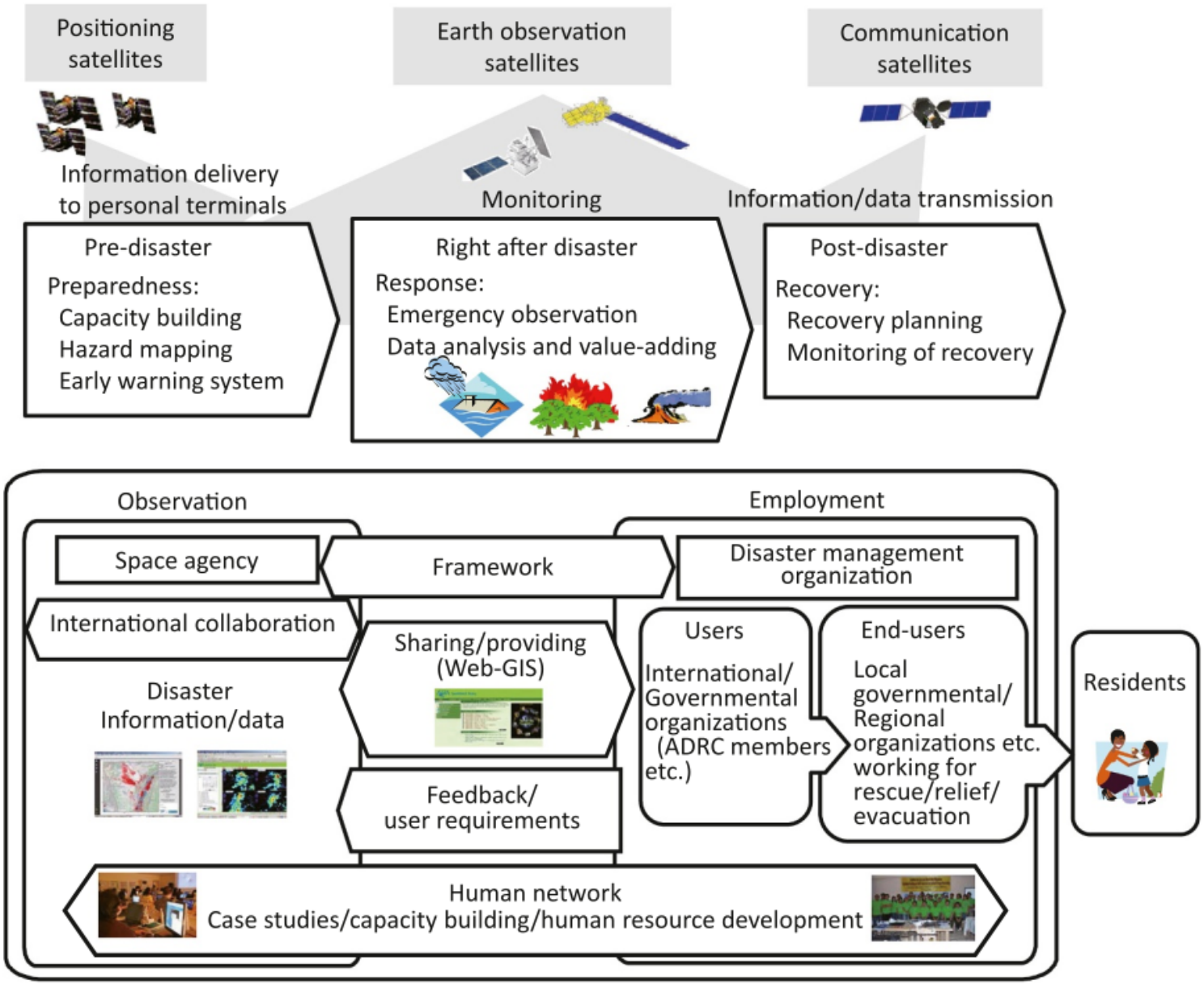

The International Charter Space and Major Disasters

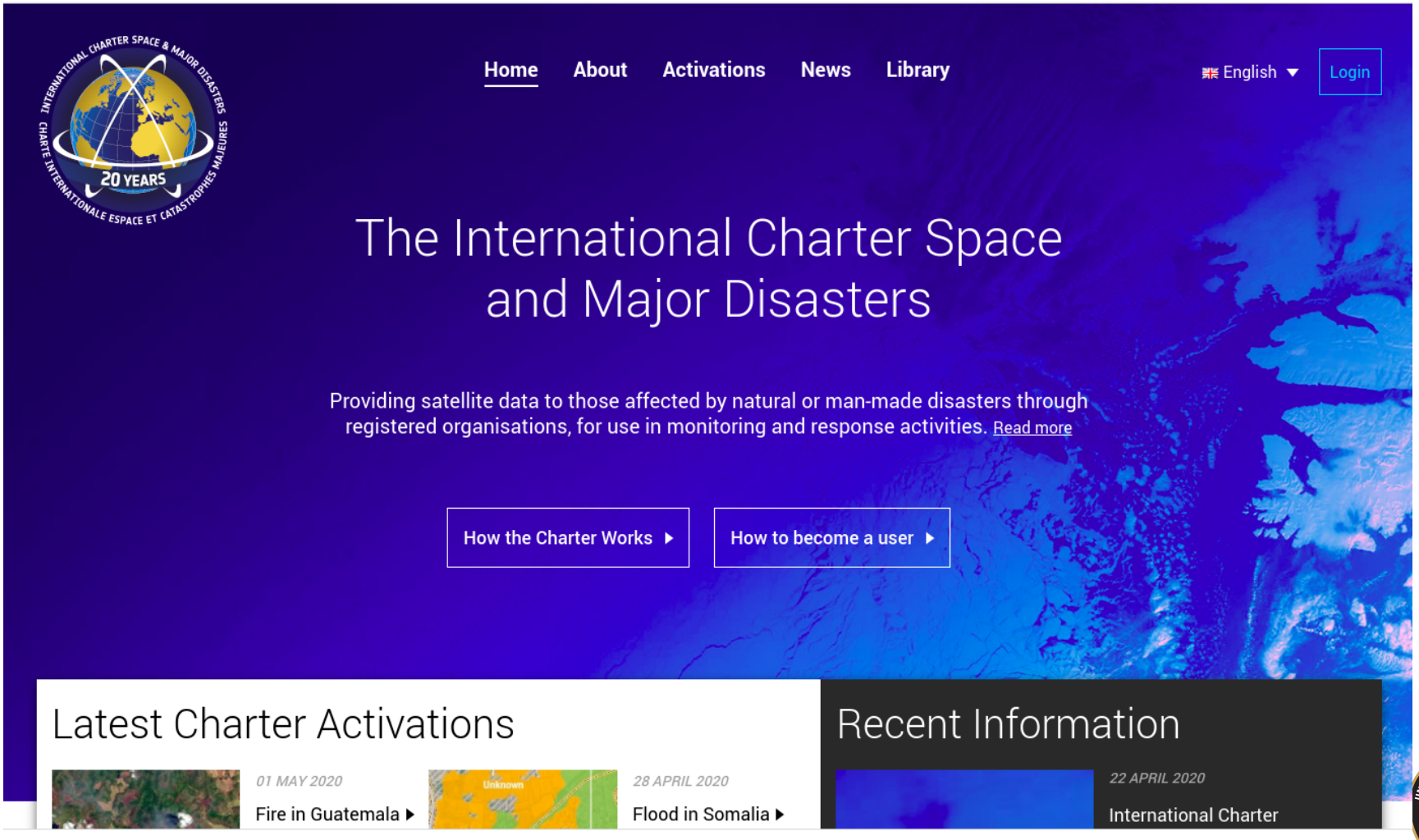

Copernicus EMS

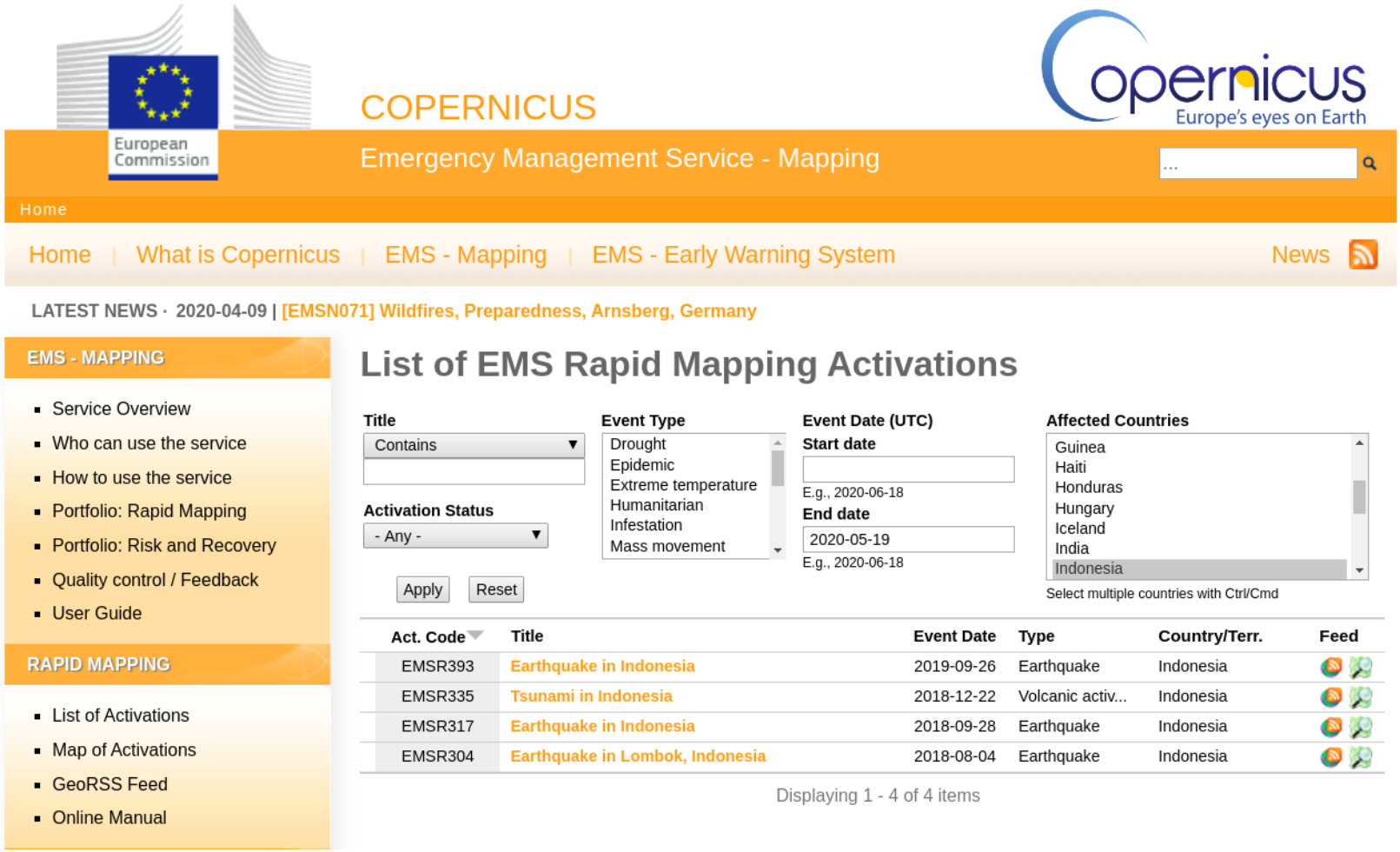

Sentinel Asia

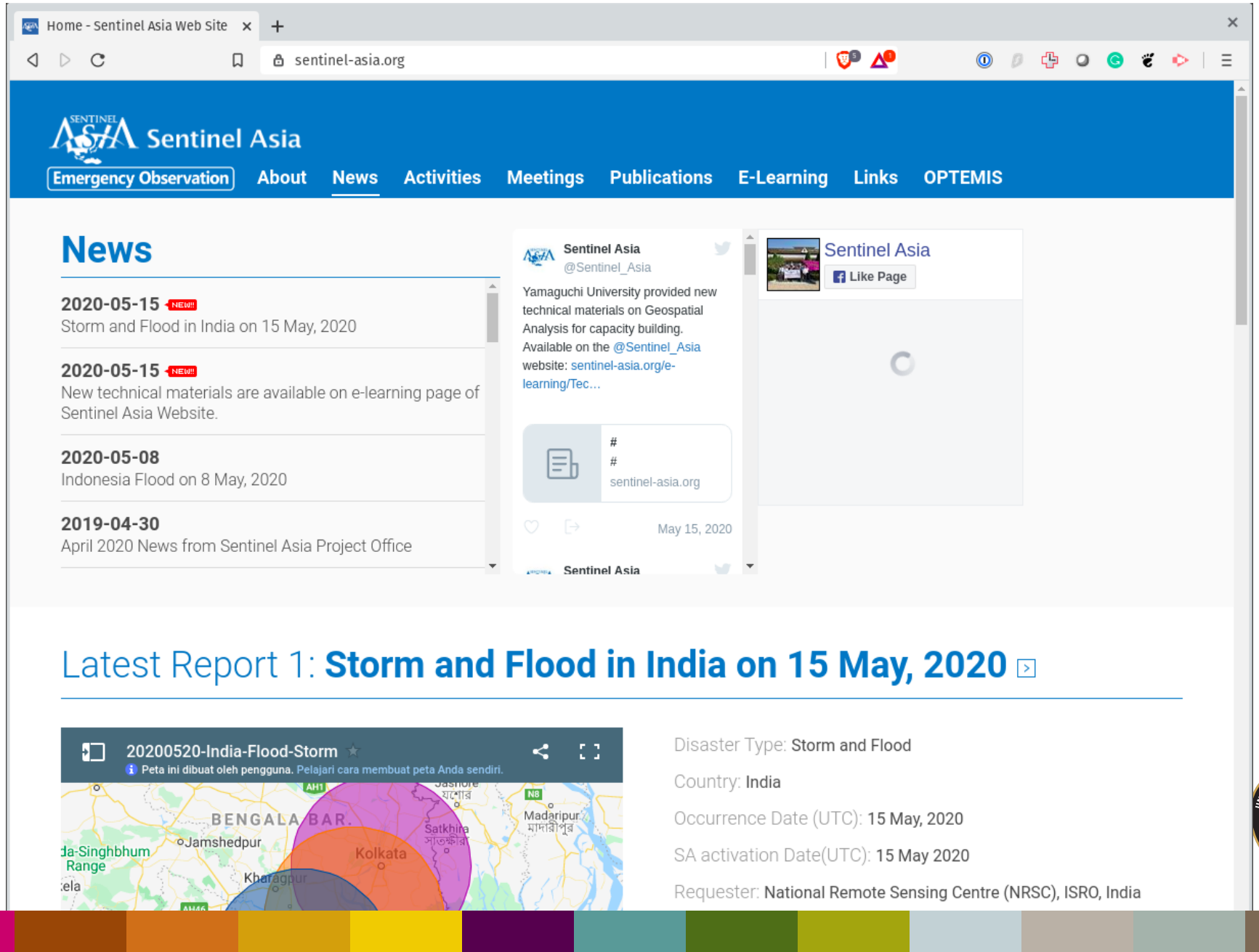

Sentinel Asia Activities in 2017

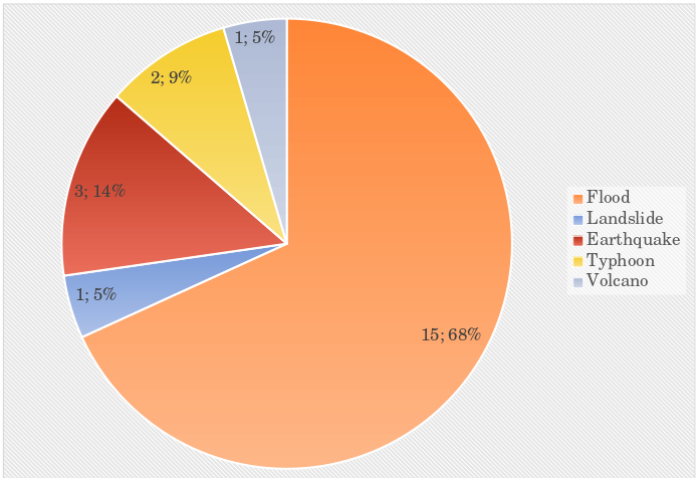

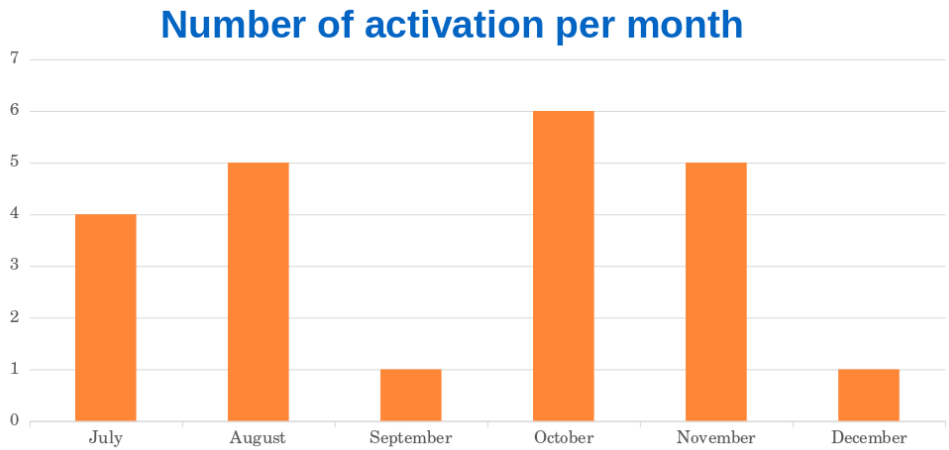

Sentinel Asia Success Story

Fire detection

Observation by satellites

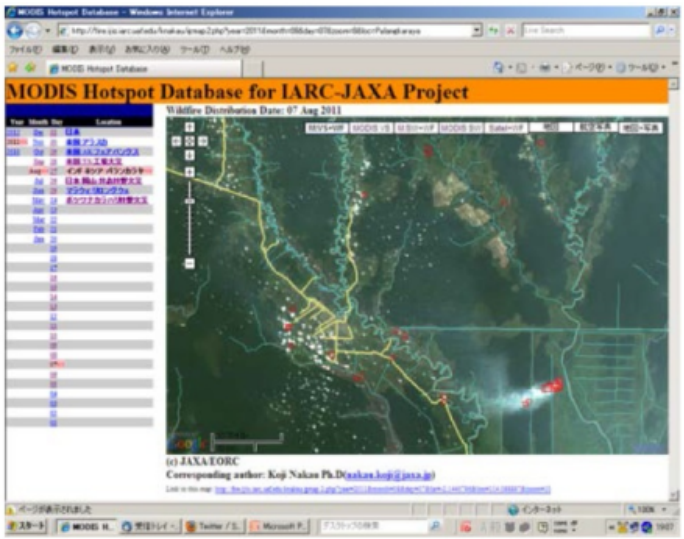

Operation at LAPAN in Jakarta

Wildfires in Palangka Raya, Kalimantan

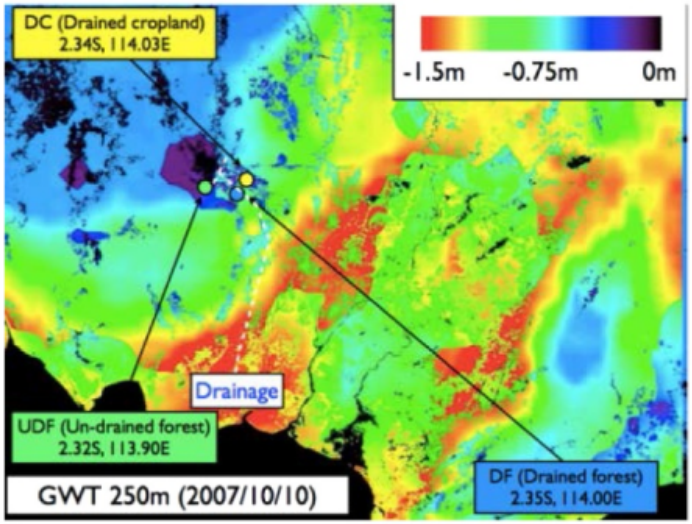

Fire information via SMS to firefighters

Firefighters

Sentinel Asia Success Story

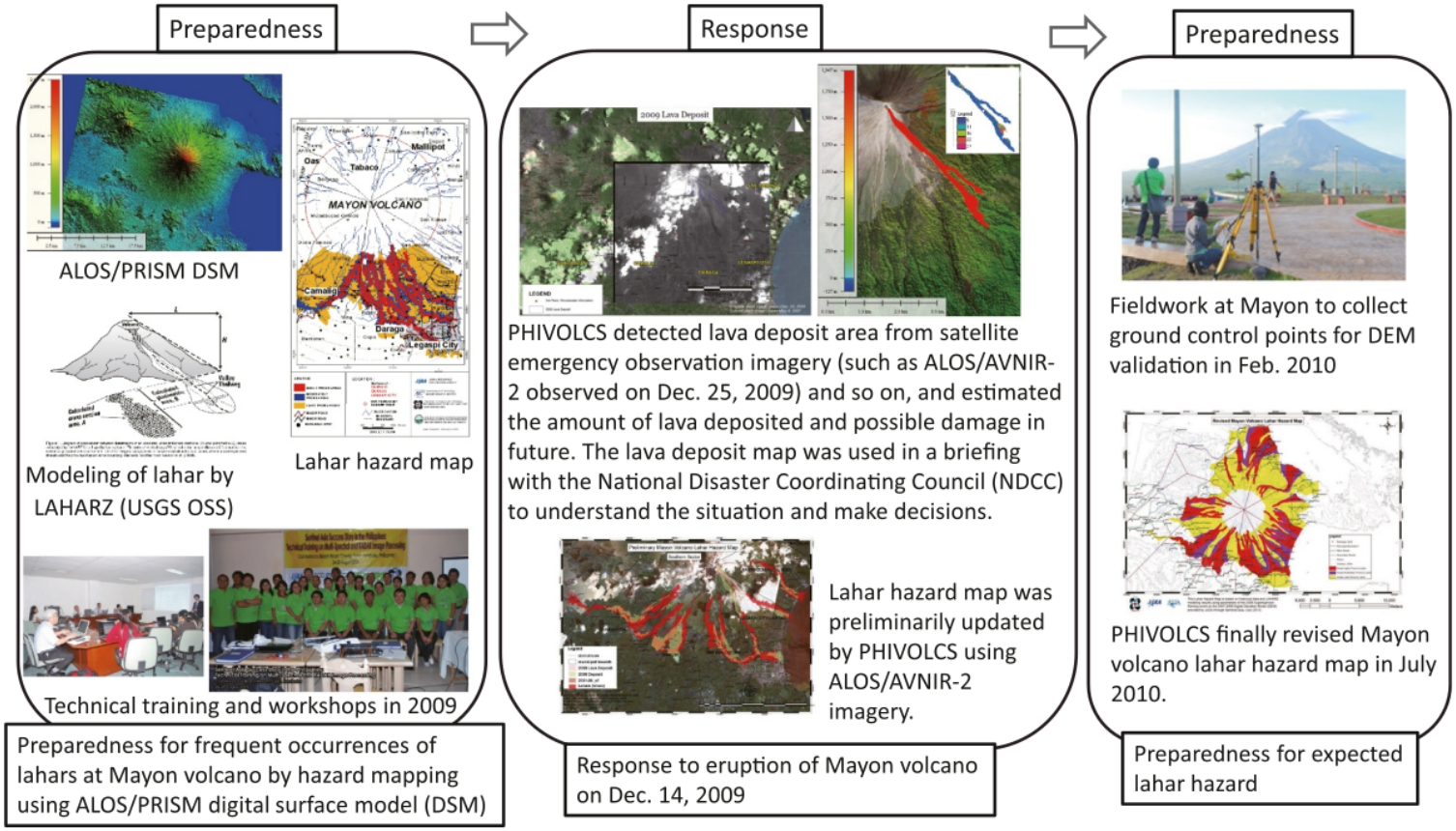

Fig. 8. Hazard mapping for lahars at Mayon volcano in the Philippines and application to response.
Source: Presentations by A. S. Daag and R. U. Solidum, Jr. of PHIVOLCS at JPT annual meetings and reply to feedback questionnaire of SA emergency observation. *

*Kaku, 2019

Sentinel Asia Success Story

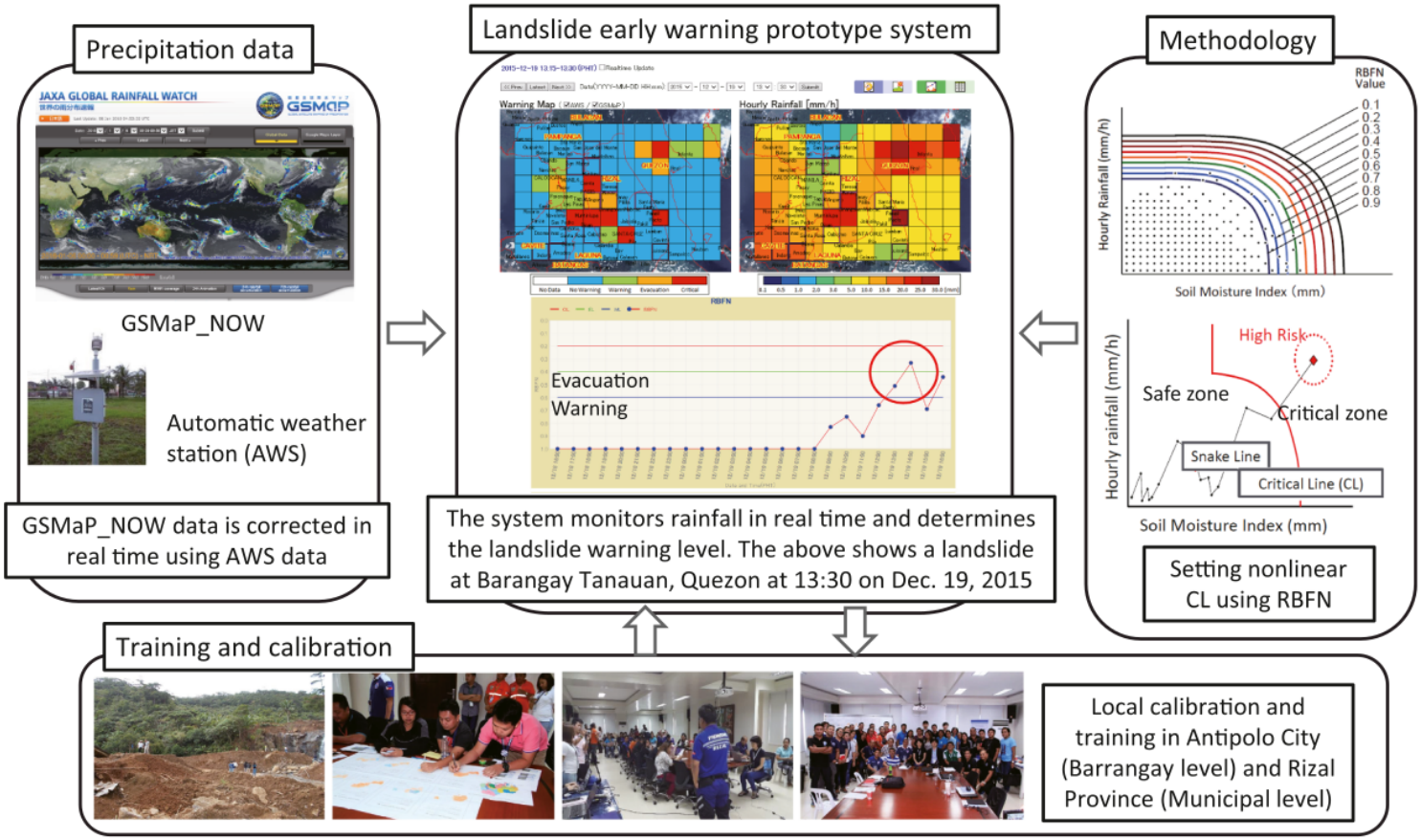

Fig. 9. Landslide early warning prototype system in the framework of the SA Success Story in the Philippines. Source: Presentation by A. S. Daag of PHIVOLCS at APRSAF-23 annual meeting.

*

*Kaku, 2019

Nepal activation 2015

Difference of coherence (Δγ) analysis

(@Kausaltar in Katmandu)

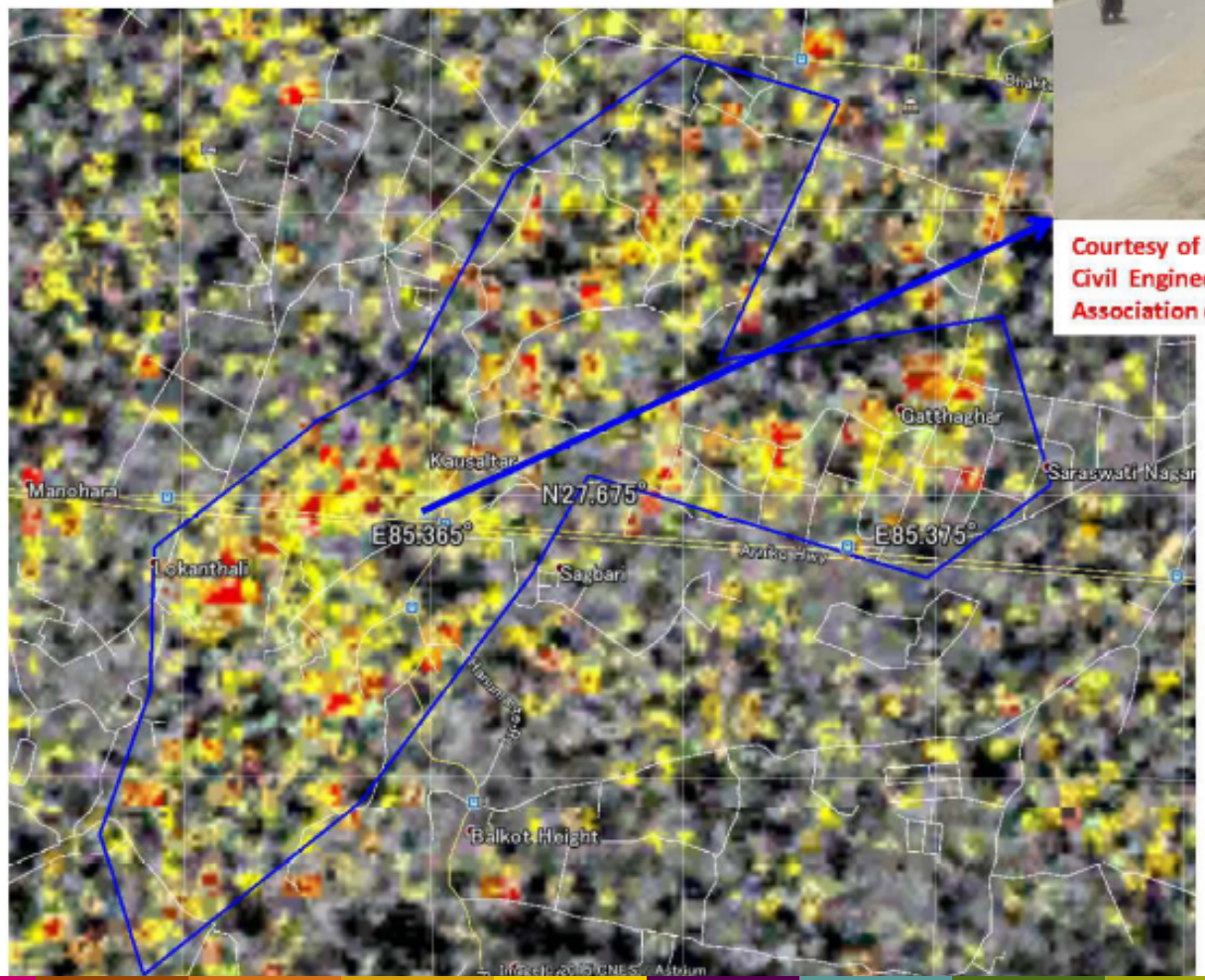

Courtesy of the Investigation team of the Japan Society of Civil Engineers, Japanese Geotechnical Society, and Japan Association of Earthquake Engineering.

Prospective damaged area

Red : $\Delta\gamma \geq 0.4$
Orange : $\Delta\gamma \geq 0.3$
Yellow : $\Delta\gamma \geq 0.2$

Sensor : PALSAR-2
Obs. date : May 2, 2015
Feb. 21, 2015
Oct. 4, 2014

Nepal activation 2015

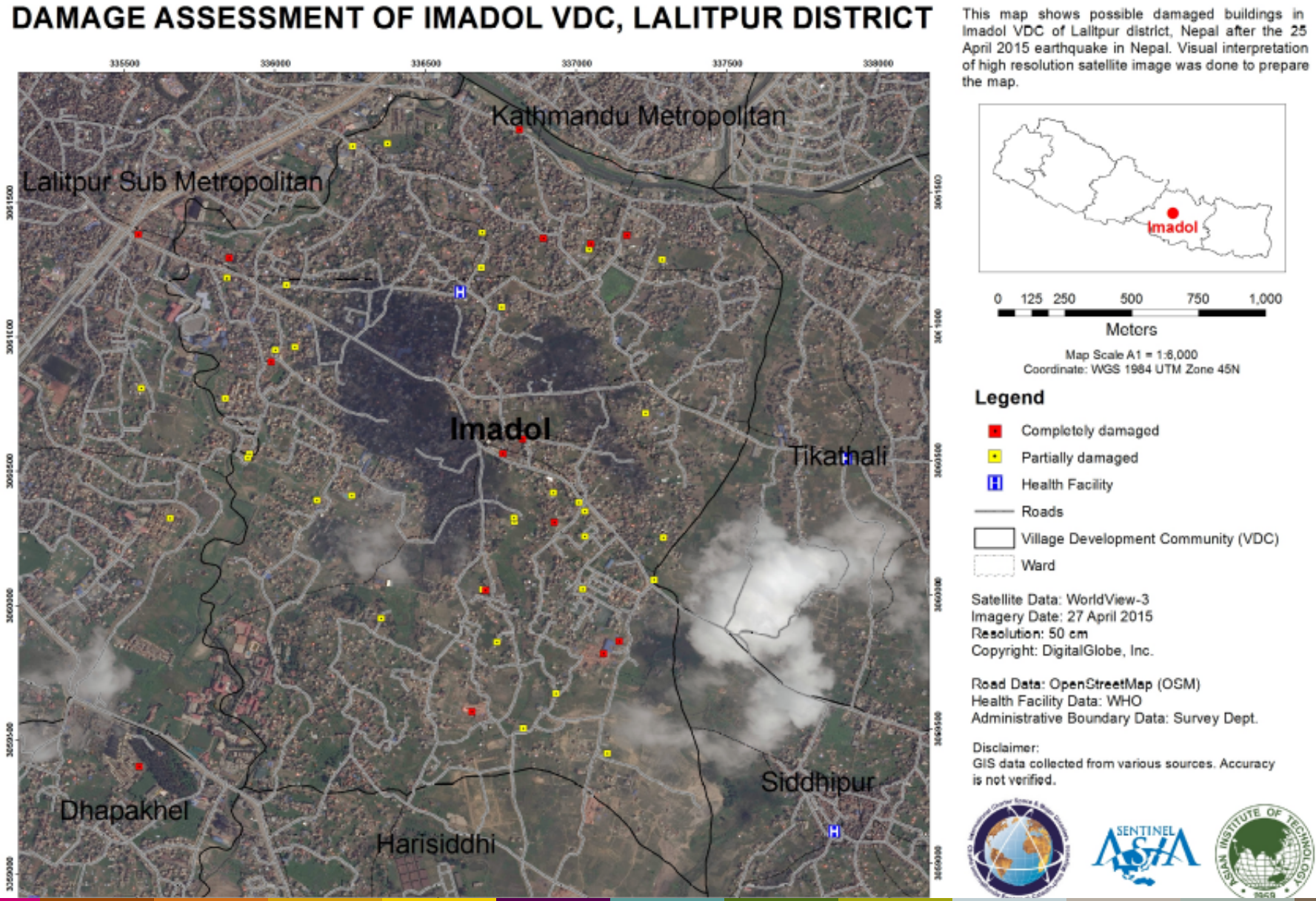

Philippines activation 2017

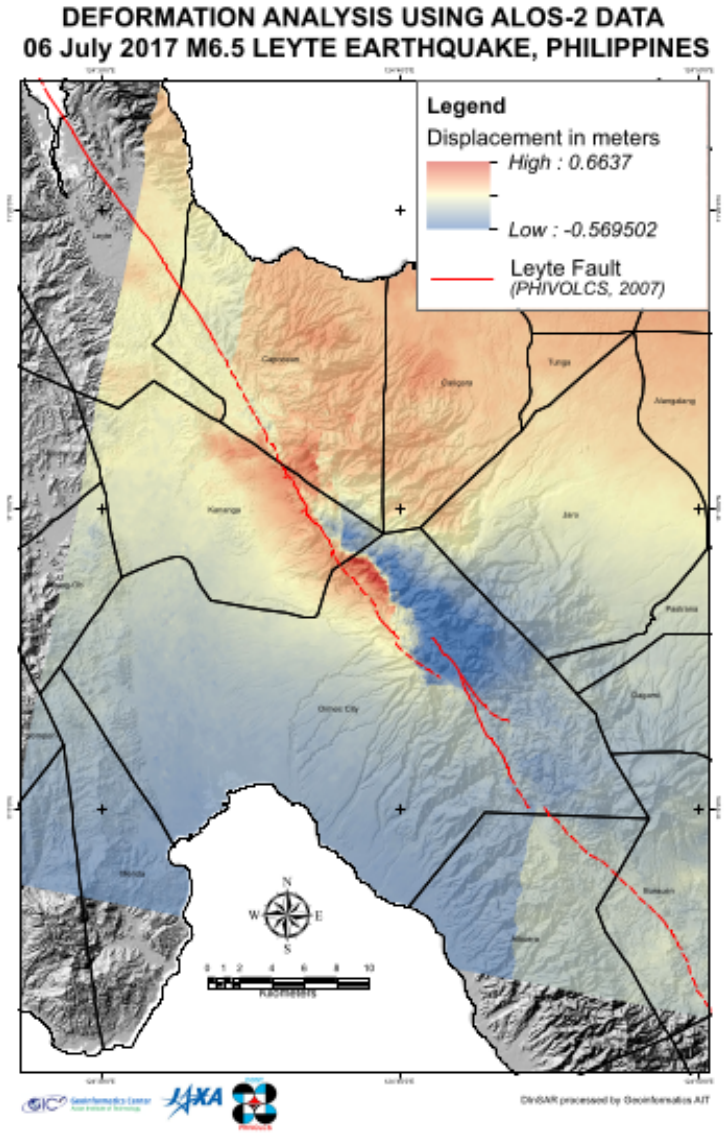

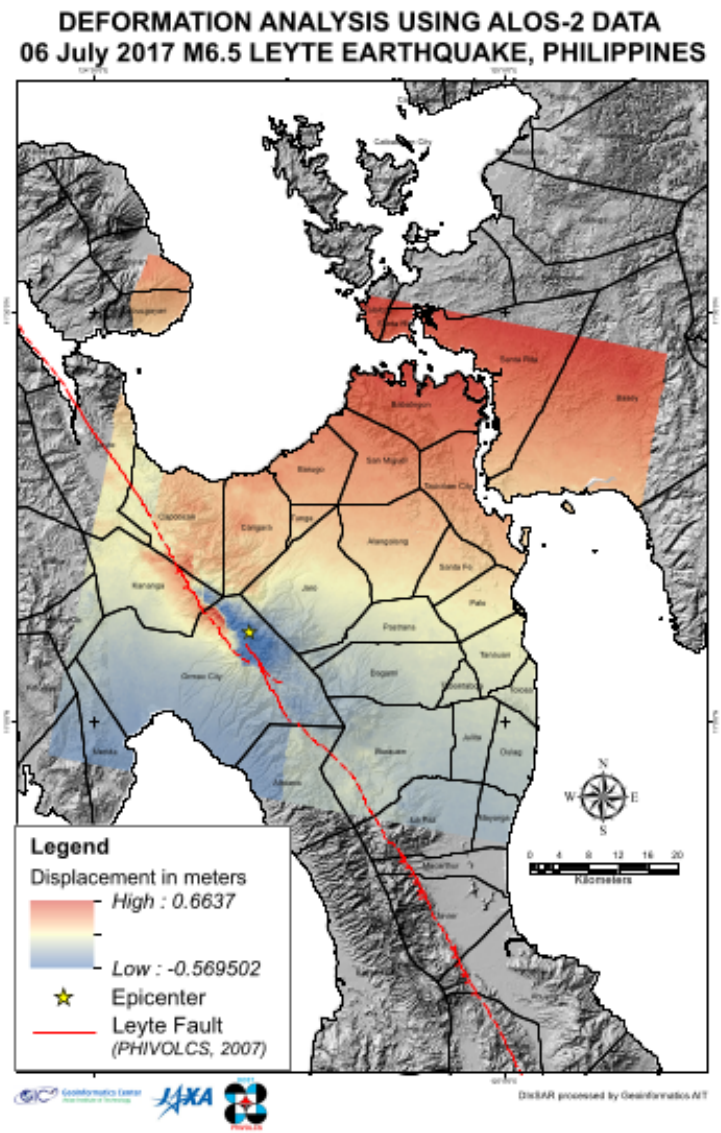

Vietnam activation 2017

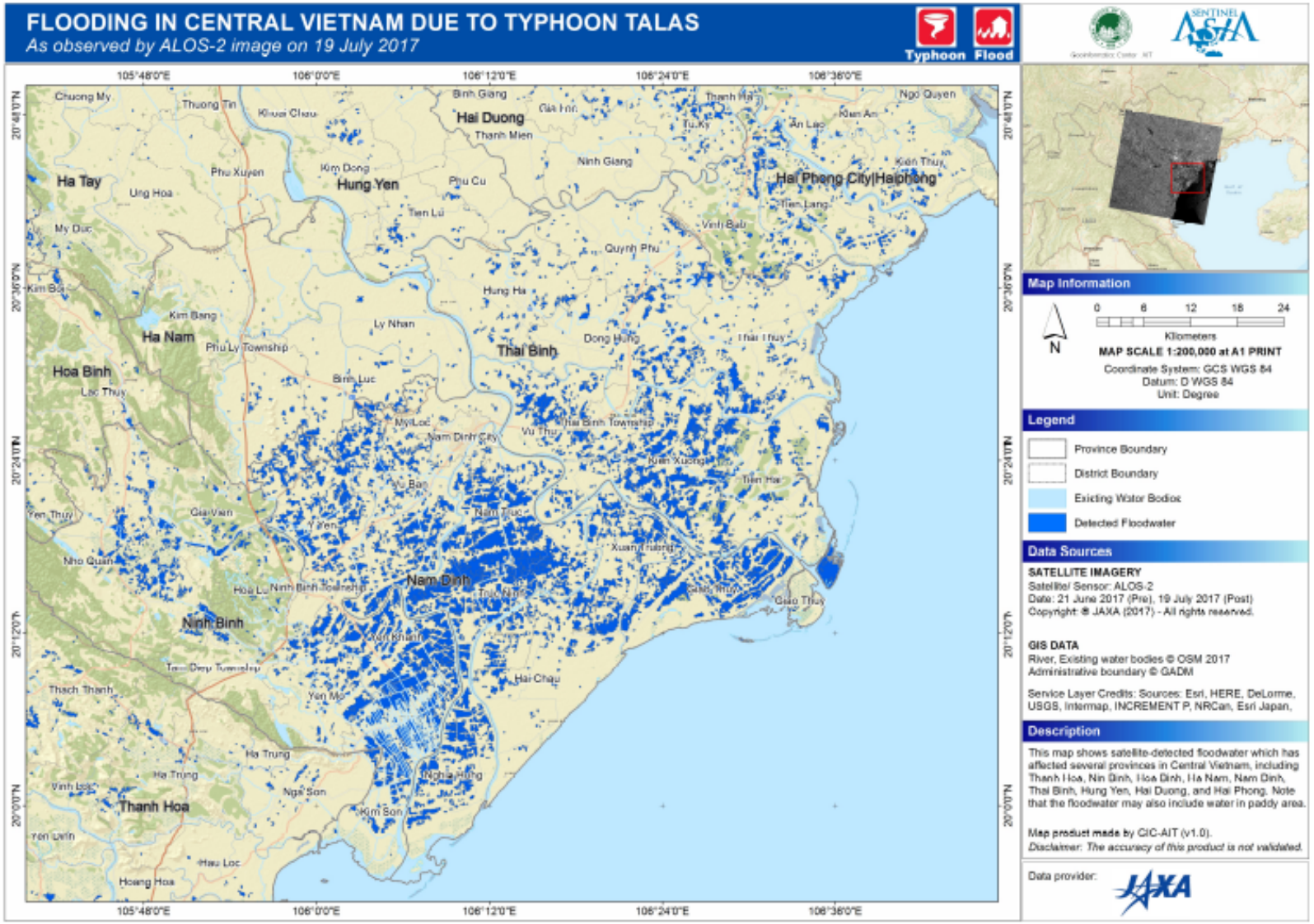

- Date : 17 July 2017 Requester : MONRE
- Disaster : Typhoon Data provided : ALOS-2

Indonesia activation 2017

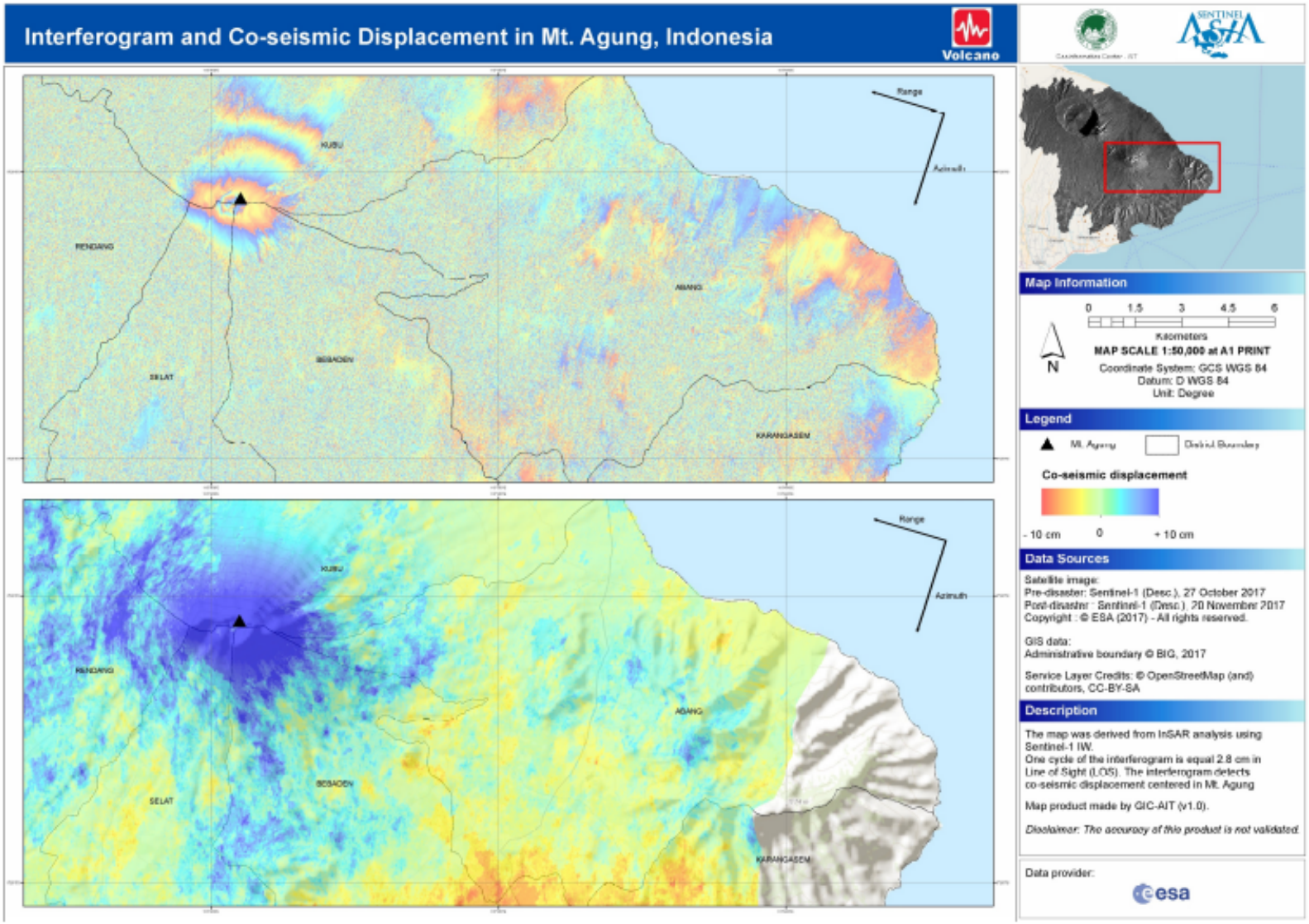

- Date : 21 November 2017 Requester : LAPAN/BNPB

Indonesia activation 2017

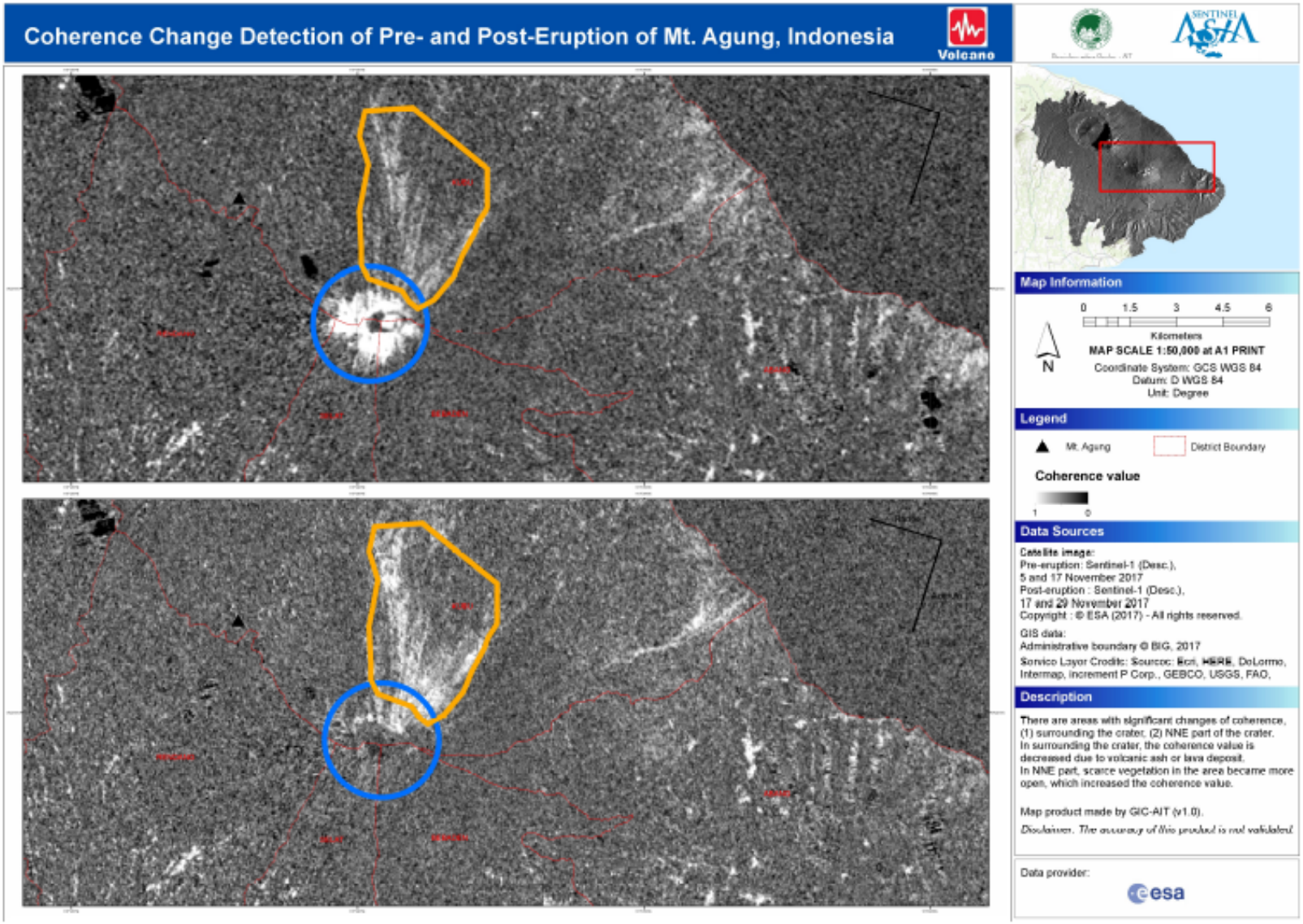

- Date : 21 November 2017 Requester : LAPAN/BNPB

Visual interpretation

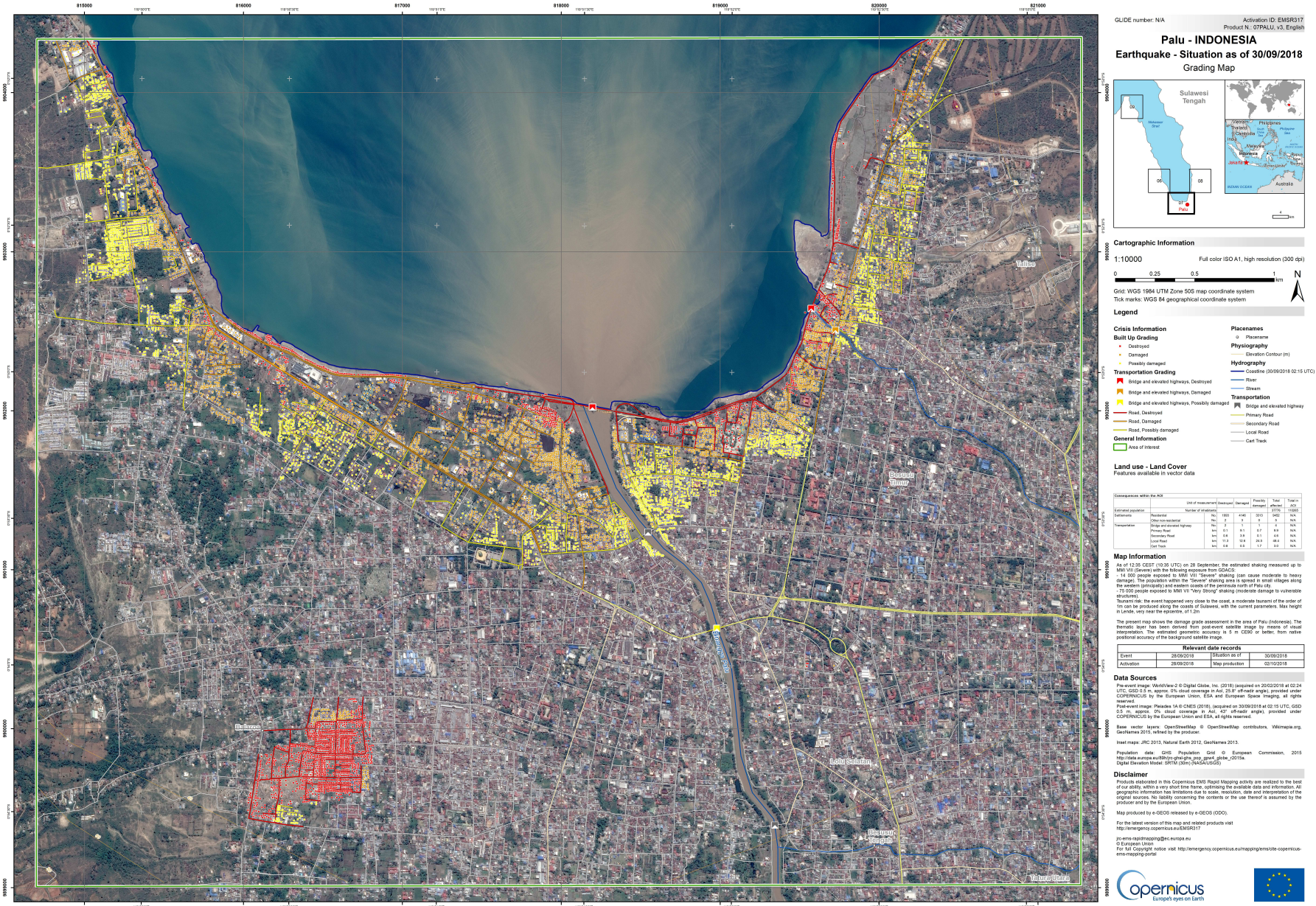

Change detection

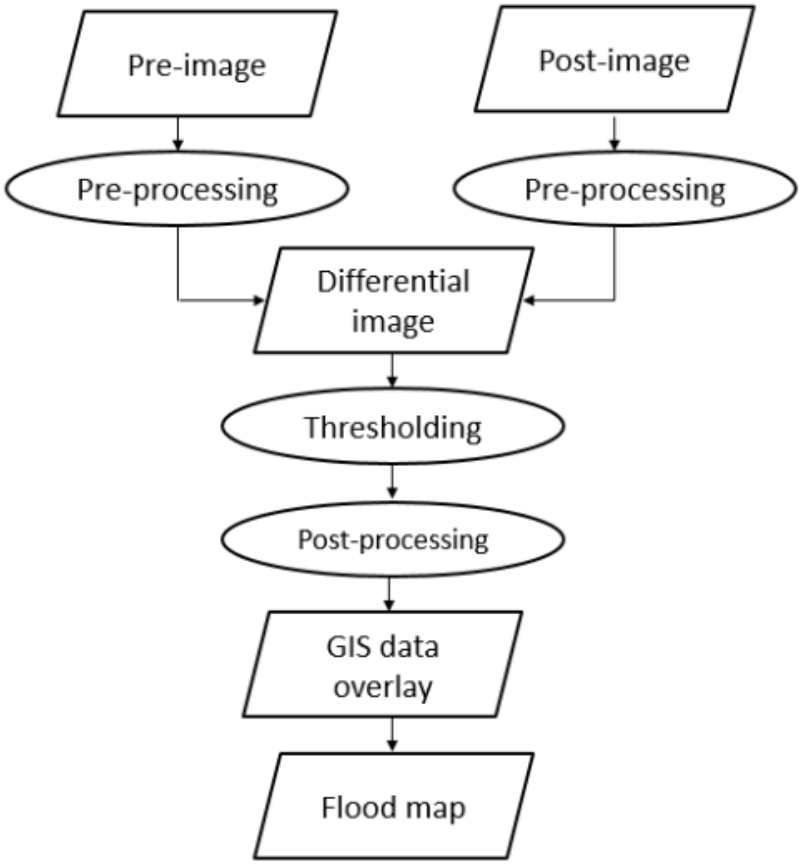

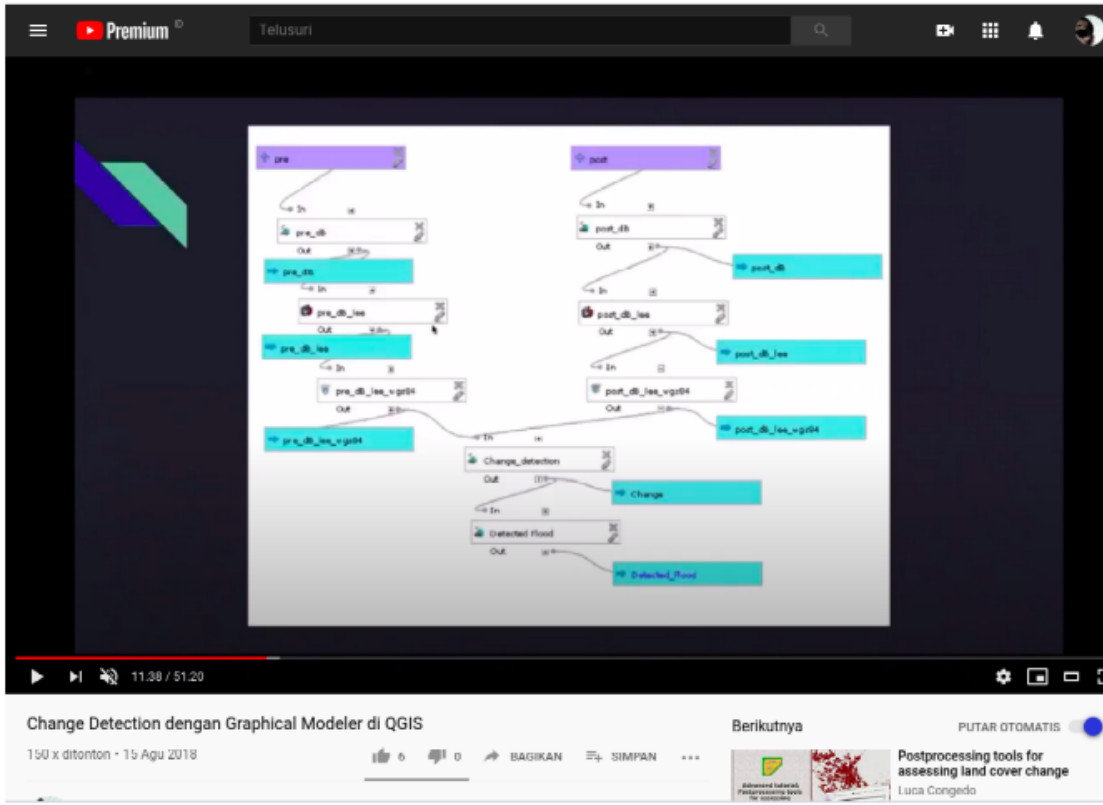

https://youtu.be/HR_7kENFGT4

InSAR

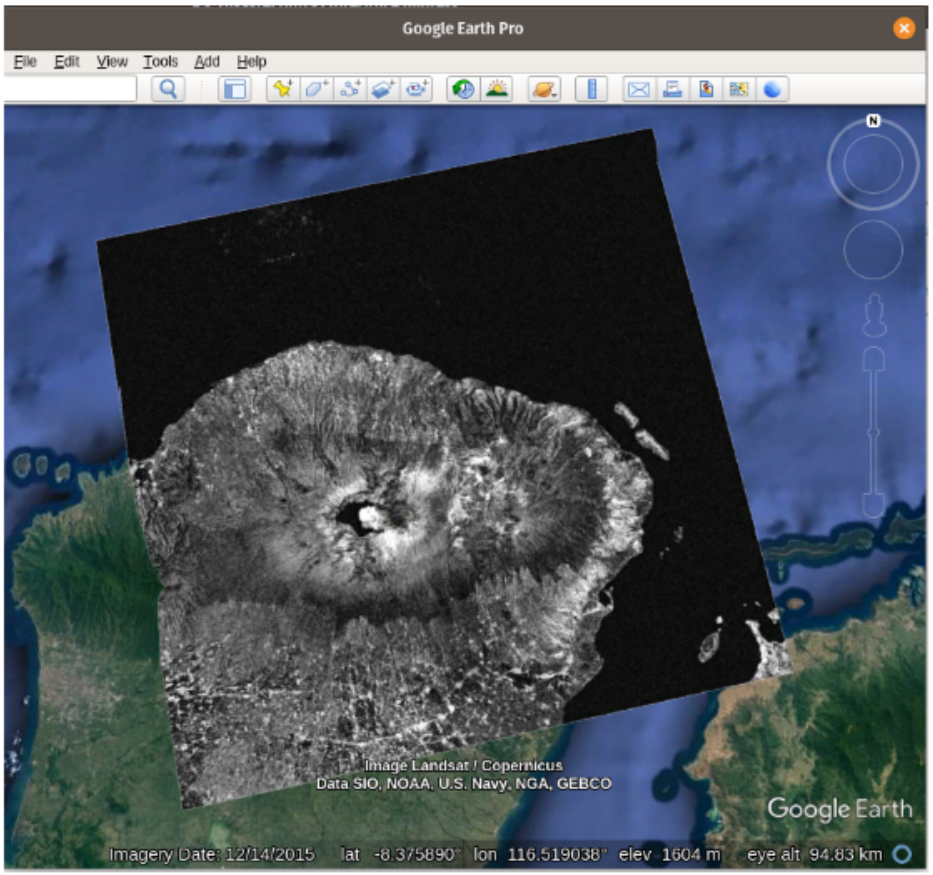
Google Earth Pro
File Edit View Tools Add Help
Image Landsat / Copernicus
Data SIO, NOAA, U.S. Navy, NGA, GEBCO
Google Earth
Imagery Date: 12/14/2015 lat -8.375890° lon 116.519038° elev 1604 m eye alt 94.83 km

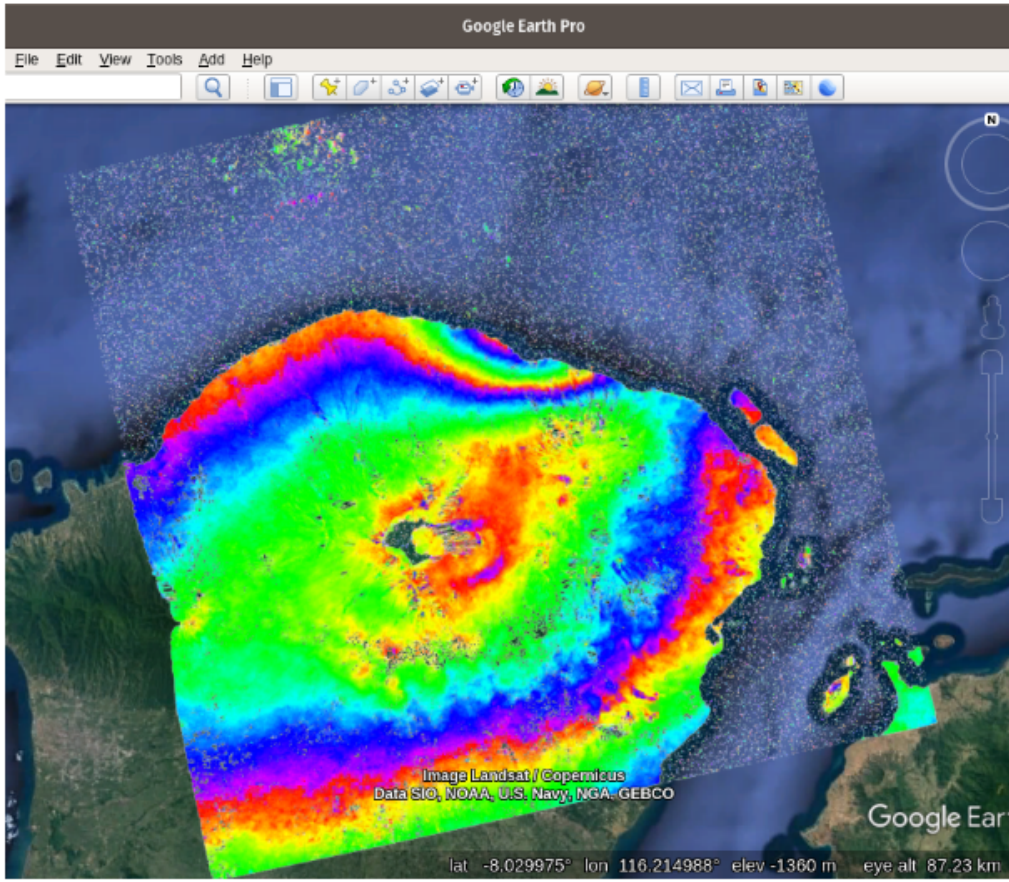
Google Earth Pro
File Edit View Tools Add Help
Image Landsat / Copernicus
Data SIO, NOAA, U.S. Navy, NGA, GEBCO
Google Ear
lat -8.029975° lon 116.214988° elev -1360 m eye alt 87.23 km

Introduction

Remote Sensing

Remote sensing is the process of detecting and monitoring the physical characteristics of an area by measuring its reflected and emitted radiation at a distance (typically from satellite or aircraft). Special cameras collect remotely sensed images, which help researchers "sense" things about the Earth.

Remote sensing system

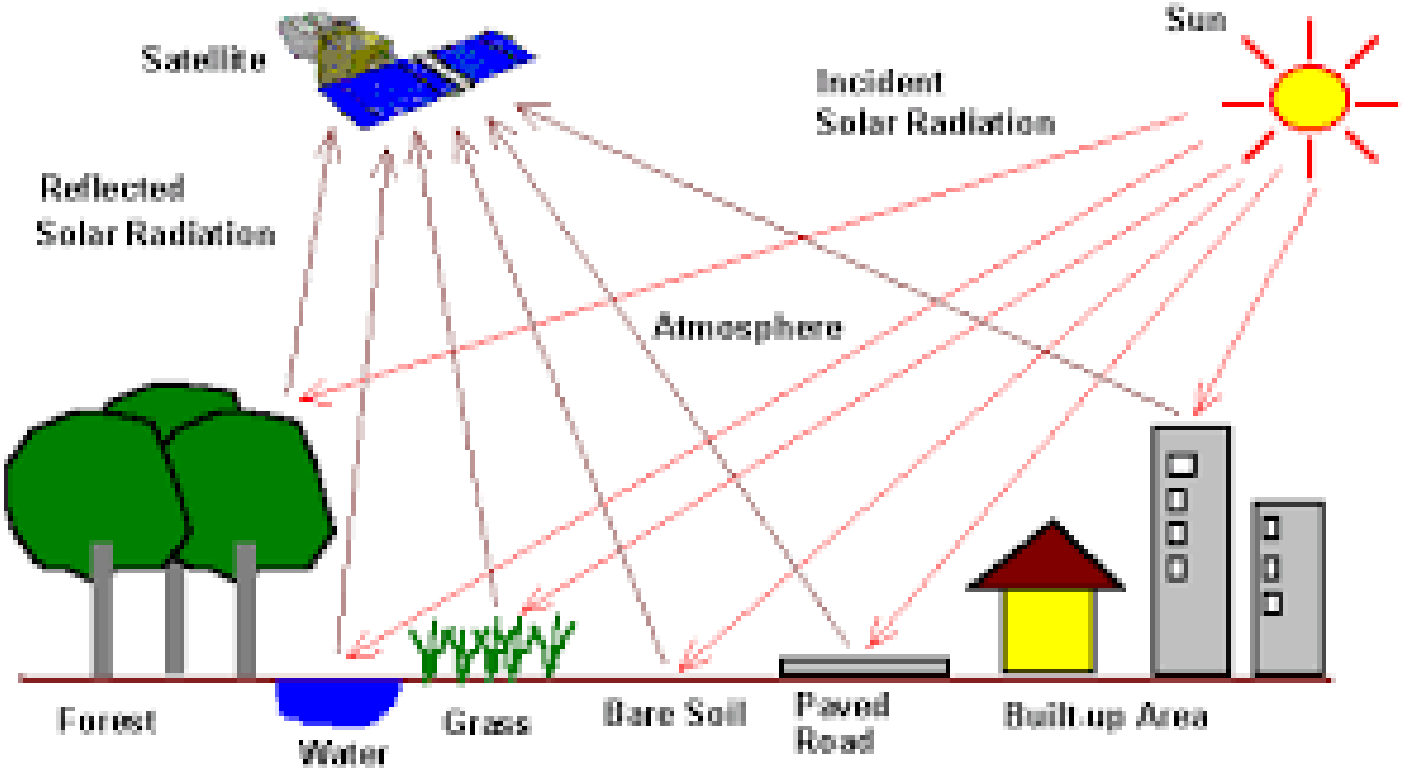

1. Spectral response

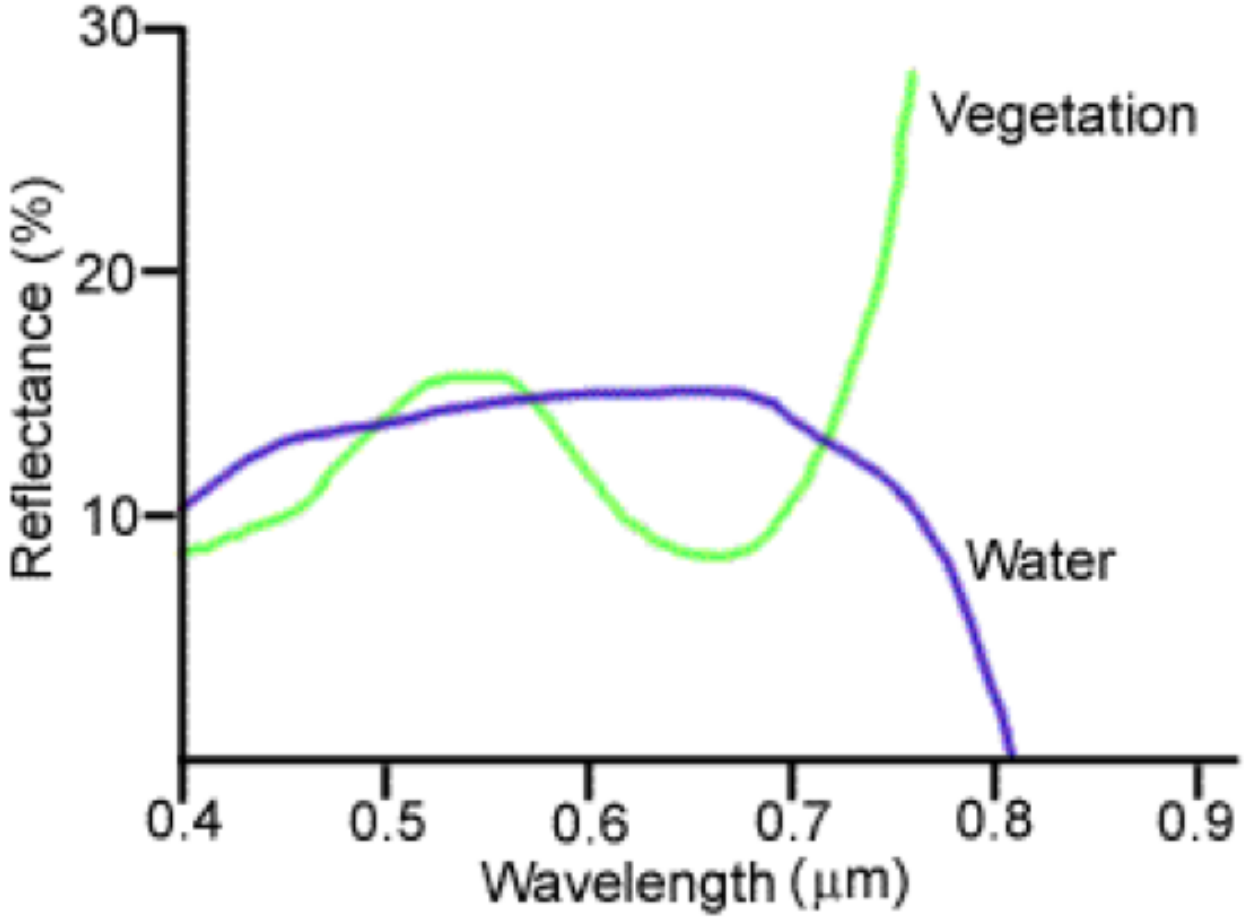

2. Everything is a number

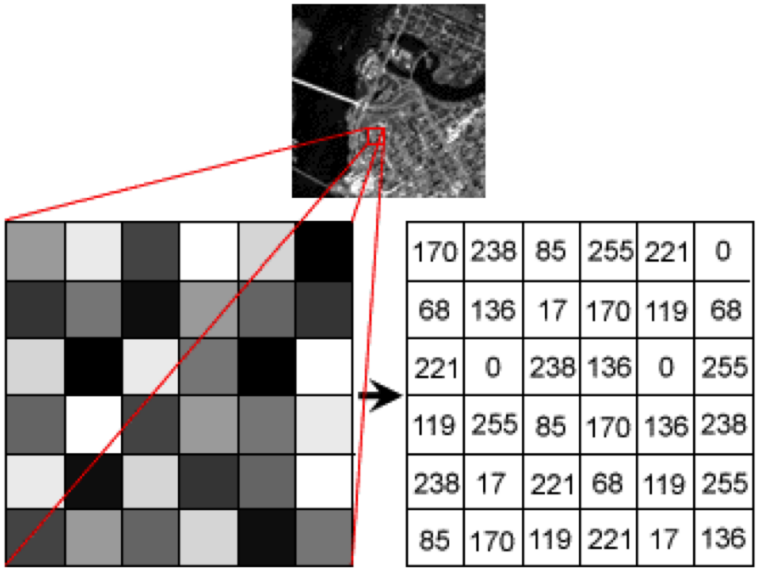

Image, pixel and digital number

- Reflected EM will be recorded by sensor in digital number.
- Visualisation will be defined by grayscale level.

3. RGB Visualisation

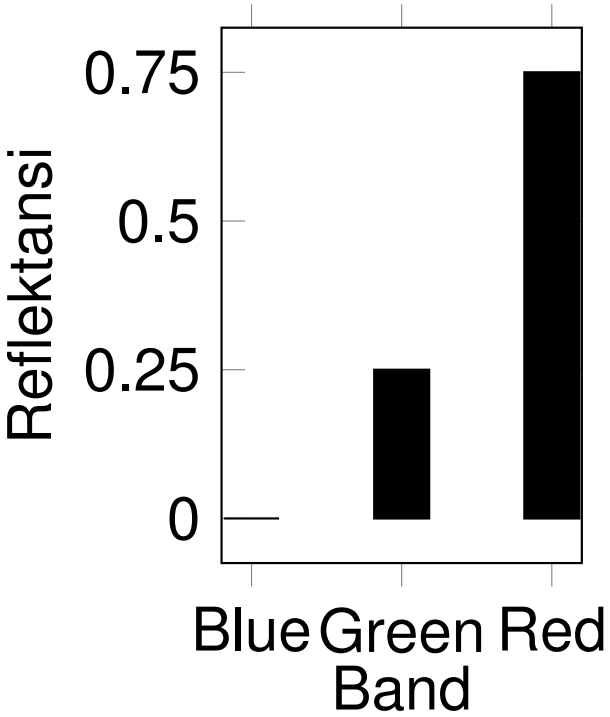

3. RGB Visualisation

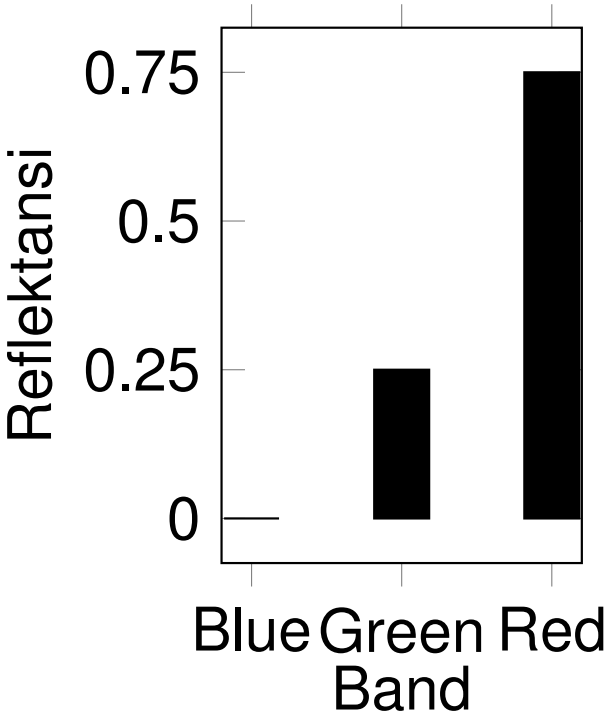

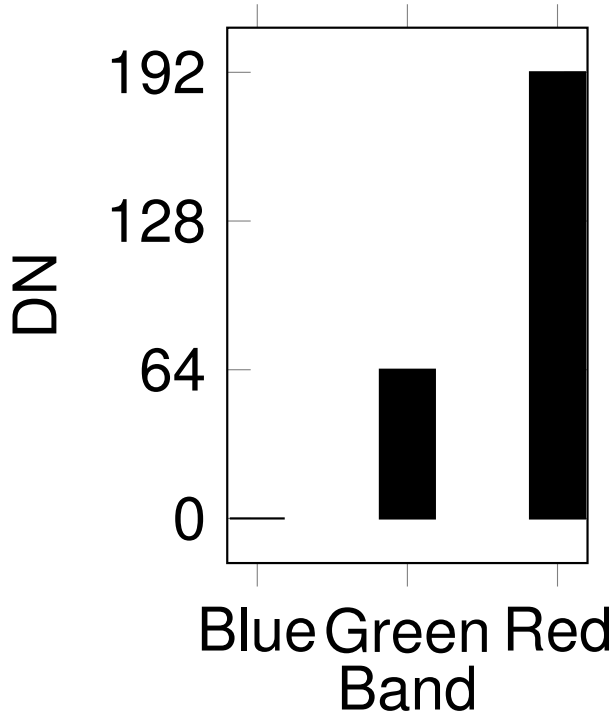

3. RGB Visualisation

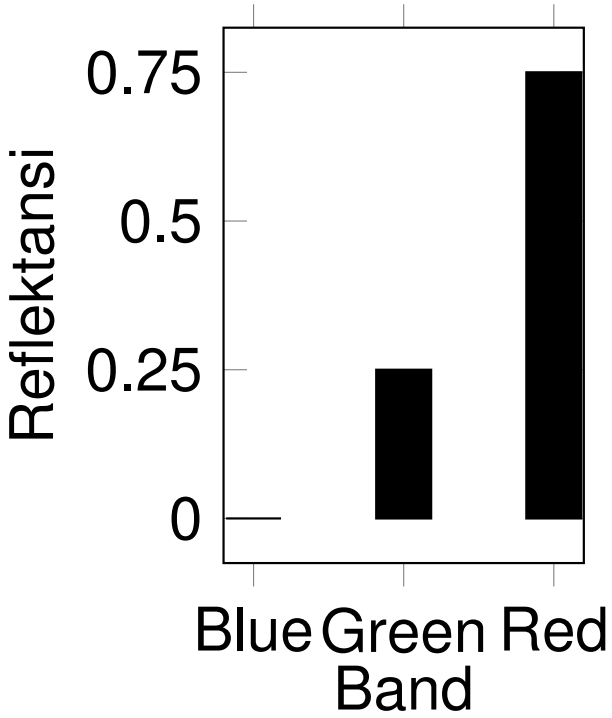

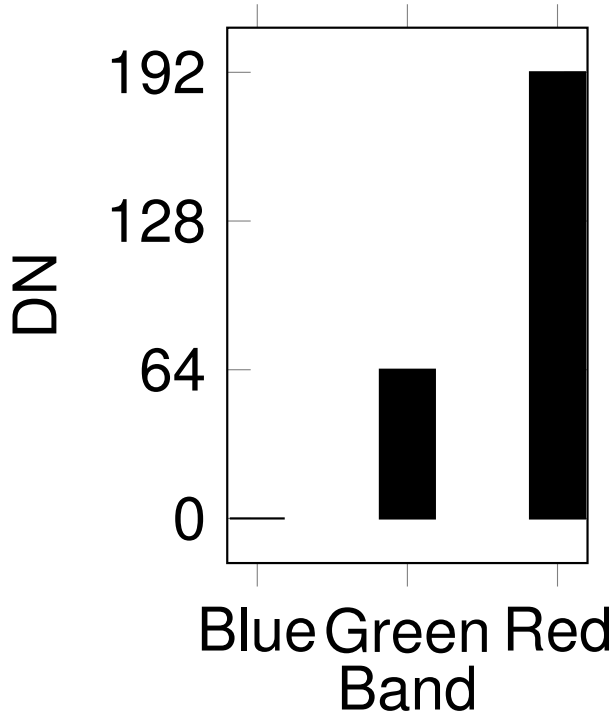

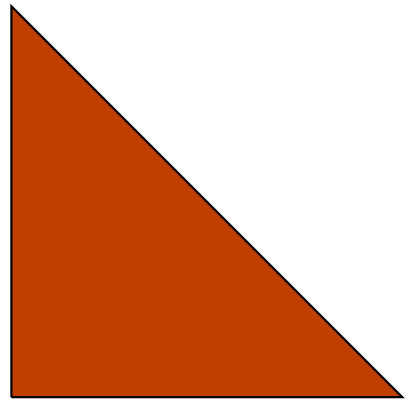

3. RGB Visualisation

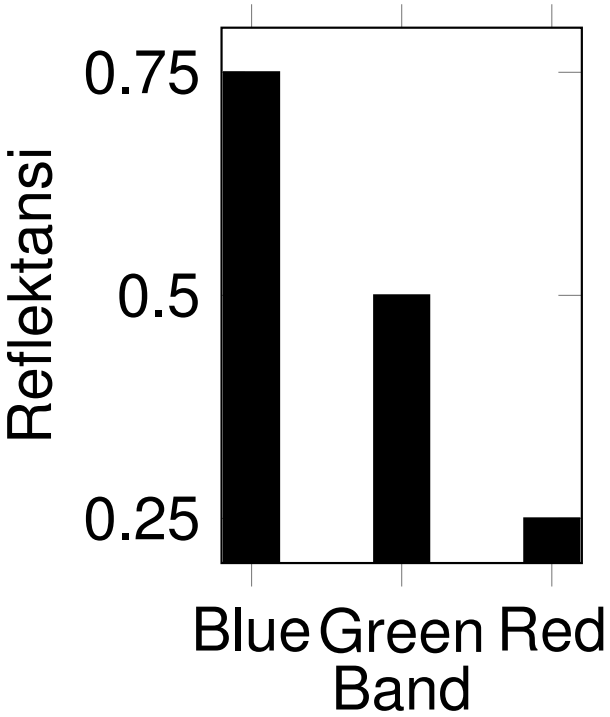

3. RGB Visualisation

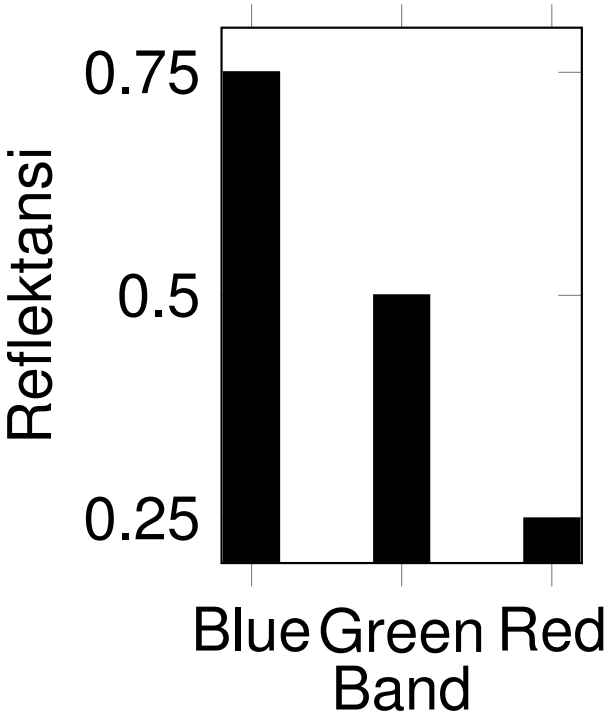

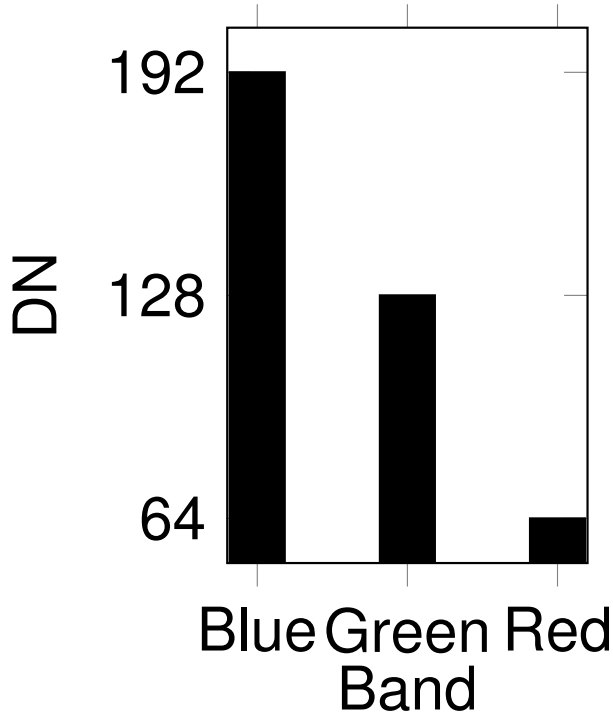

3. RGB Visualisation

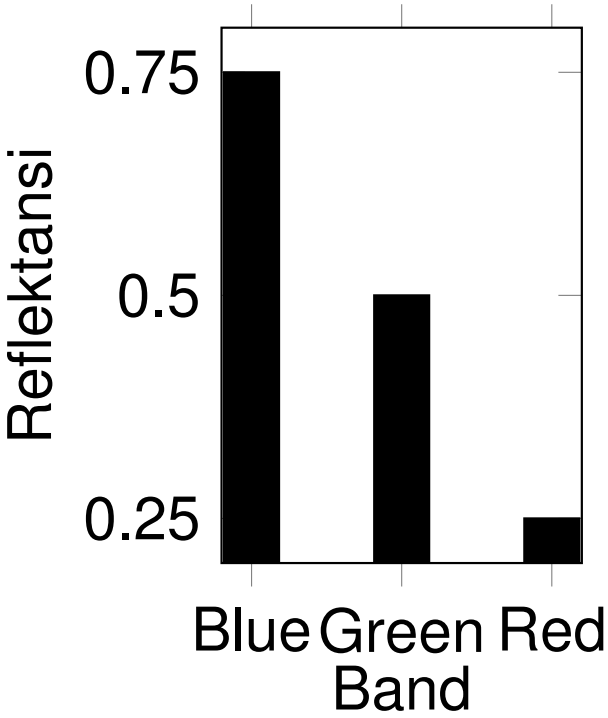

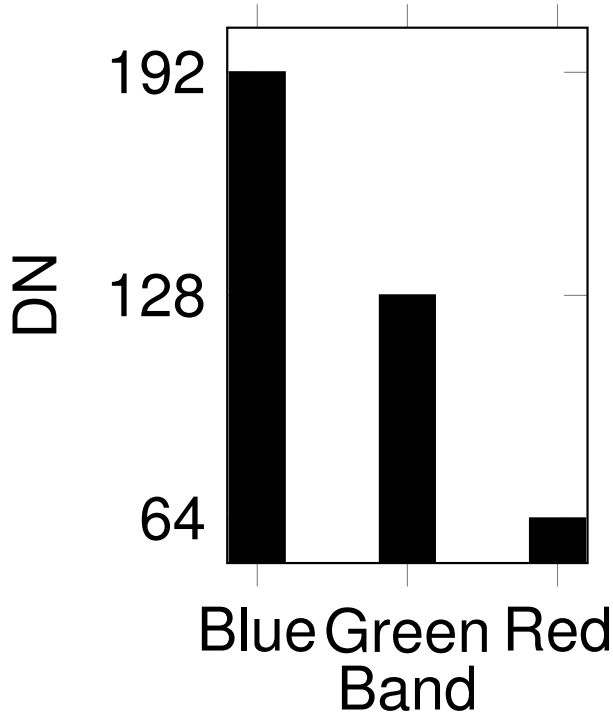

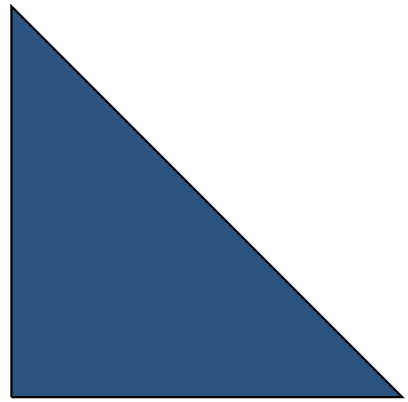

Blue channel

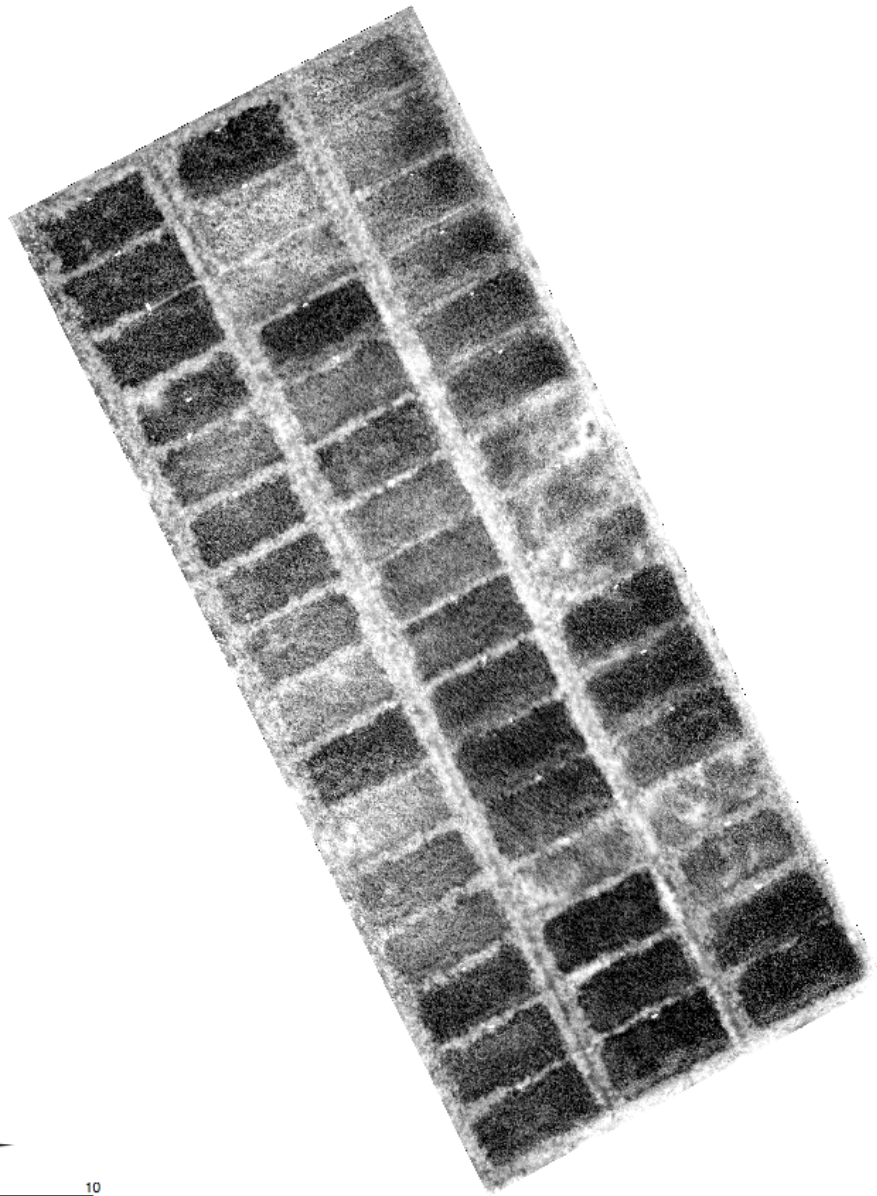

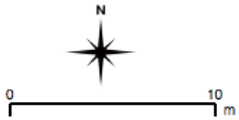

Green channel

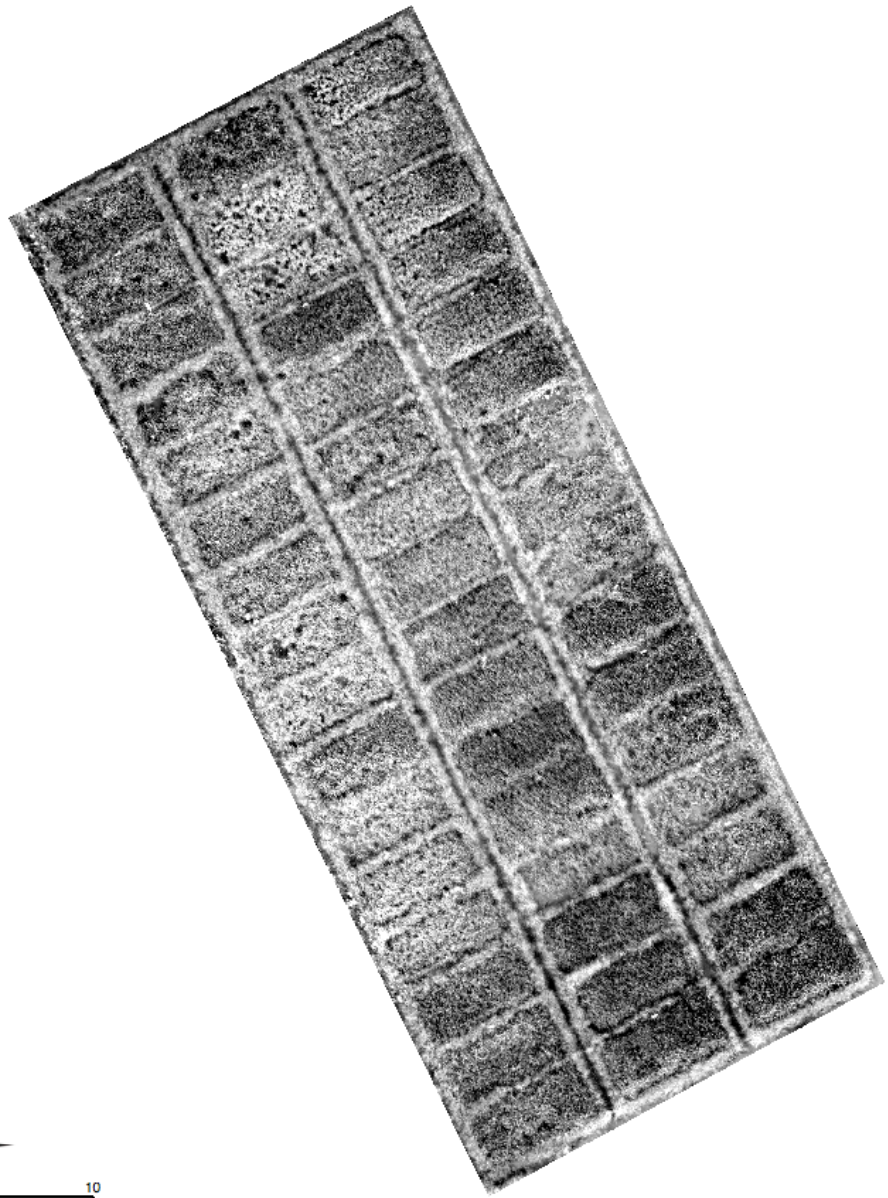

Red channel

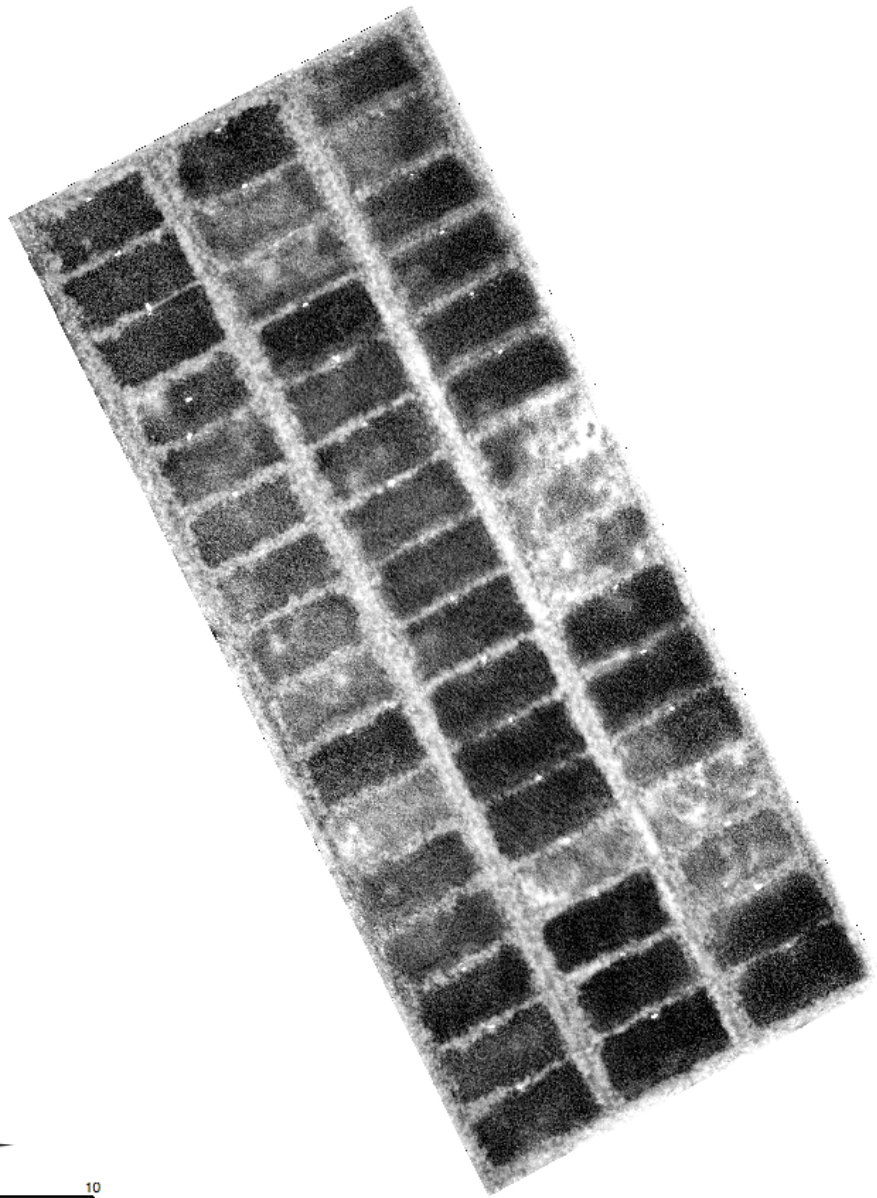

Red edge channel

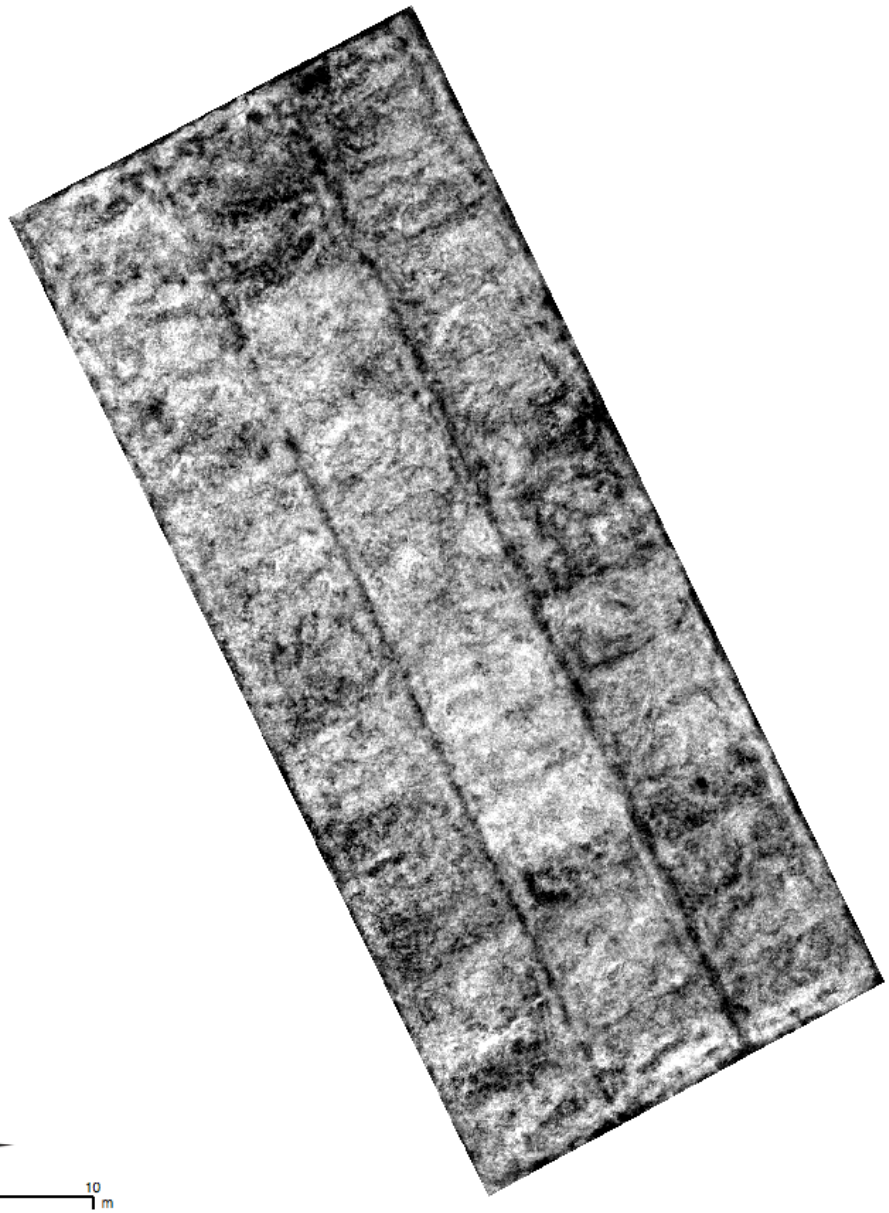

Near infra-red (NIR) channel

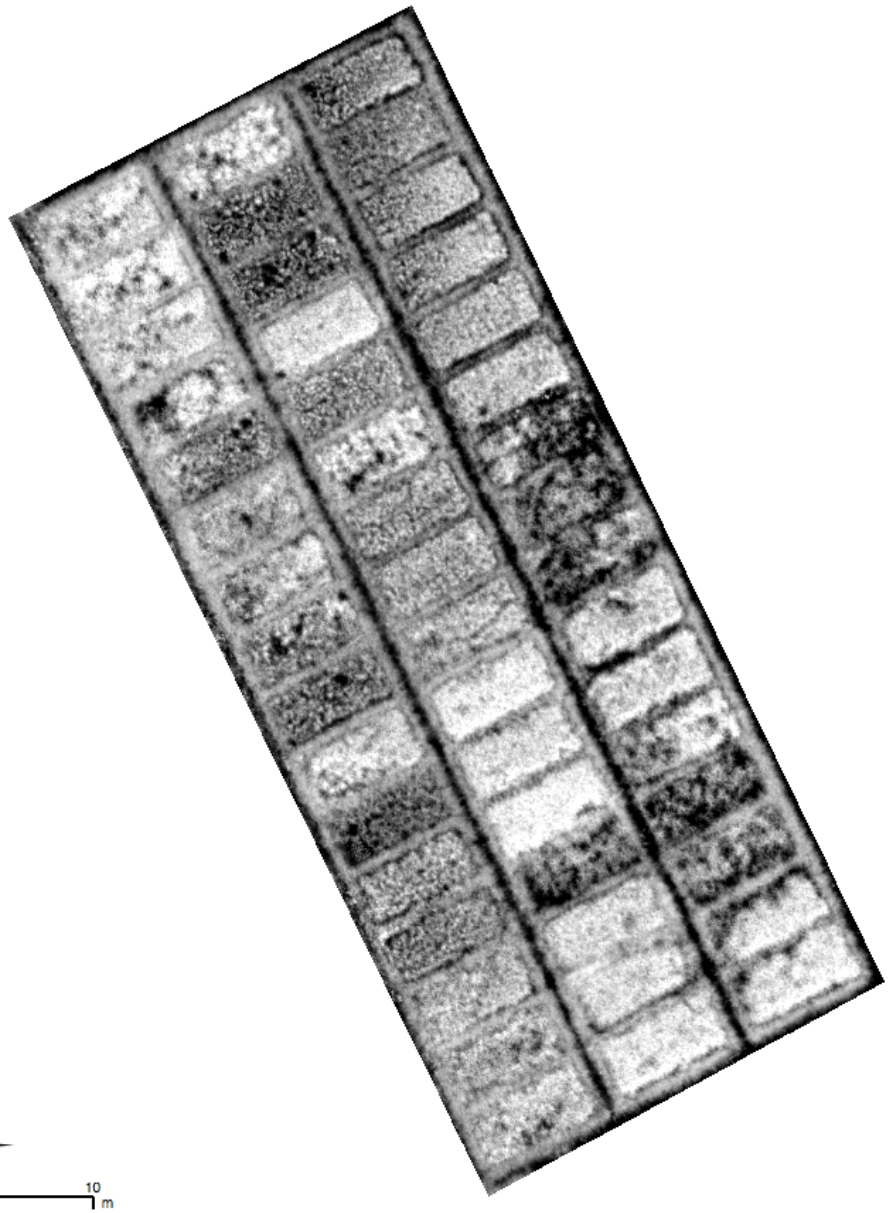

RGB = Red:Green:Blue

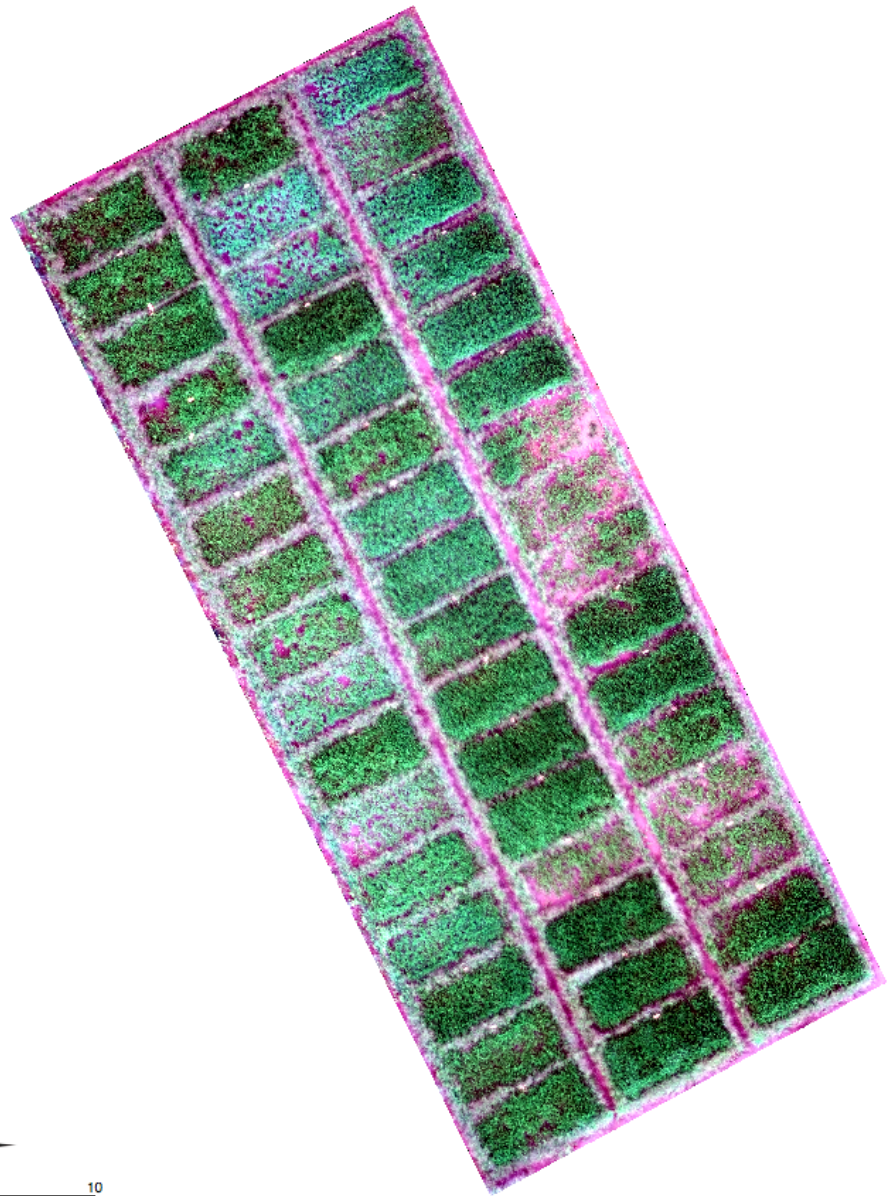

RGB = NIR:Red:Green

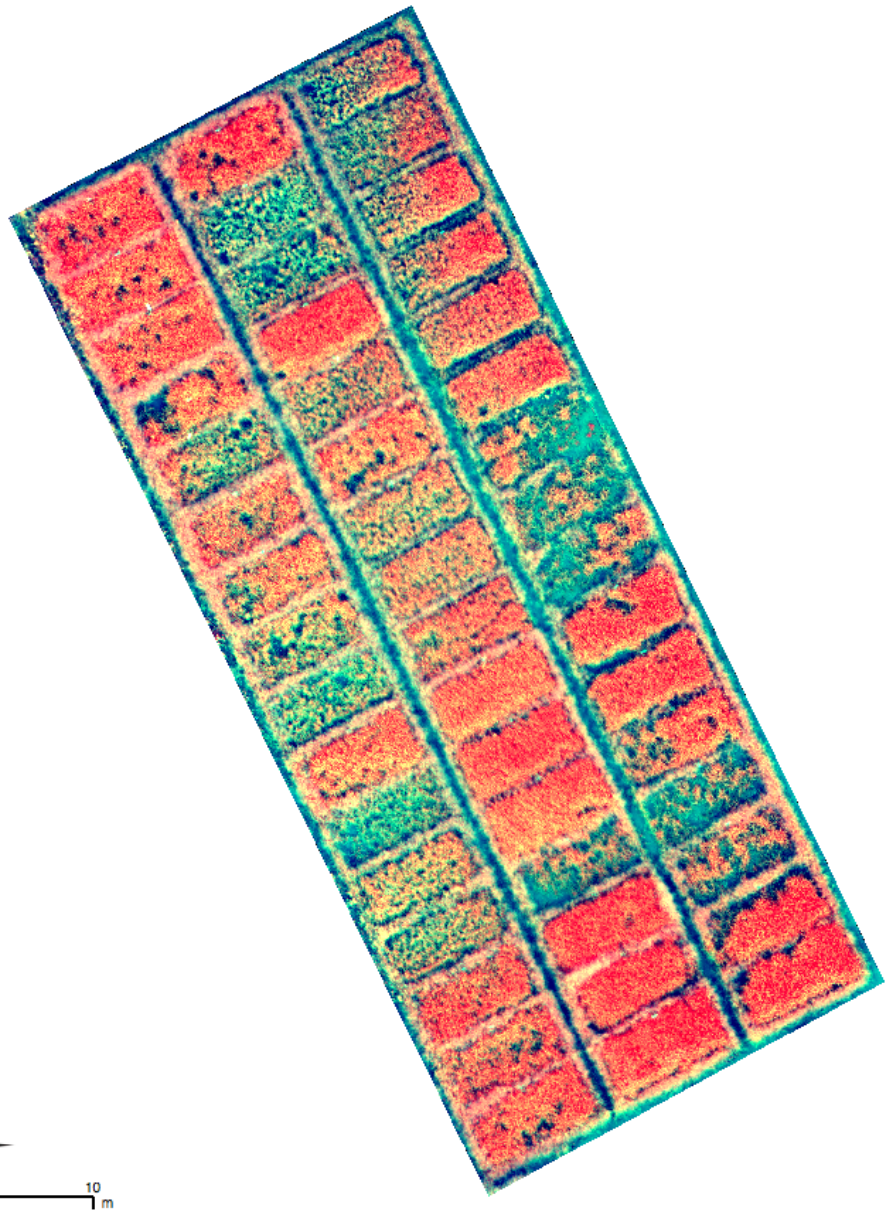

4. Minimizing errors

5. Classification

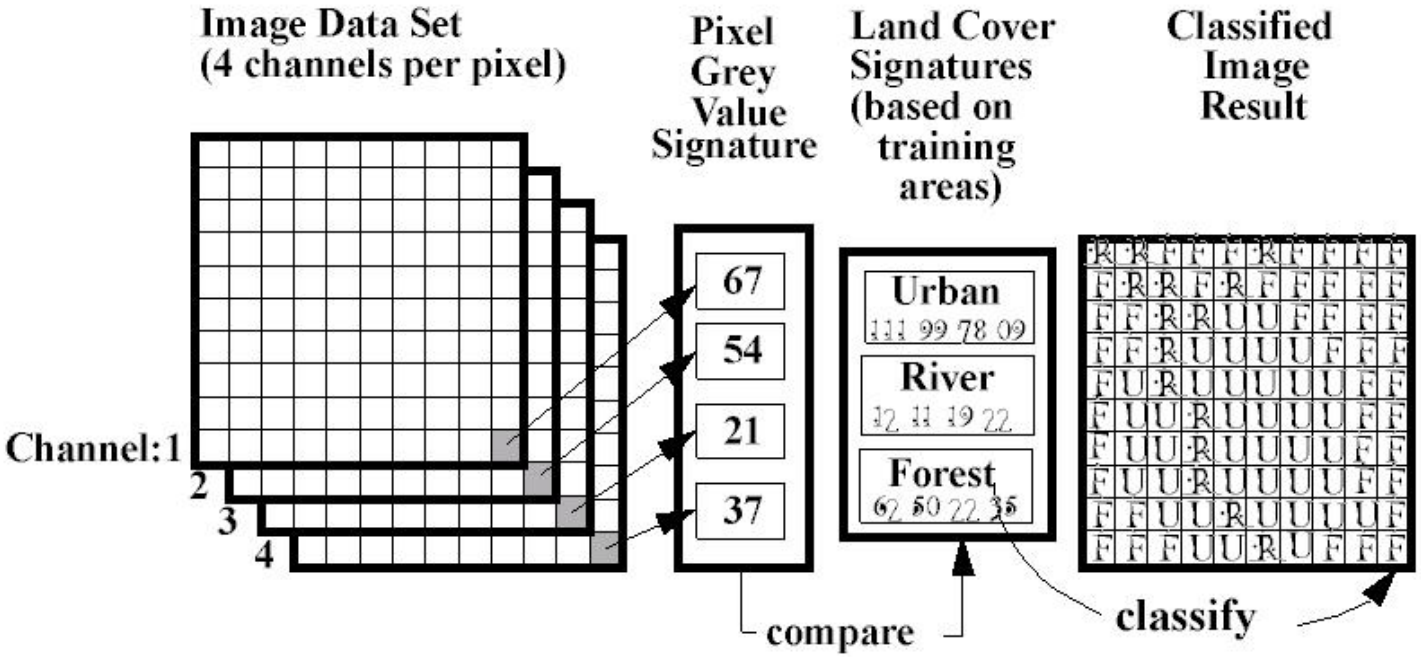

Supervised classification

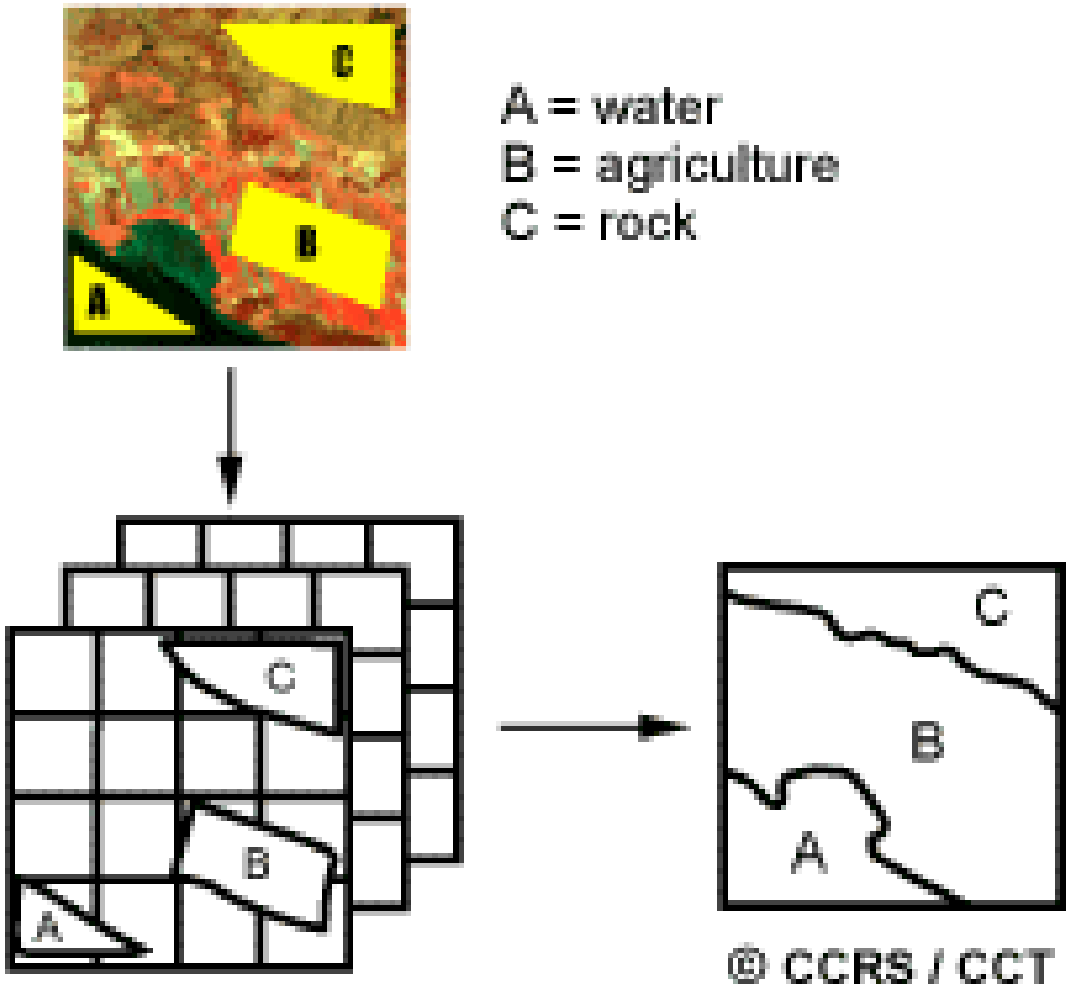

Unsupervised classification

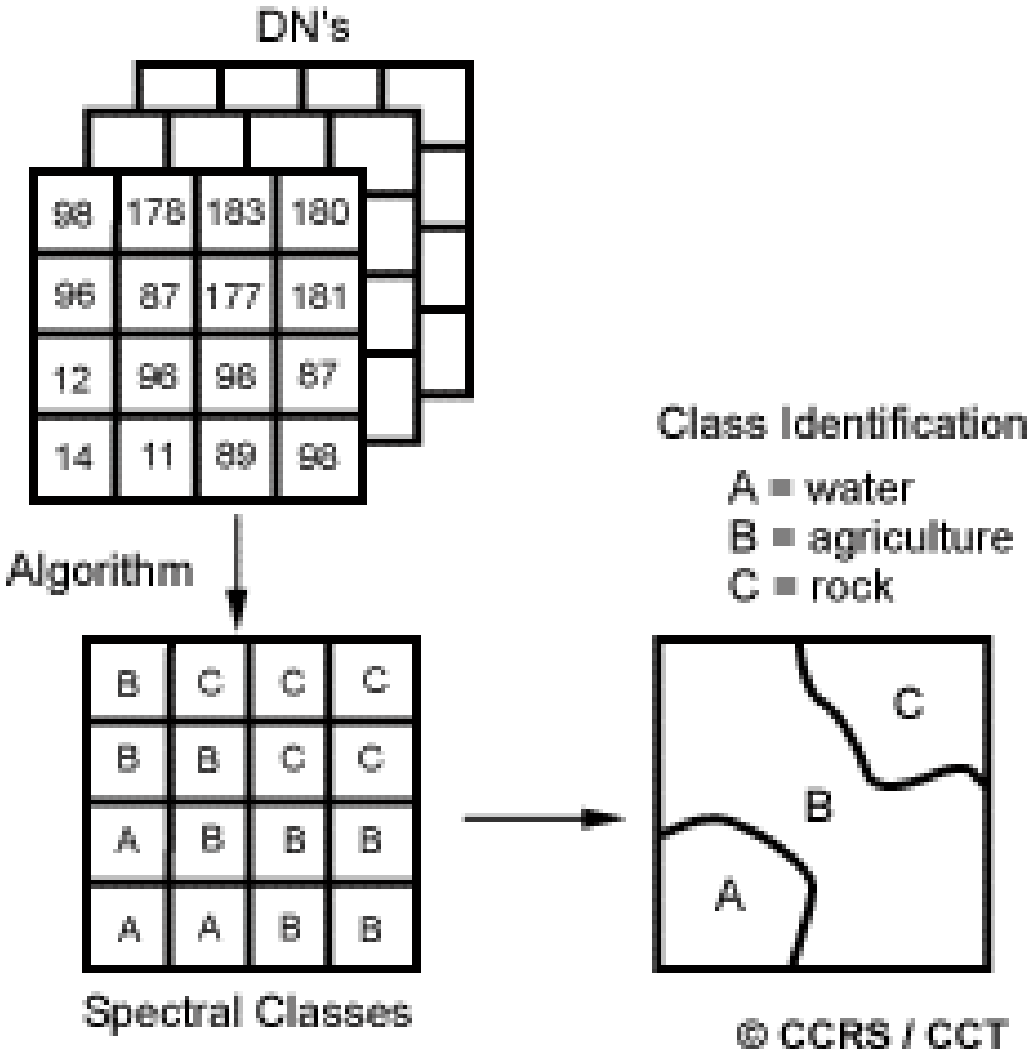

Introduction

Geodesy

Geodesy is a scientific discipline that deals with the measurement and representation of the Earth's surface in a three-dimensional, time-varying space. A topographic map is essential for the thematic mapping of geological and environmental information.[a]

[a] Jung Hum Yu, 2011

RADAR spectrum

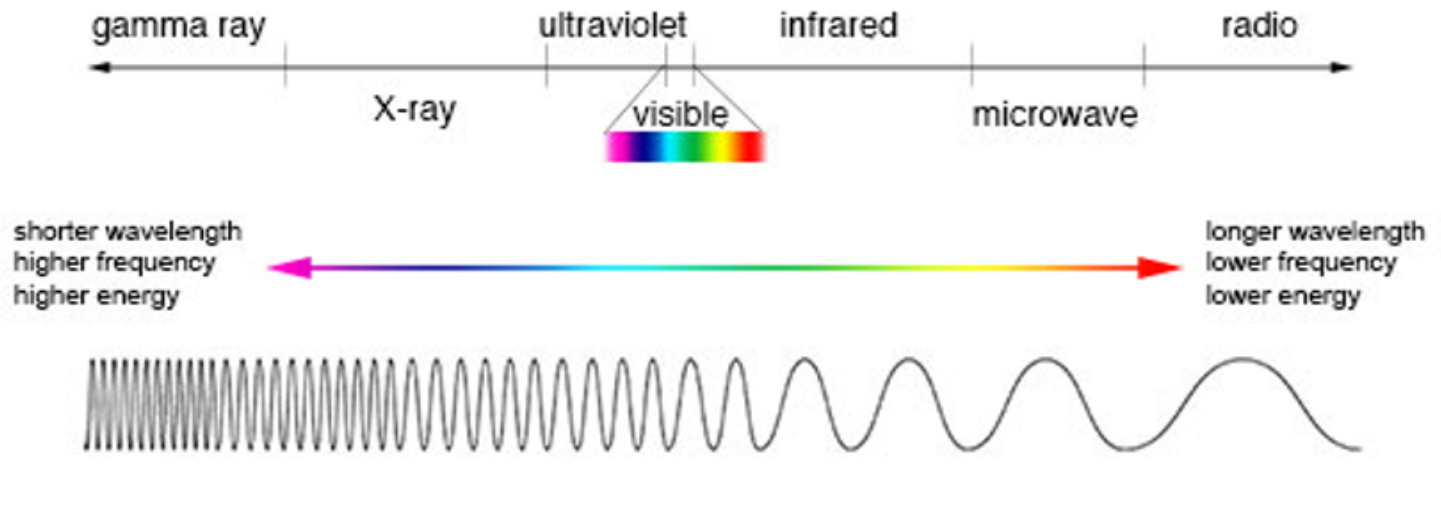

‖

- Radar was investigated by A.H. Taylor and L.C. Young in 1922 (Wilkinson 1987). Side Looking Airborne Radar (SLAR), which has a continuous strip mapping capability, was developed in the 1950s. ¶

‖ https://www.capellaspace.com/sar-101-an-introduction-to-synthetic-aperture-radar/

¶ Jung Hum Yu, 2011

Echolocation

HOW SAR WORKS

THINK ECHOLOCATION, LIKE A WHALE

- SAR sends out energy, bounces that energy off something and returns the energy as information that:
  - Is multi-dimensional
  - Includes: time, geometry, signal data & elevation
  - Is commonly formed into an image
- With this, we can measure: speed, distance, direction & presence

THESE MEASUREMENTS ARE REPEATABLE FOR HIGH PRECISION RESULTS

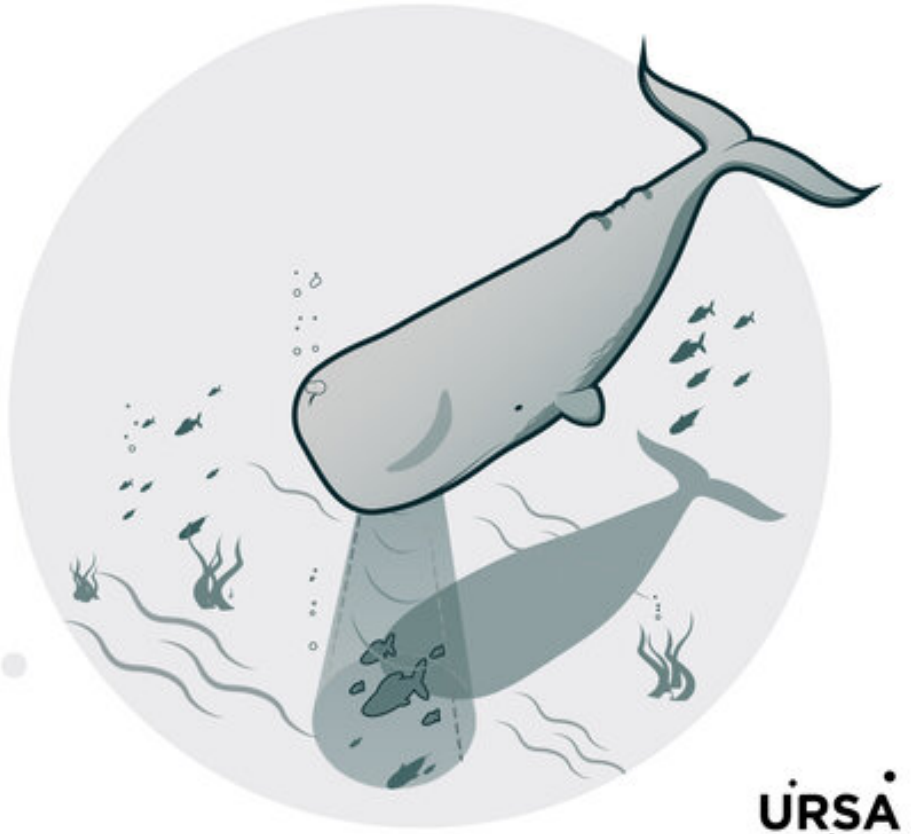

https://www.liamjcullen.com/

Why side-looking radar

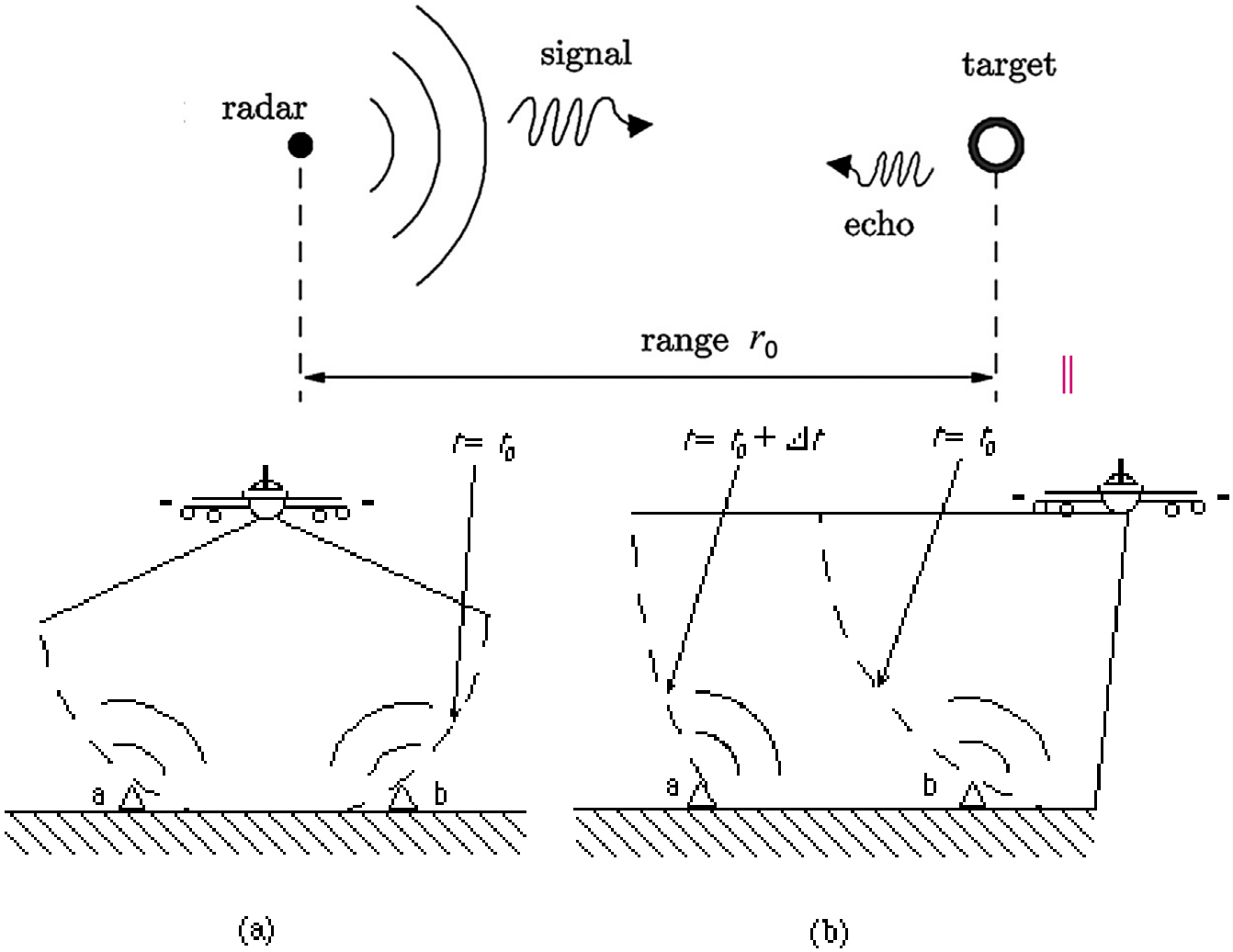

‖ http://dx.doi.org/10.1016/B978-0-12-809254-5.00005-1

¶ http://www.csr.utexas.edu/projects/rs/whatissar/rar.html

Why side-looking radar

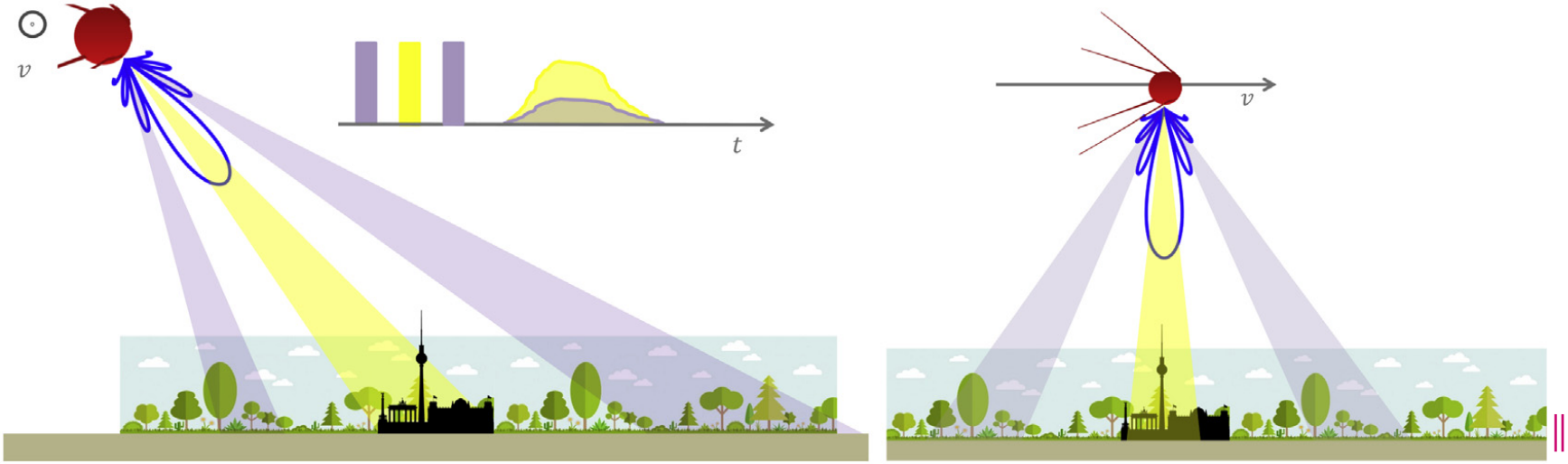

[||] Emery and Camps. 2017.

RADAR geometry

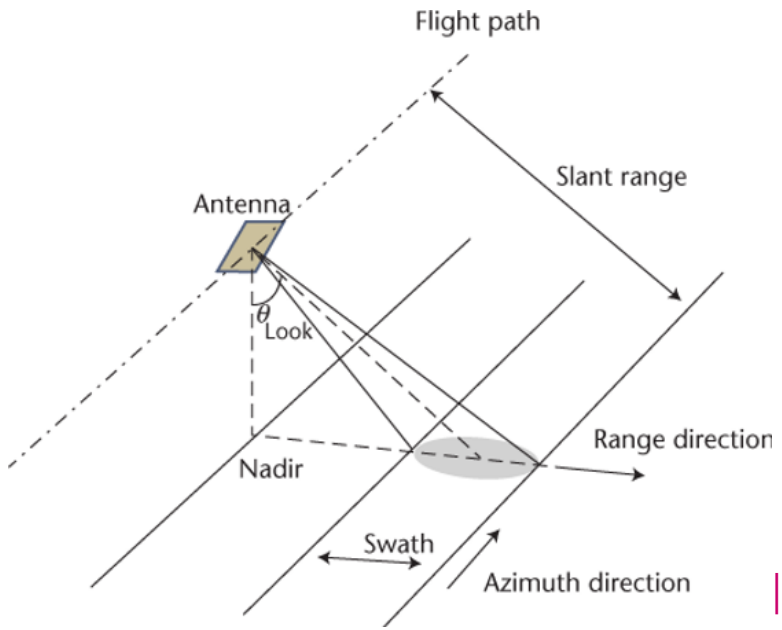

- SLAR has two major types: real aperture radar and synthetic aperture radar, where the word “aperture” means antenna.
- Real aperture radar uses a fixed length antenna ranging in length from 1- 2m.
- Synthetic aperture radar also uses similar length antenna however it can synthesize a much longer antenna which has an improved resolution.

Real Aperture Radar

SIDE-LOOKING RADAR
(REAL-APERTURE RADAR)

Active sensor !

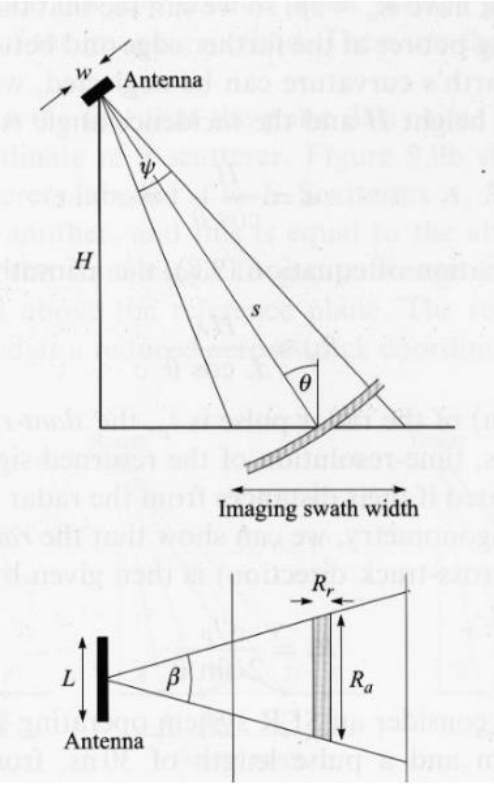

Emission of a short pulse: $t_p = 30$ ns

Across-track resolution obtained by time-resolving the signal

$$R_r = \frac{c t_p}{2 \sin\theta}$$

if $t_p = 30$ ns, $\theta = 35^\circ$ then $\mathbf{R_r = 8\ m}$

Along-track resolution is poor

$$R_a = \frac{H\lambda}{L \cos\theta}$$

if $H = 800$ km, $\lambda = 24$ cm, $L = 10$ m
$\theta = 35^\circ$ then $\mathbf{R_a = 24\ km}$

https://www.slideserve.com/kalare/reading-and-modelling

Synthetic Aperture Radar

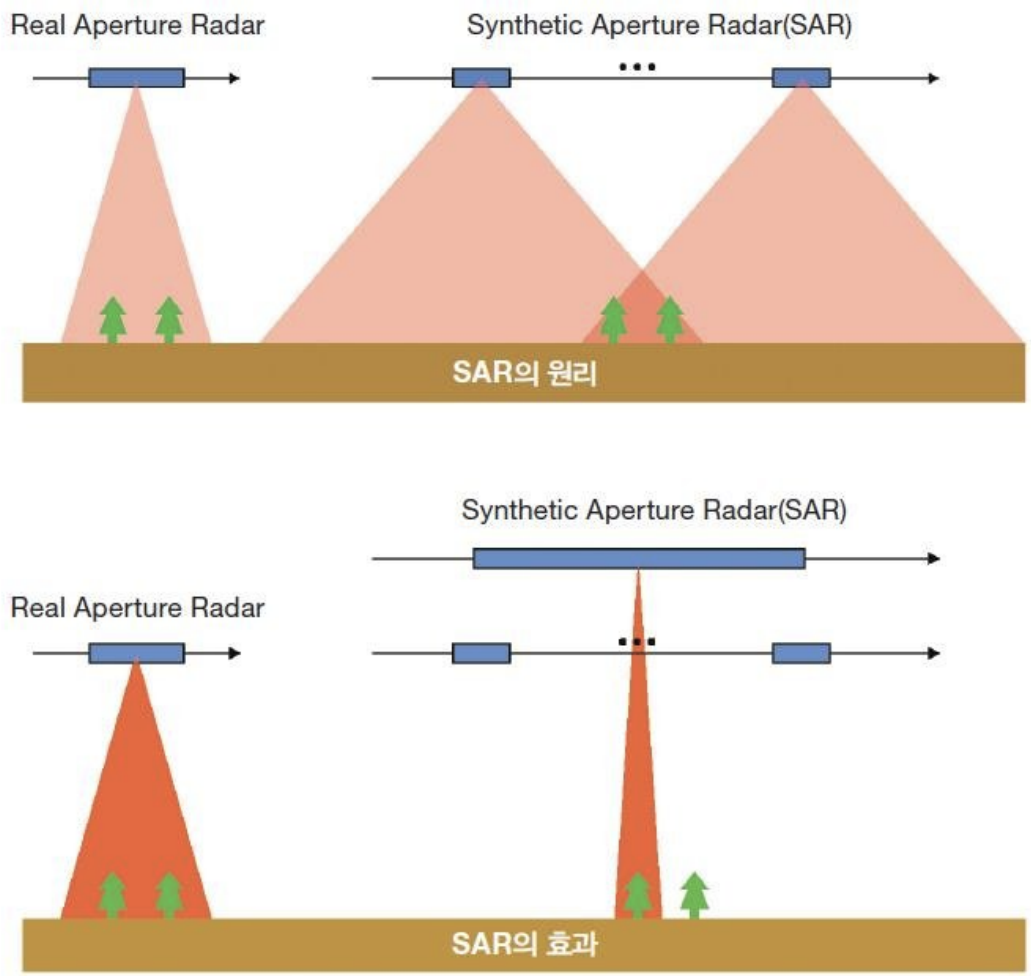

https://m.post.naver.com/viewer/postView.nhn?volumeNo=15131559&memberNo=253010

Across-track resolution (slant range)

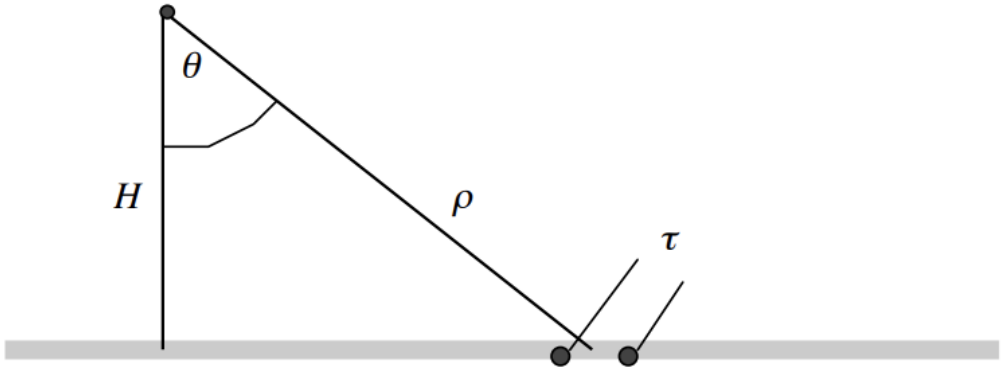

θ	-	look angle
H	-	spacecraft height
B	-	bandwidth of radar
τ	-	pulse length $1/B$
C	-	speed of light

$$\Delta r = \frac{C\tau}{2}$$ - slant range resolution

$$R_r = \frac{C\tau}{2}\frac{1}{\sin\theta}$$ - ground range resolution

https://igppweb.ucsd.edu/ fialko/insar/sar_summary.pdf

Along-track / azimuth resolution)

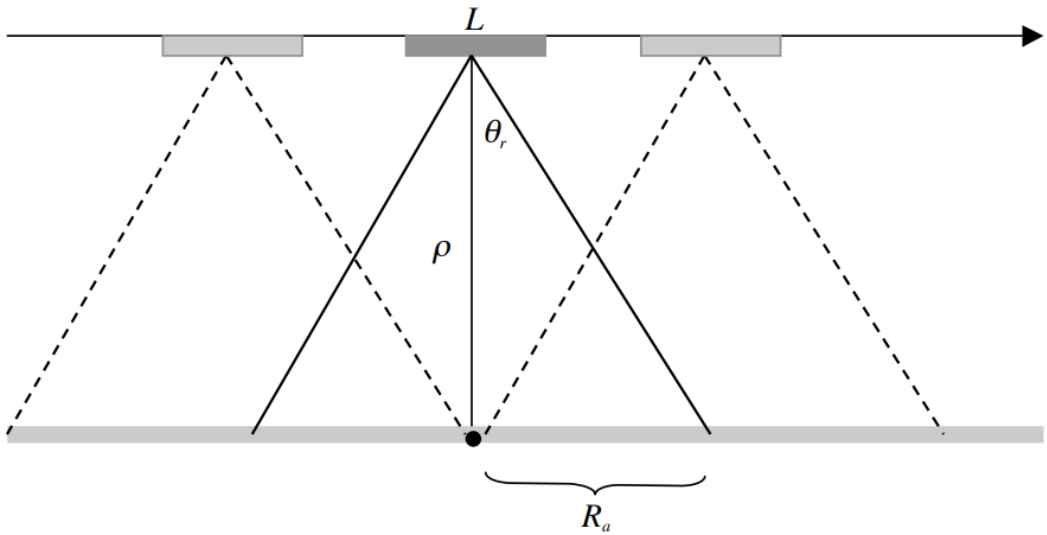

L - length of radar antenna
ρ - nominal slant range $H/\cos\theta$
λ – wavelength of radar

$\sin\theta_r = \lambda / L$ - diffration resolution

$R_a = \rho \sin\theta_r = \frac{\rho\lambda}{L} = \frac{\lambda H}{L\cos\theta}$ - half - length of ground illumination

https://igppweb.ucsd.edu/ fialko/insar/sar_summary.pdf

Spotlight mode

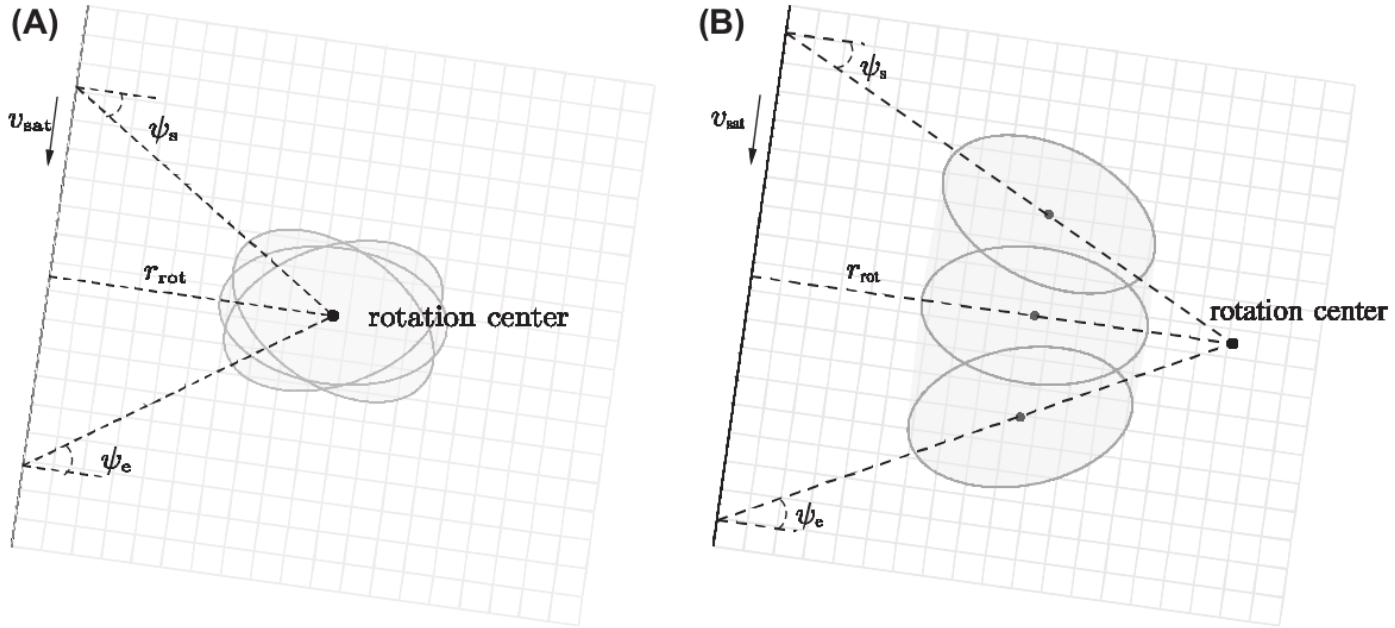

FIGURE 5.80

Steering laws, footprints, and scene size for staring (A) and sliding (B) spotlight acquisition modes. In the sliding configuration, a longer azimuth scene size is traded off for a coarser illumination time and azimuth resolution.

Emery and Camps. 2017

ScanSAR mode

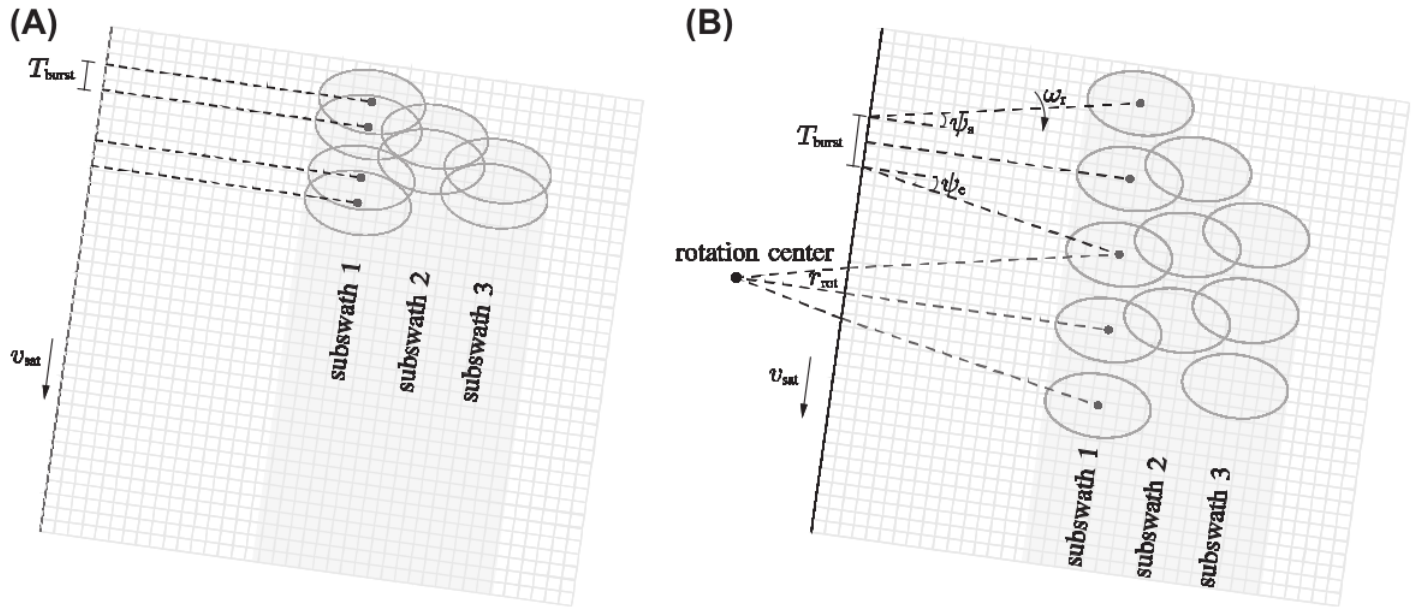

FIGURE 5.82

Steering laws, footprints, and scene size for ScanSAR (A) and terrain observation by progressive scans (TOPS) (B) acquisition modes. The azimuth steering of the TOPS mode allows for the illumination of the scene with more homogeneous radiometric qualities.

Emery and Camps. 2017

ScanSAR mode

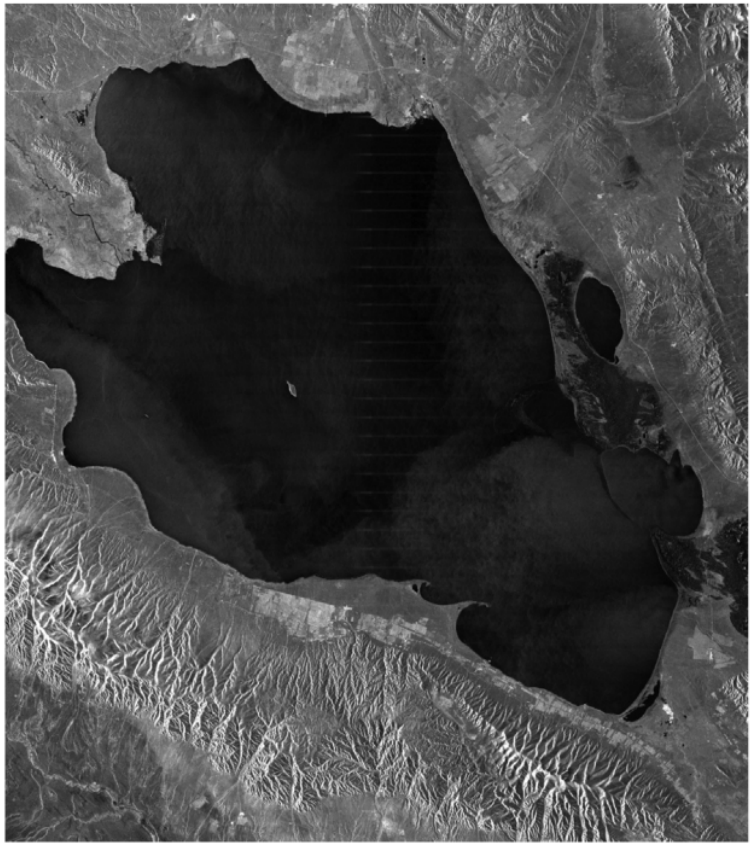

FIGURE 5.83

TerraSAR-X ScanSAR image over Qinghai Lake, China. The periodic horizontal white stripes in the lake are due to a noise scaling effect due to scalloping. The distance between the stripes corresponds to the duration of the radar bursts. Note azimuth ambiguities can also be observed in the lake.

Emery and Camps. 2017

TOPS mode

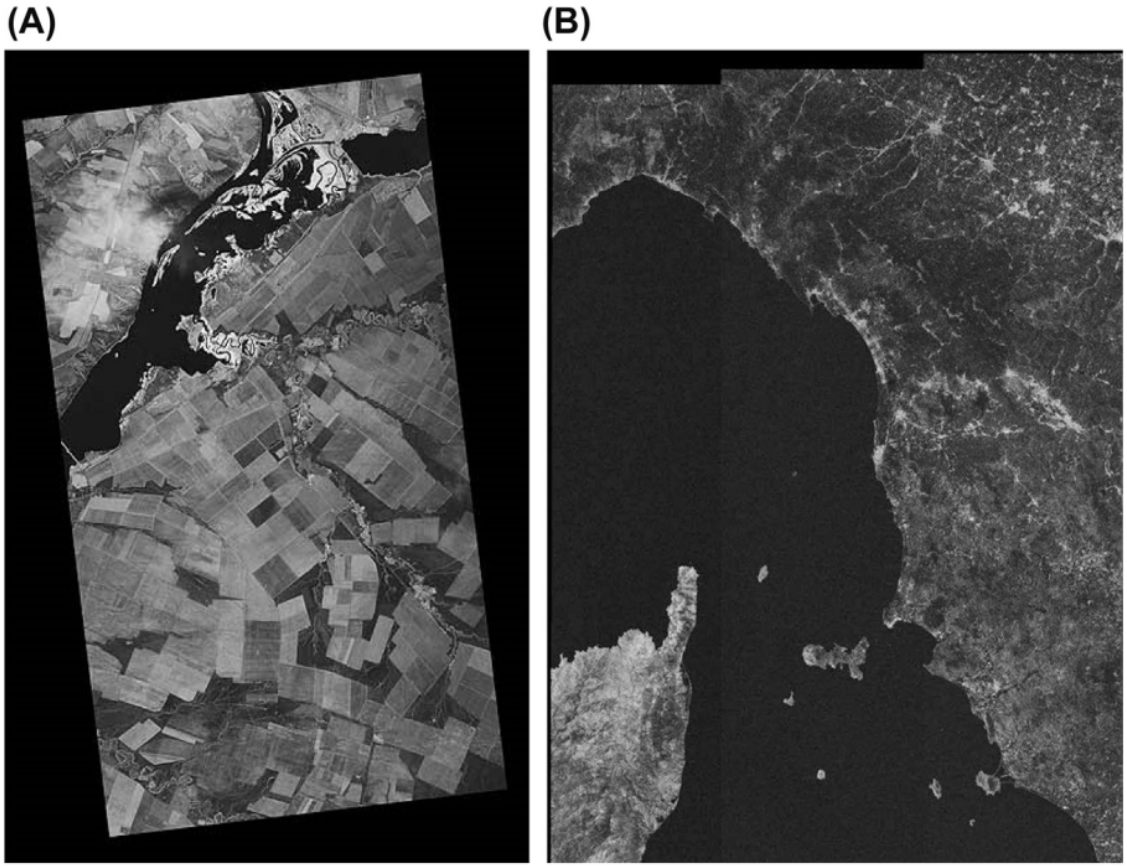

FIGURE 5.84

First synthetic aperture radar images acquired by (A) TerraSAR-X and (B) Sentinel-1 in the terrain observation by progressive scans (TOPS) acquisition mode. TerraSAR-X image acquired over the south Russian Steppes about 500 km northeast of the Black Sea and about 50 km west of Volgograd. Sentinel-1A mosaic of the first S-1A TOPS interferogram (two slices) in IW mode around the Gulf of Genoa, Italy, acquired on August 7 and 19. Range extension, 250 km; azimuth extension, 340 km.

Emery and Camps, 2017

Modes comparison

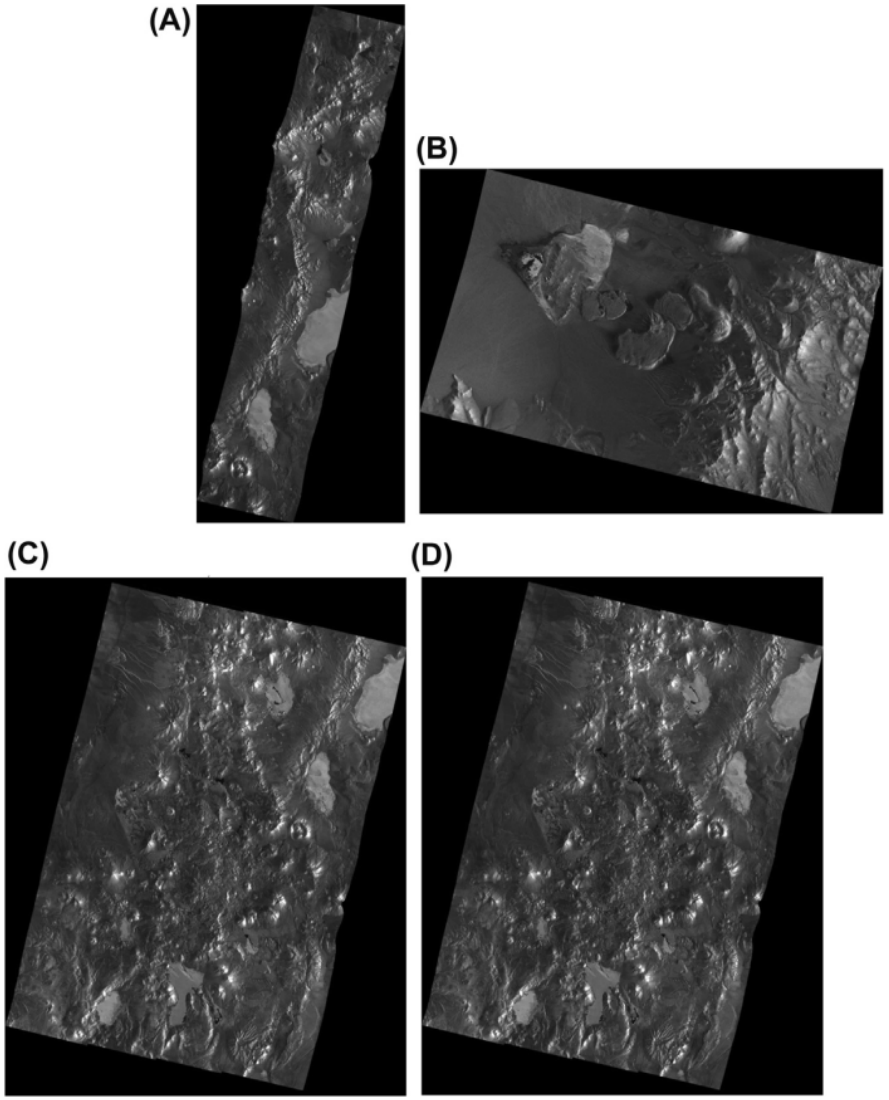

FIGURE 5.81

Geocoded TerraSAR-X images over the Atacama Desert, Chile. Stripmap (A), sliding spotlight (B), ScanSAR (C), and terrain observation by progressive scans (TOPS) modes (D). The vertical direction corresponds to north.

SAR missions

Table 5.4 List of All Spaceborne Synthetic Aperture Radar Missions Over the Past 40 years

Sensor	Frequency Band/ Polarization	Agency
Seasat	L/HH	NASA/JPL
ERS-1/2	C/VV	ESA
JERS-1	L/HH	JAXA
SIR-C/X-SAR	L/quad, C/quad, X/VV	NASA/JPL, DLR, ASI
Radarsat-1	C/HH	CSA
SRTM	C/HH + VV, X/VV	NASA/JPL, DLR, ASI
ENVISAT/ASAR	C/dual	ESA
ALOS/PalSAR	L/quad	JAXA
TerraSAR-X/TanDEM-X	X/quad	DLR/Astrium
Radarsat-2	C/quad	CSA
COSMOSkyMed-1/4	X/dual	ASI/MiD
RISAT-1	C/quad	ISRO
HJ-1C	S/VV	
Kompsat-5	X/dual	KARI
PAZ	X/quad	CDTI
ALOS-2	L/quad	JAXA
Sentinel-1a/1b	C/dual	ESA
Radarsat constellation-1/2/3	C/quad	CSA
SAOCOM-1/2	L/quad	CONAE/ASI

‖Emery and Camps. 2017

SAR Data Acquisitions

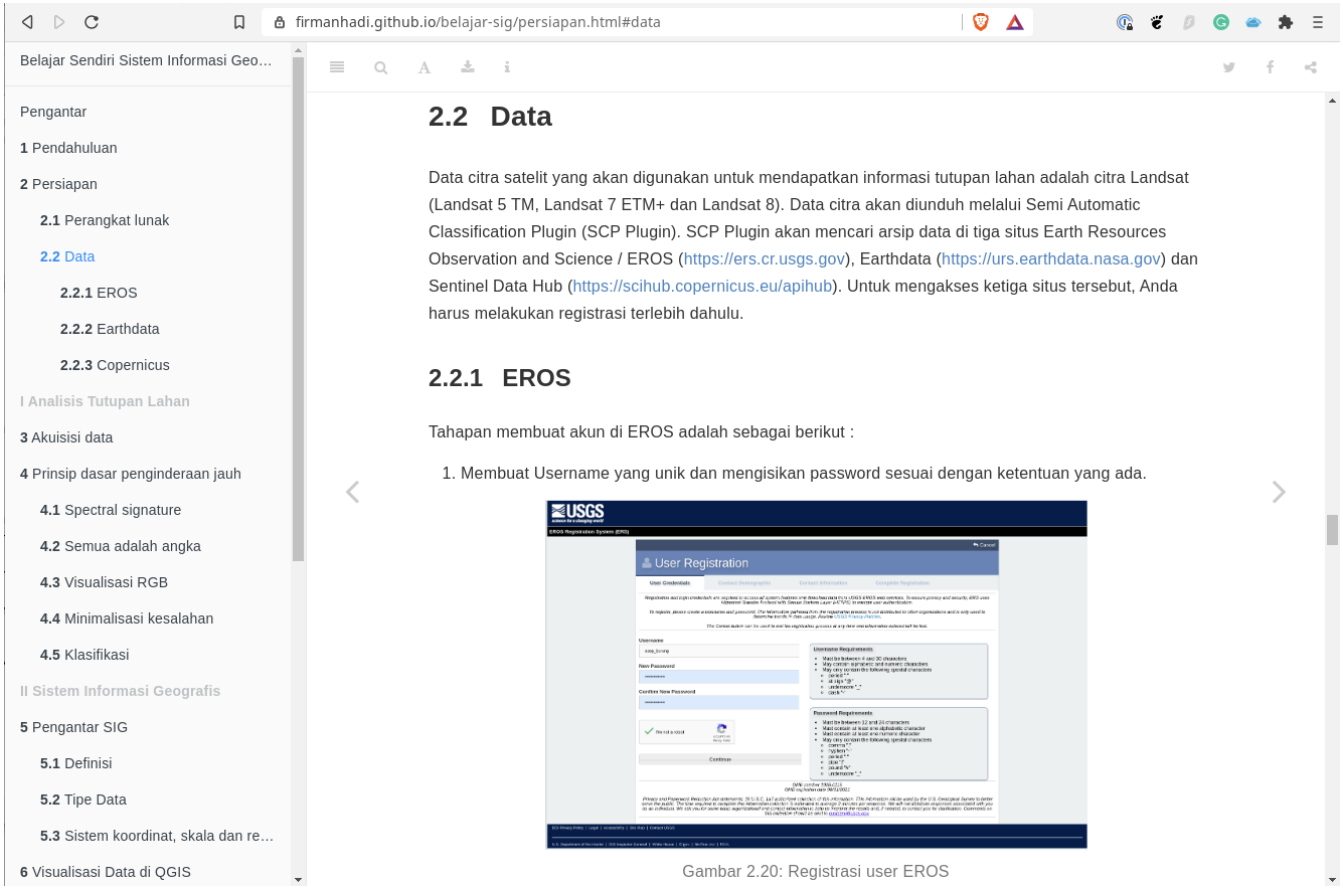

Gambar 2.20: Registrasi user EROS

SAR Wavelength

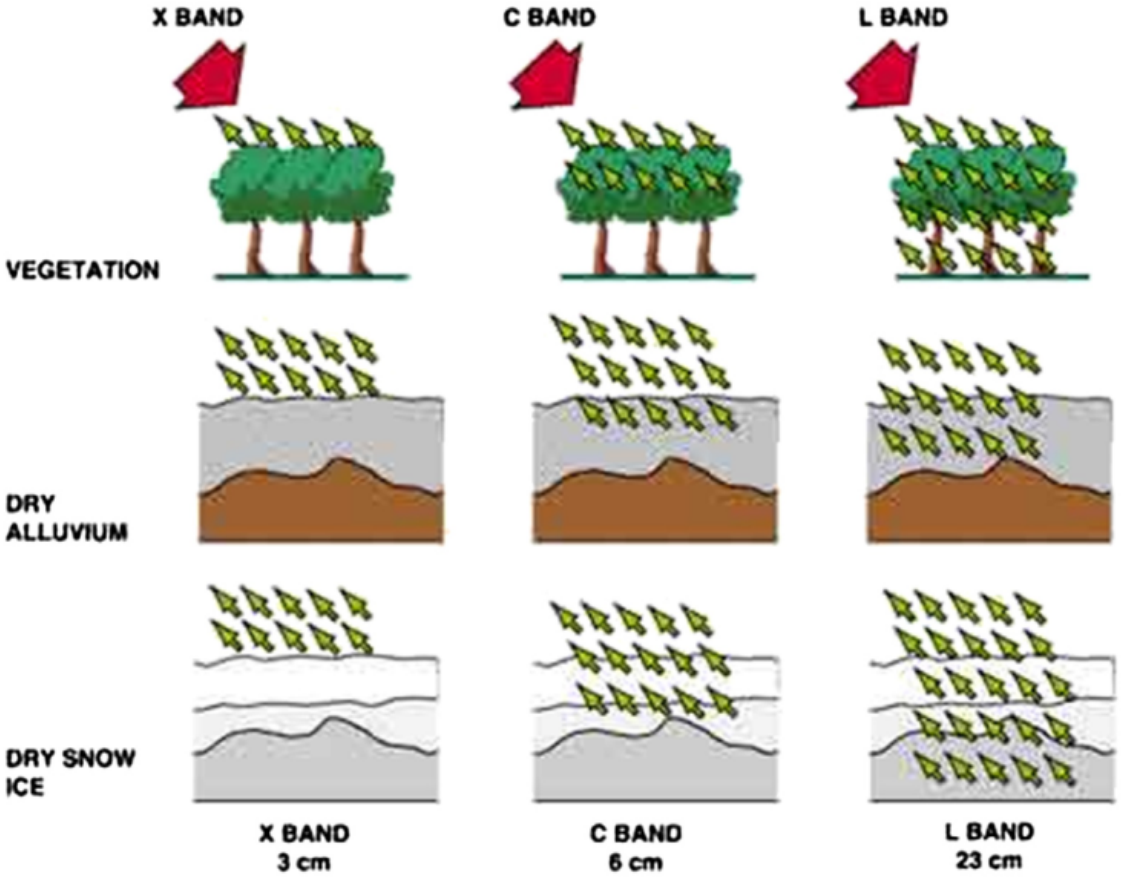

FIGURE 5.34

The effect of increasing radar wavelength on its ability to sense through a tree canopy.

Emery and Camps. 2017

SAR Polarization

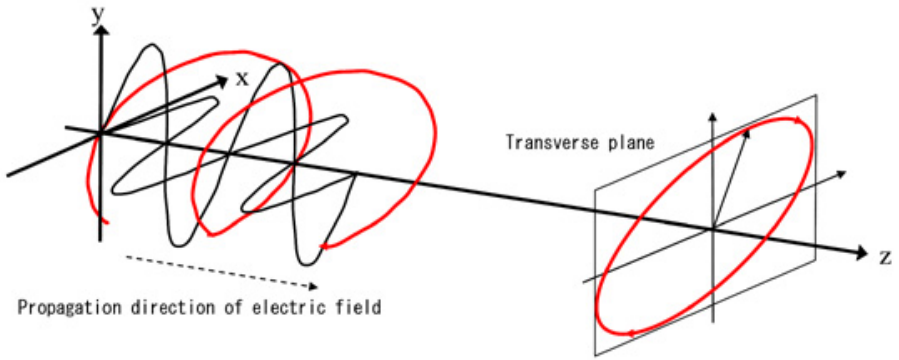

(i) Locus of an elliptically polarized wave

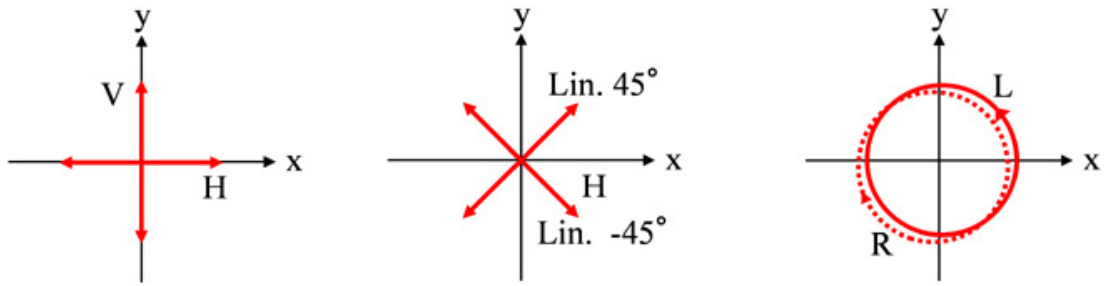

(a) Horizontal polarization, Vertical polarization

(b) Linear 45 degree polarization, Linear -45 degree polarization,

(c) Left circular polarization, Right circular polarization

(ii) Typical polarizations

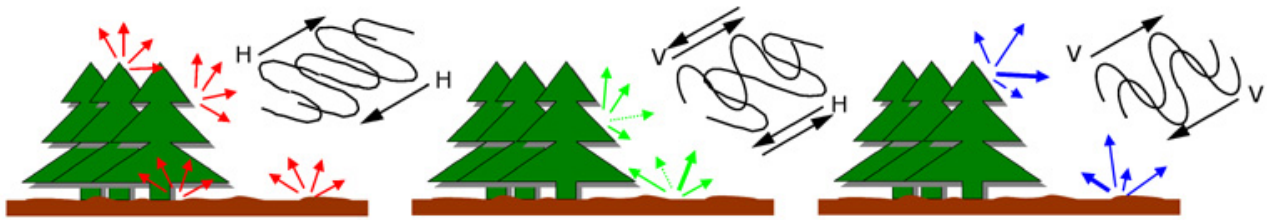

(a) HH

(b) HV and VH

(c) VV

(iii) Scattering with respect to polarization

https://www.eorc.jaxa.jp/ALOS/en/img_up/pal_polarization.htm

SAR Polarization

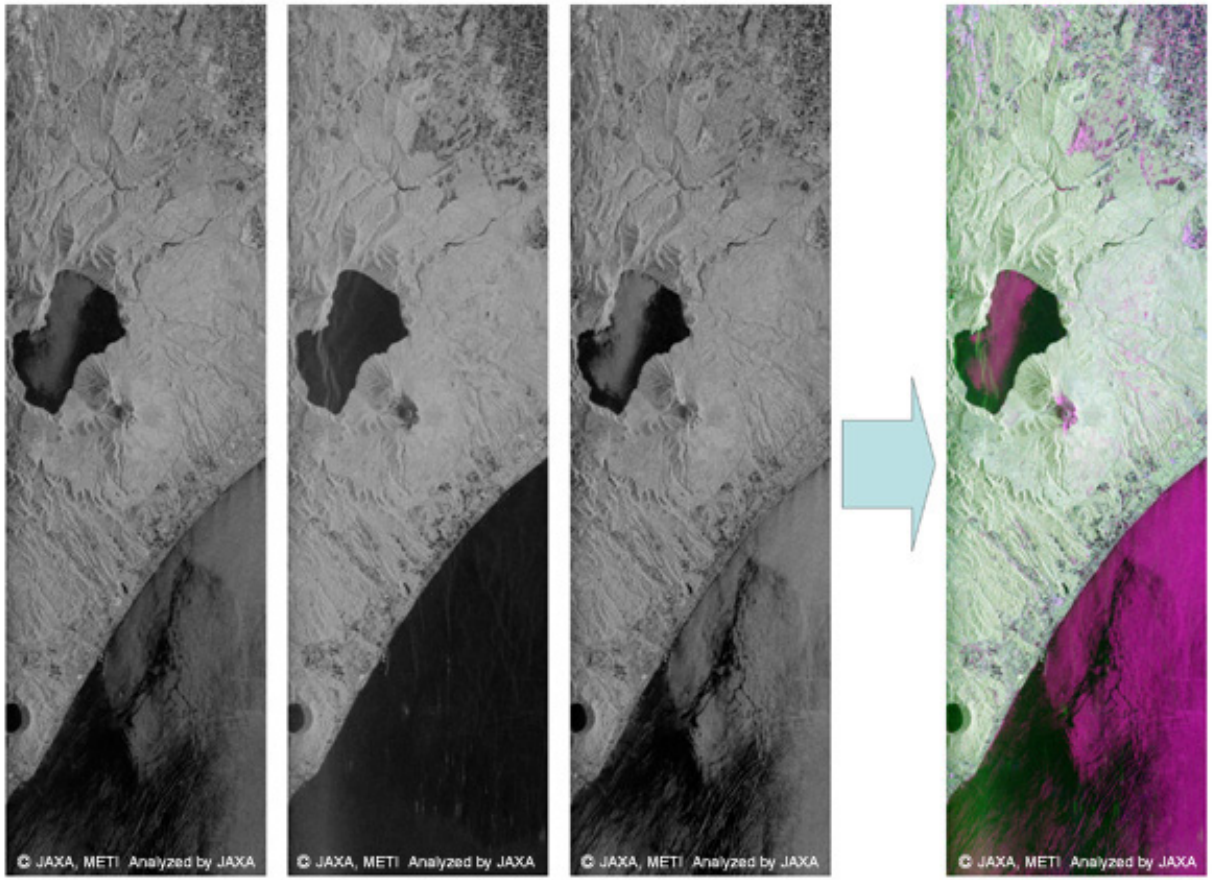

https://www.eorc.jaxa.jp/ALOS/en/img_up/pal_polarization.htm

Backscatter value interpretation table

Table 5.2 Exemplary Values of Radar Backscatter for Typical Artificial Surface, Surface Scatterers, and Volume Scatterers

Radar Brightness	σ_0 (dB)	Target Examples
Very high backscattering	>0	Artificial objects and urban areas, ascending terrain slopes, very rough surfaces, very steep incident angles
High backscattering	−10 to 0	Rough surfaces (e.g., dense vegetation, forests, open water with wind), volumes (e.g., multiyear ice, marginal sea ice)
Moderate backscattering	−20 to −10	Moderately rough surfaces (e.g., vegetation, crops, first-year ice, open water with little wind)
Low backscattering	>−20	Smooth surfaces (e.g., calm water, roads, very dry soil, deserts)

Note the values are just representative and will change as a function of several parameters of the acquisition, such as wavelength and/or polarization.

Multi-frequency composites

- Combination of multiple SAR frequency bands.
- Synergy of different backscatter mechanisms.

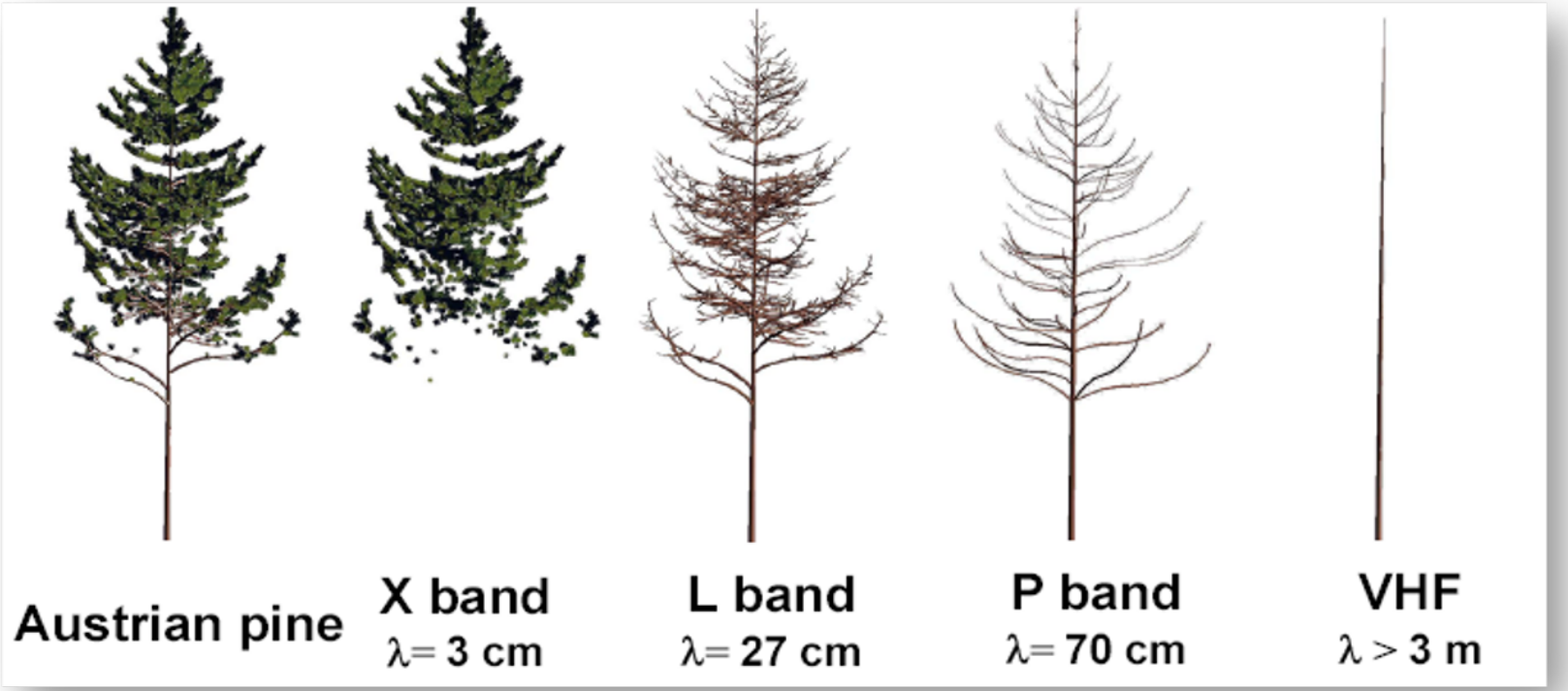

Multi-frequency composites

- Combination of multiple SAR frequency bands.
- Synergy of different backscatter mechanisms.

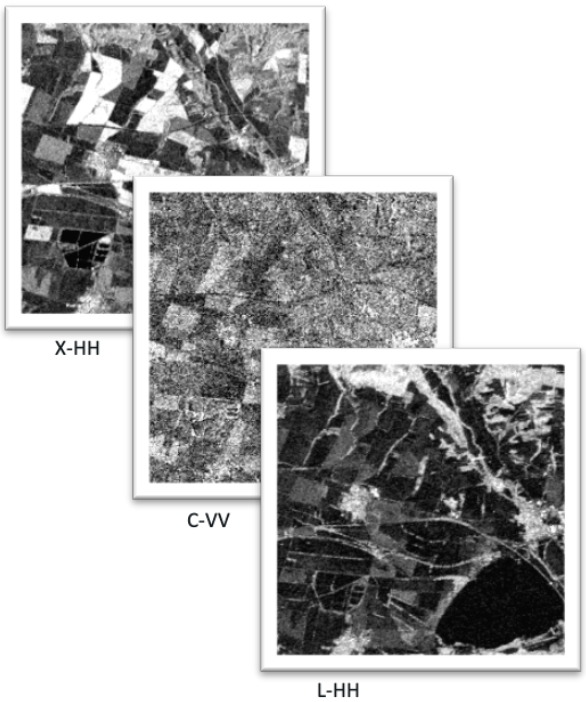

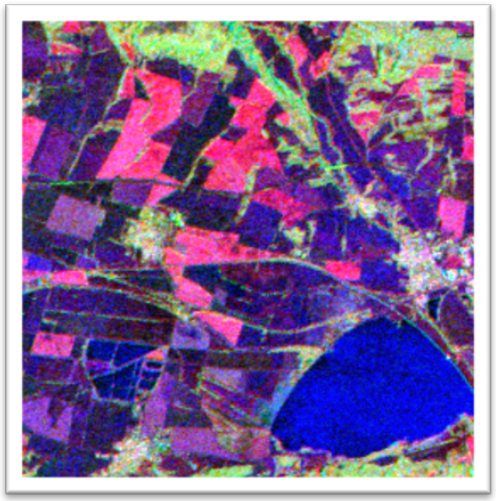
R: X-HH | G: L-HH | B: C-VV

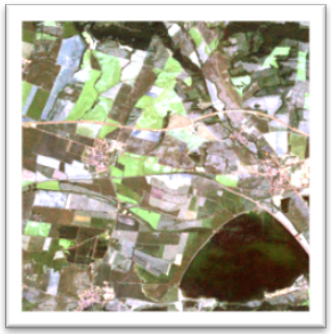
Landsat R: B 1 G: B 2 B: B 3


R: X-HH | G: L-HH | B: X-HV

Multi-temporal composites

- Combination of multiple dates of SAR acquisitions.
- Colors indicating changes.

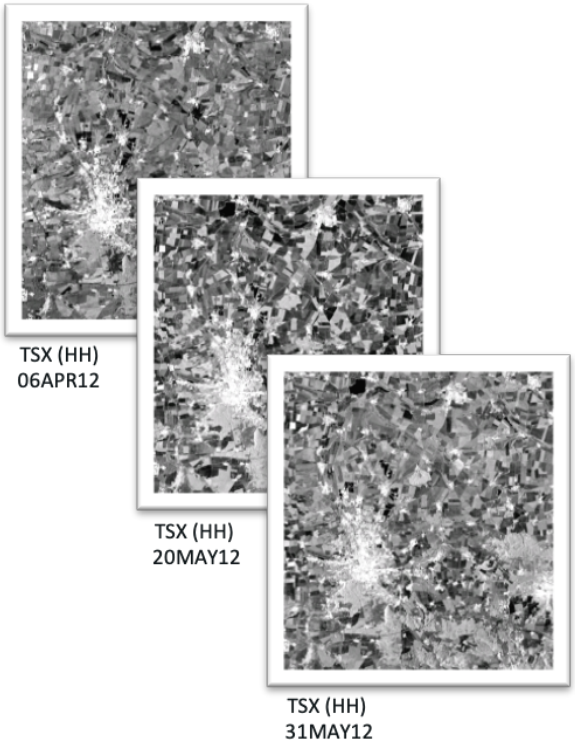

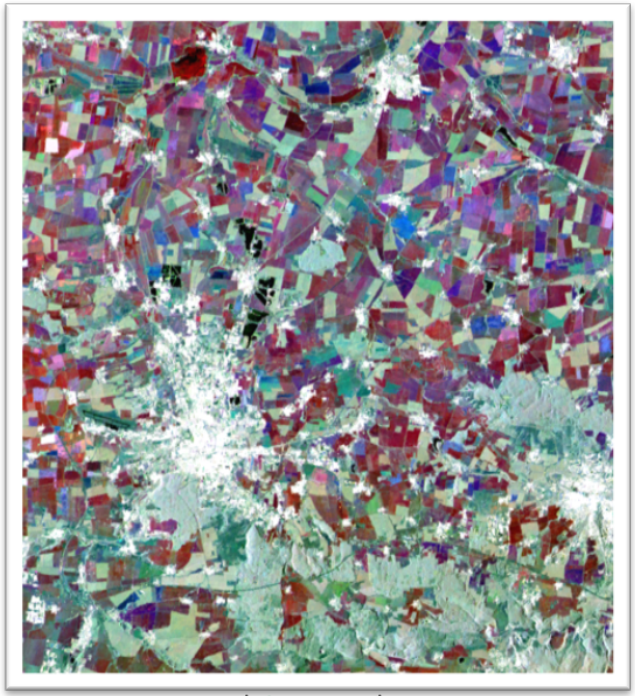

R: 06APR | G: 20MAY | B: 31MAY © DLR

© Google Earth

Multi-polarization Products

- Combination of multiple polarizations.
- Colors indicating different backscatter mechanism.

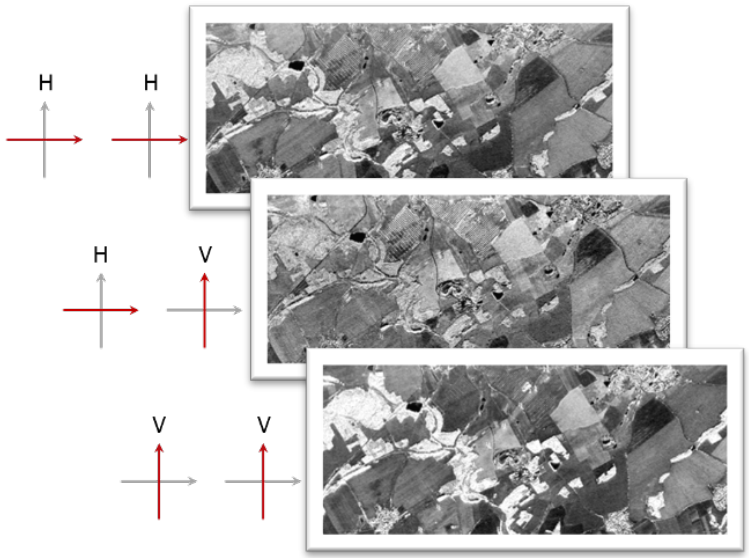

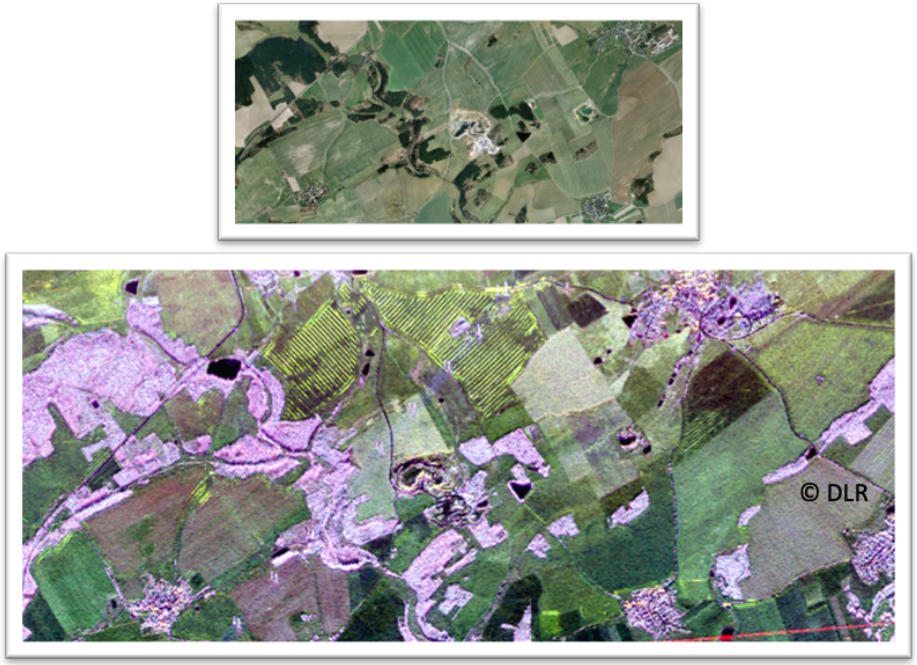

R: HH | G: VV | B: HV

Multi-product Composites

- Combination of multiple products derived from SAR data.
- Increase class separability

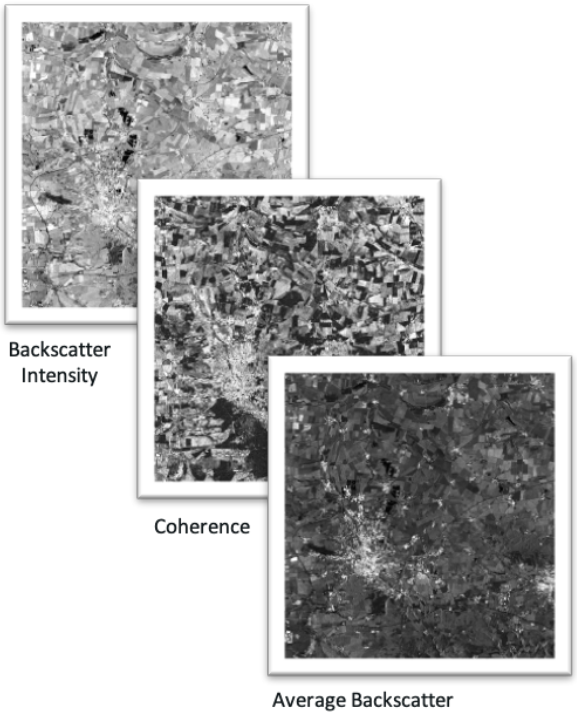

R: Intensity| G: Coherence| B: Ø Backscatter © DLR

© Google Earth

SAR Imagery and Speckle

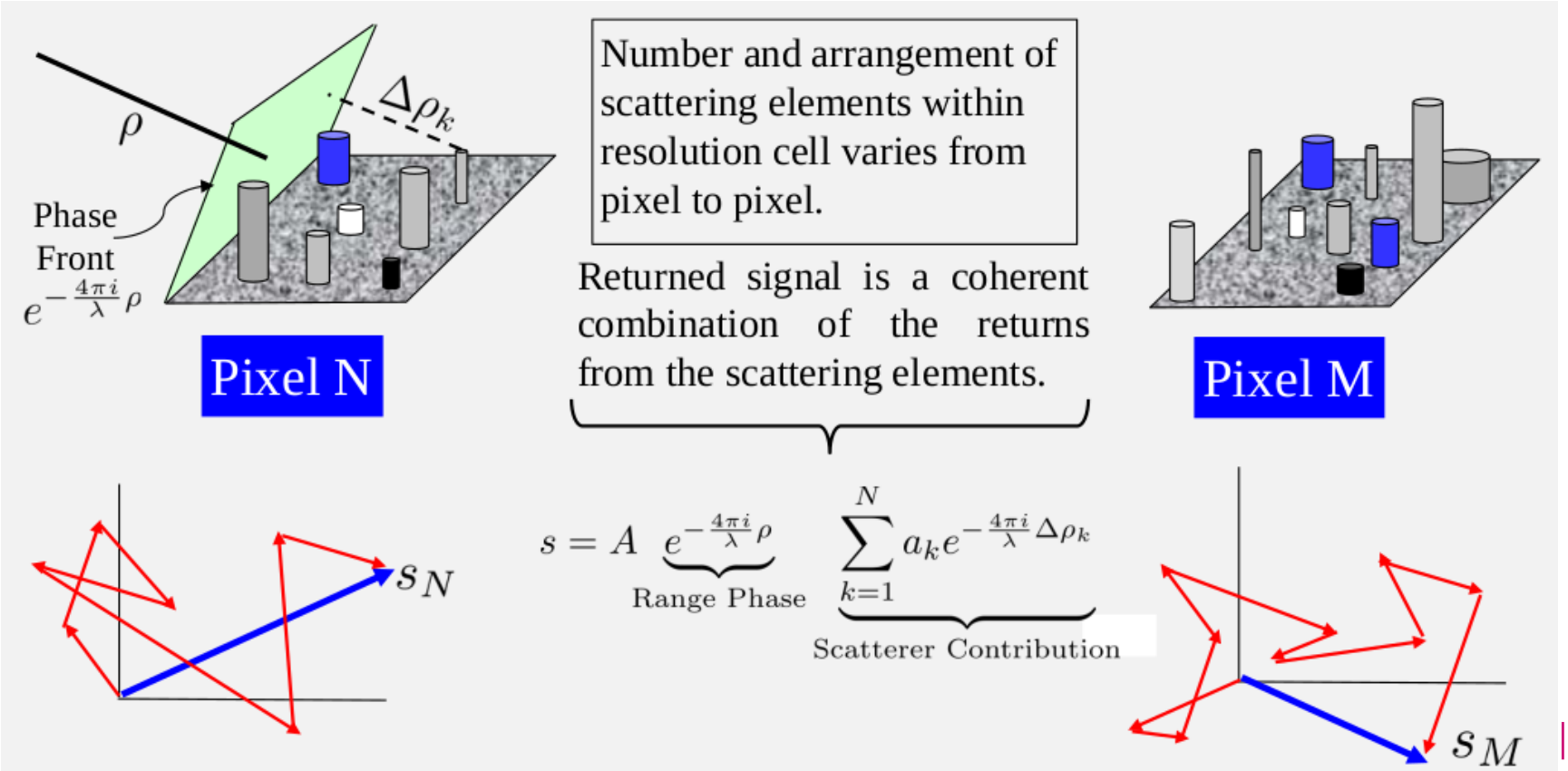

Eric Fielding. 2017

SAR Phase

The phase of the radar signal is the number of *cycles of oscillation* that the wave executes between the radar and the surface and back again.

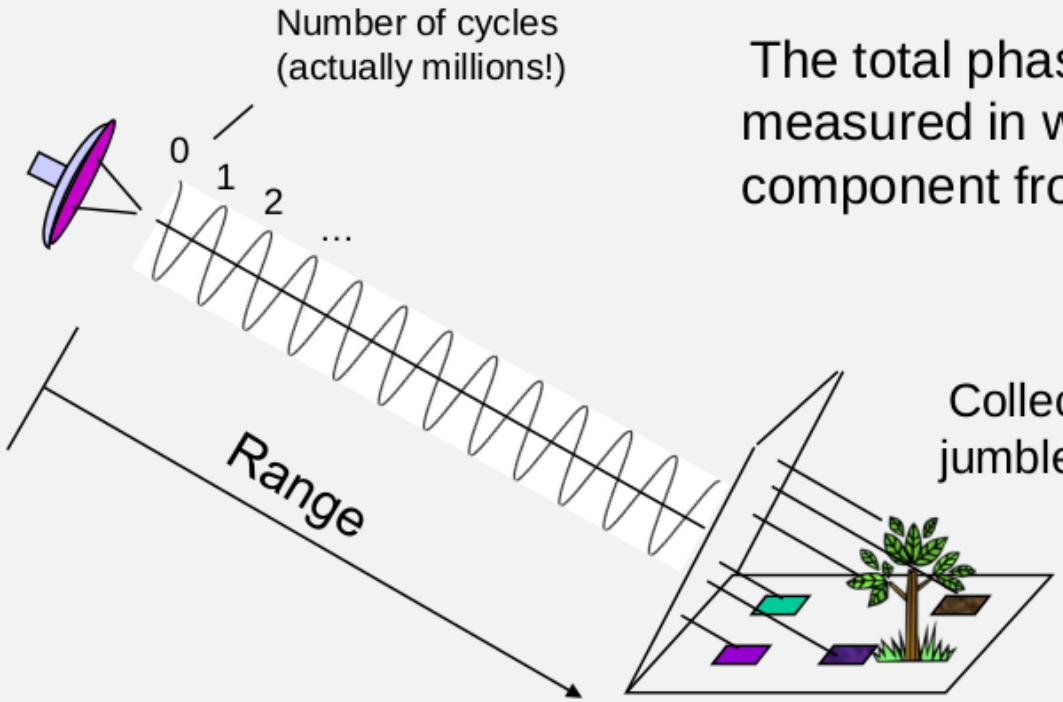

The total phase is two-way range measured in wave cycles + random component from the surface

Collection of random path lengths jumbles the phase of the echo

Only *interferometry* can sort it out!

Eric Fielding. 2017

InSAR

- Radars measure the amplitude and delay of the backscattered echoes
- The delay information is stored in the phase of the received signal with subwavelength accuracy
- The ranging accuracy of the phase measurement is low due to a mixing with many other components of the measurement (speckle noise).
- We need to access the differential phase of the two SAR images acquired from different times or from different positions. [a]

[a] Emery and Camps. 2017

Types of SAR Interferometry

Cross-Track Interferometer

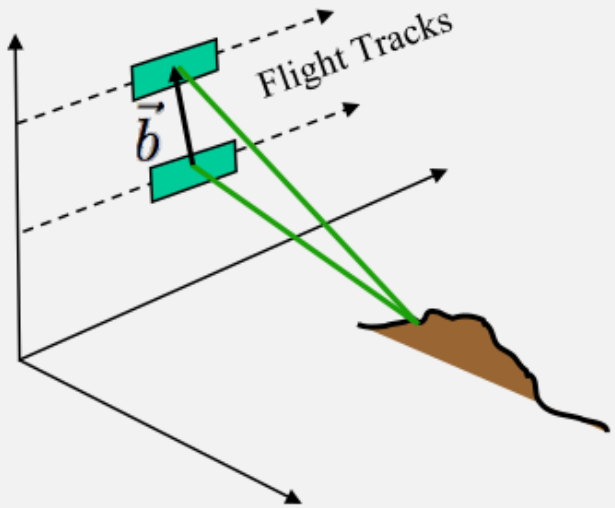

- Dual antenna single pass interferometers
- Single antenna repeat pass interferometers
  ==> Topography and Deformation

Along-Track Interferometer

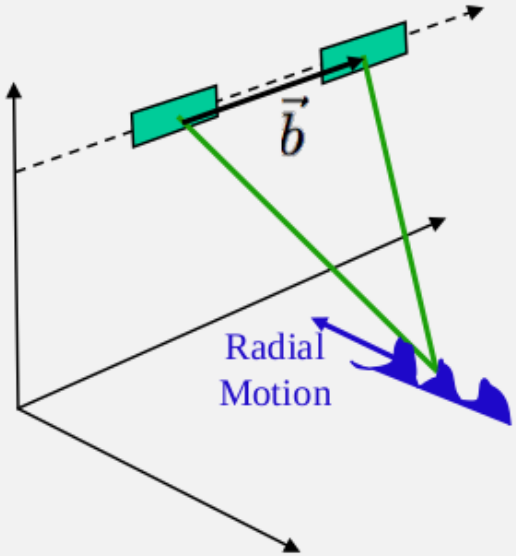

- Dual antenna single pass interferometer
- Along-track separation
  ==> Radial velocity

Slid

Eric Fielding. 2017

Interferometry for Topography

Measured phase difference:

$$\otimes\phi = -\frac{2\pi}{\lambda}\delta\rho$$

Triangulation:

$$\sin(\theta - \alpha) = \frac{(\rho + \delta\rho)^2 - \rho^2 - B^2}{2\rho B}$$

$$z = h - \rho\cos\theta$$

Critical Interferometer Knowledge:
- Baseline, (B,α) to mm's
- System phase differences, to deg's

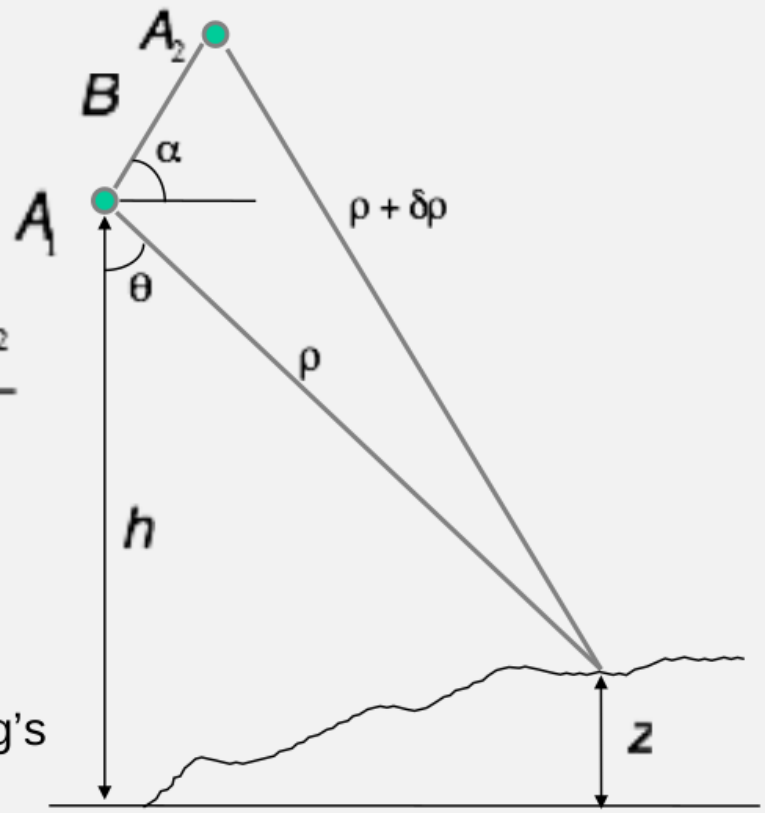

Eric Fielding. 2017

Data Collection Options

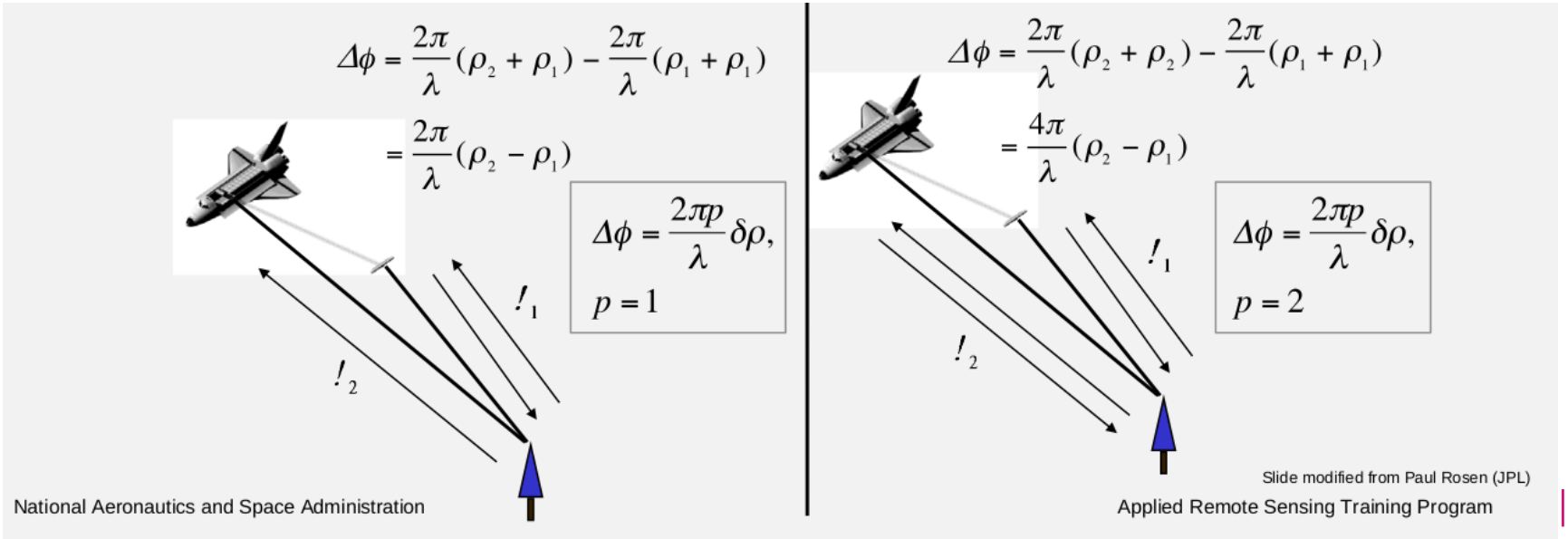

Eric Fielding. 2017

Data Collection Options

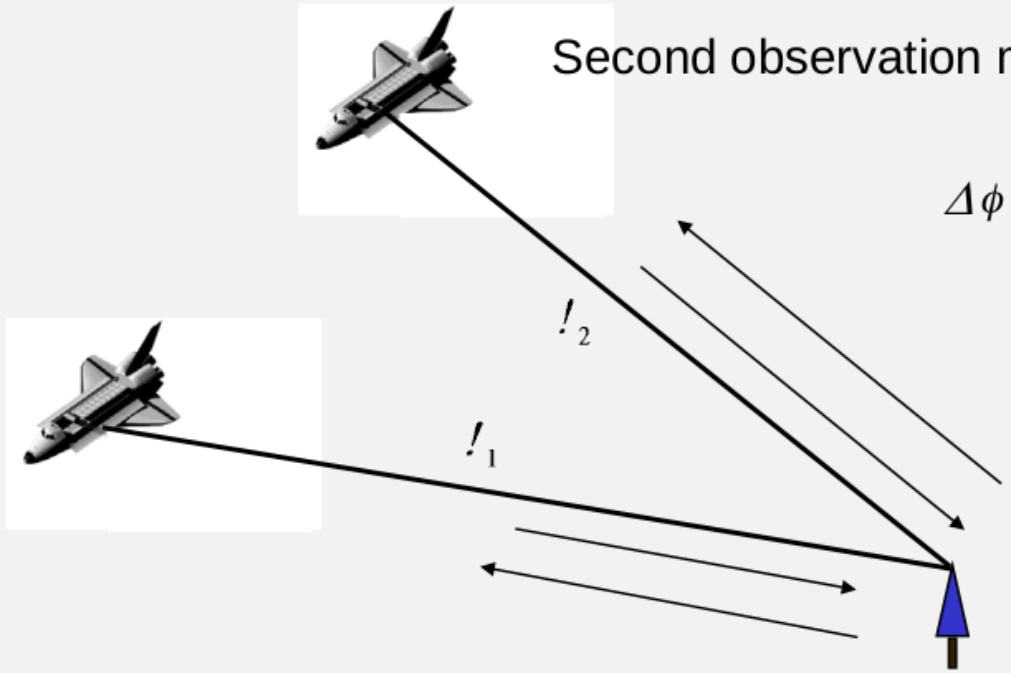

Eric Fielding. 2017

Differential Interferometry

When two observations are made from the same location in space but at different times, the interferometric phase is proportional to any change in the range of a surface feature directly.

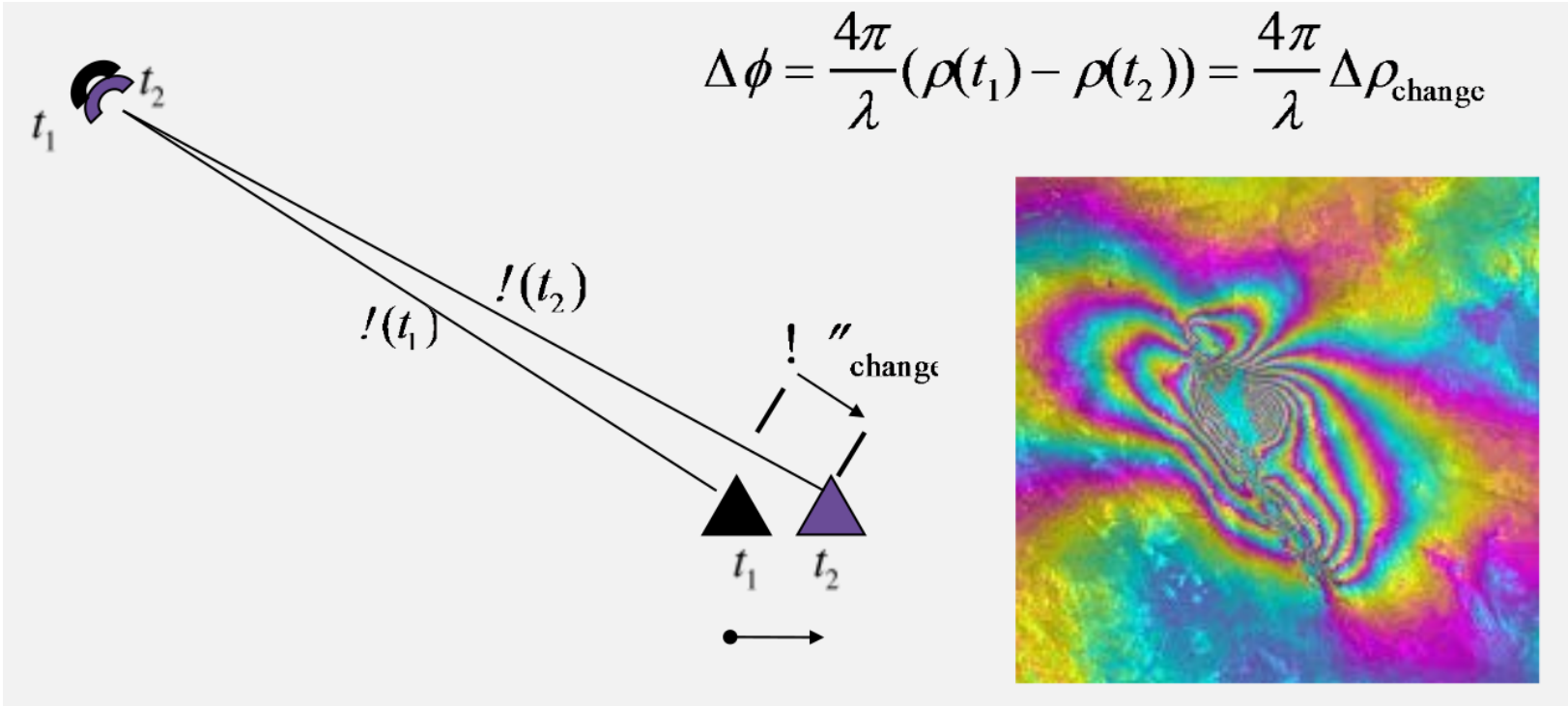

Eric Fielding. 2017

Differential Interferometry and Topography

Generally two observations are made from different locations in space and at different times, so the interferometric phase is proportional to topography and topographic change.

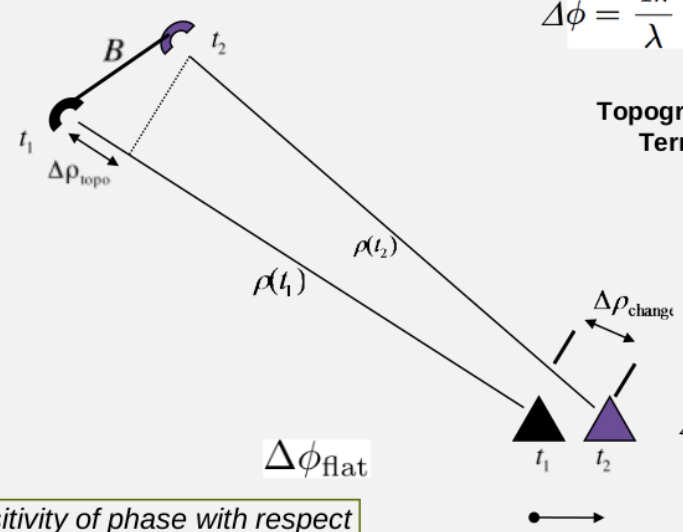

$$\Delta\phi = \frac{4\pi}{\lambda}\left(-\langle\hat{\ell},\vec{b}\rangle + \langle\hat{\ell},\vec{D}\rangle\right)$$

Topography Term

Change Term

$$\Delta\phi = \frac{4\pi}{\lambda}(\Delta\rho_{change} - \Delta\rho_{topo})$$

$$\Delta\phi = \frac{4\pi}{\lambda}(\Delta\rho_{change} - b\sin(\theta-\alpha))$$

$$\Delta\phi_{flat} = \frac{4\pi}{\lambda}\left(\Delta\rho_{change} - \frac{b_\perp h_T}{\rho\sin\theta}\right)$$

Note: Sensitivity of phase with respect to change is much greater than with respect to topographic relief

If topography is known, then second term can be eliminated to reveal surface change

Slide modified from Paul Rosen (JPL)

National Aeronautics and Space Administration

Applied Remote Sensing Training Program

Eric Fielding. 2017

Correlation Theory

- InSAR signals decorrelate due to:
  - Thermal and Processor Noise.
  - Differential Geometric and Volumetric Scattering.
  - Rotation of Viewing Geometry
  - Random Motions Over Time
- Decorrelation relates to the local phase standard deviation of the interferogram phase
  - Affects height and displacement accuracy.
  - Affects ability to unwrap phase.

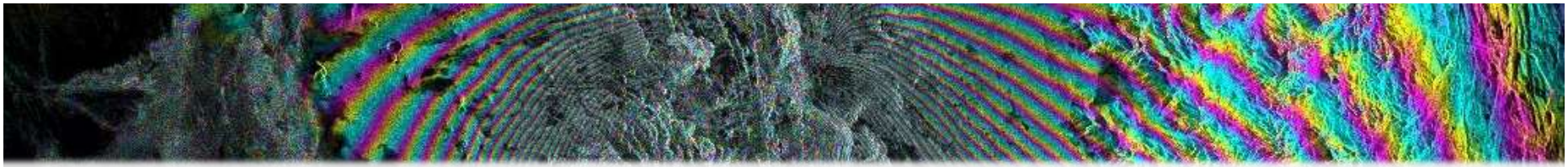

GEOS 657 – MICROWAVE REMOTE SENSING

GRADUATE-LEVEL COURSE AT THE UNIVERSITY OF ALASKA FAIRBANKS

Lecturer:
Franz J Meyer, Geophysical Institute, University of Alaska Fairbanks, Fairbanks; fjmeyer@alaska.edu

Lecture 15: InSAR Time Series Analysis Basics & PS-InSAR: Time Series Analysis using Point Targets

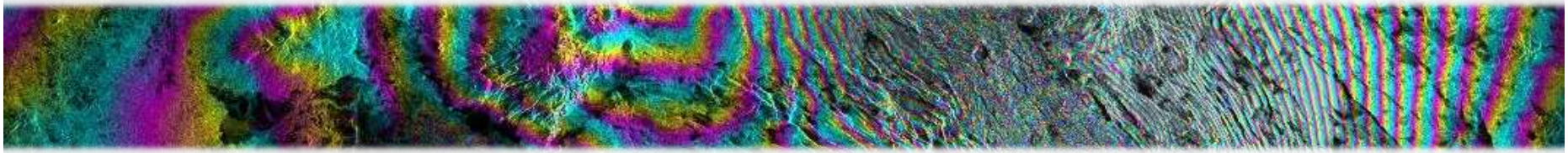

ASF UAF UNIVERSITY OF ALASKA FAIRBANKS UAF COLLEGE OF NATURAL SCIENCE & MATHEMATICS University of Alaska Fairbanks

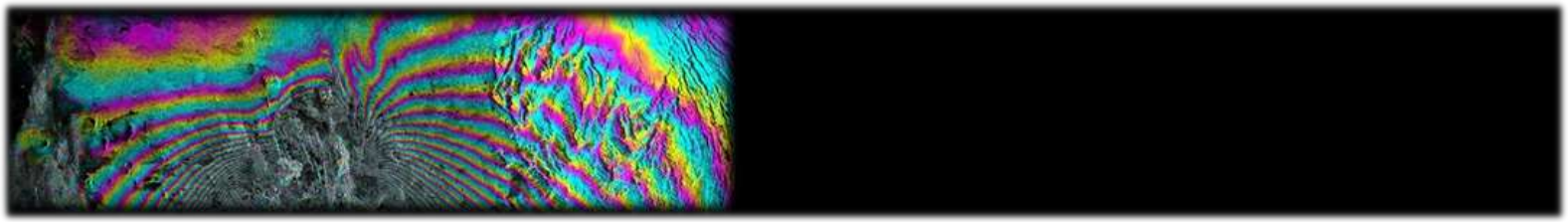

THE BASIC CONCEPTS OF INSAR TIME SERIES ANALYSIS

Study Deformation Across Time Scales

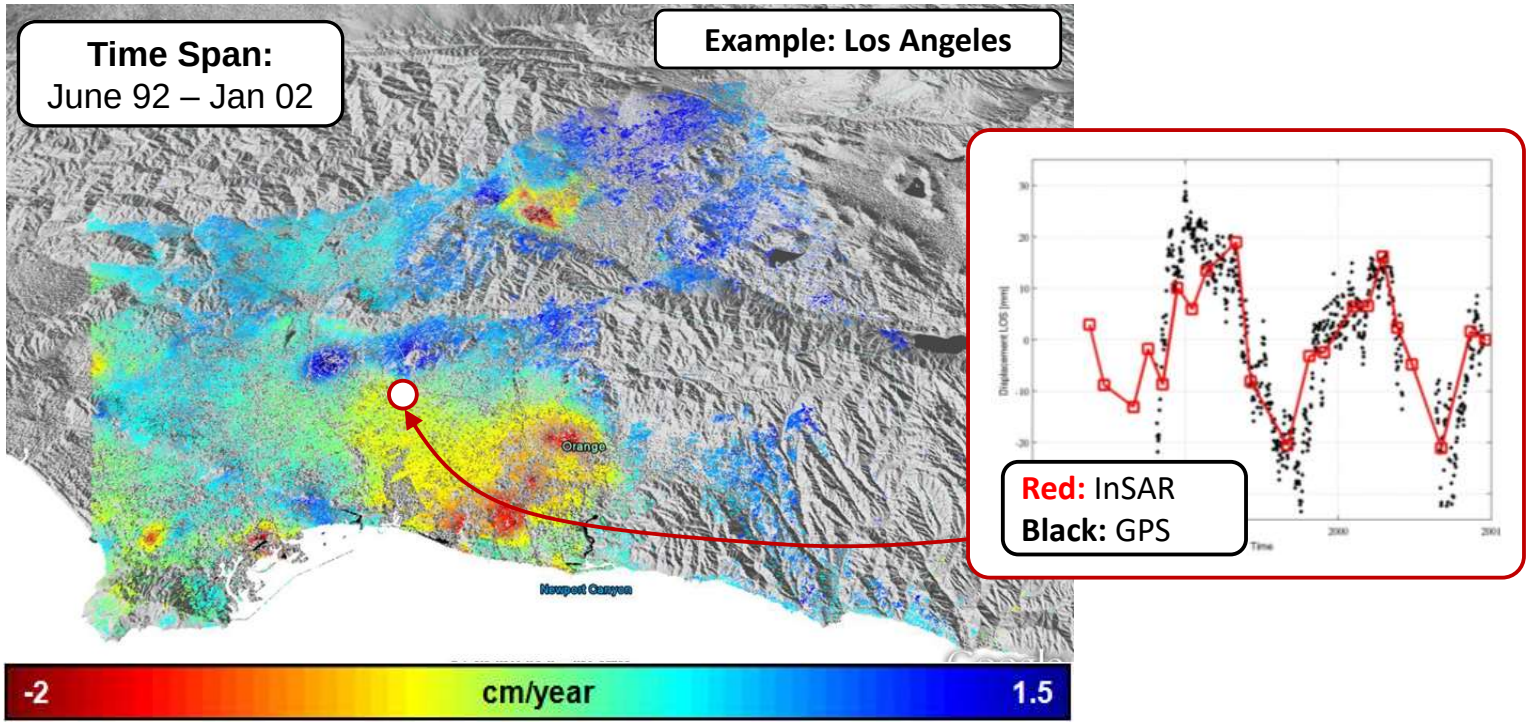

Why Use Time Series Analysis?

Two compelling reasons

1. **Study temporally extended phenomena**
   - Volcanic inflation
   - Landslides
   - Inter-seismic slip
   - Groundwater-related subsidence

2. **Improved estimation of deformation signal** by exploiting time series to remove
   - Atmosphere
   - Topography (DEM errors)
   - and other noise sources

Treatment of Error Sources and Limitations Through InSAR Time Series Analysis

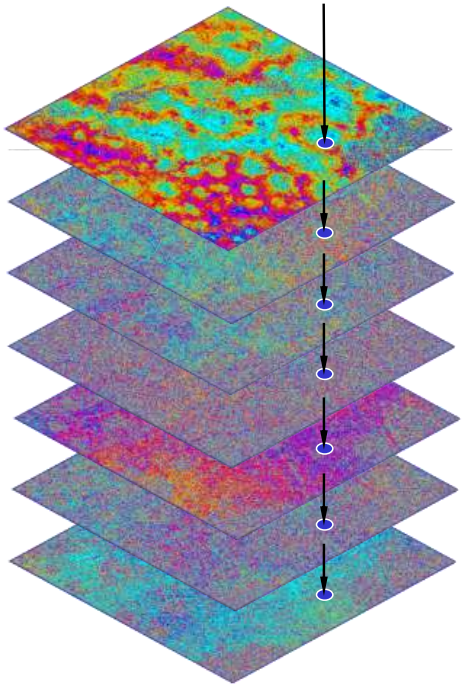

Concepts included in Time Series InSAR

1. **Use many ($N \gg 2$) interferograms (ifgrms) spanning long time span**
   - → $N \gg 2$ observations and only two unknowns (topography h; deformation v)
   - → Suppression of noise (atmosphere; orbit errors; noise) *[response to Limitation 4 in Lecture 13]*
   - → Improve precision of deformation estimates *[response to Limitation 2 in Lecture 13]*
2. **Find patches that are coherent in all ifgrms**
   - → Sophisticated algorithm required to identify pixels that are coherent over long time frames *[response to Limitation 2 in Lecture 13]*
3. **Analyze phase of coherent pixels over time & across space**

Separate Phase Components With Time Series Analysis

Main interest | Nuisance

$$\phi = \phi_{defo} + \phi_{topo} + \phi_{atmo} + \phi_{noise}$$

smooth in time (usually)

proportional to spatial baseline

random in time – smooth in space
orbit error similar

random in time and space

Separate components based on their temporal, spatial and baseline characteristics

Rationale of InSAR Time Series Analysis

Input

Time series of SAR images

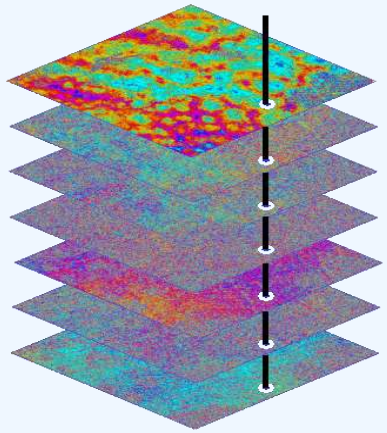

Processing

Key steps

- Interferogram formation
- Unwrapping
- Isolate deformation

Output

Deformation

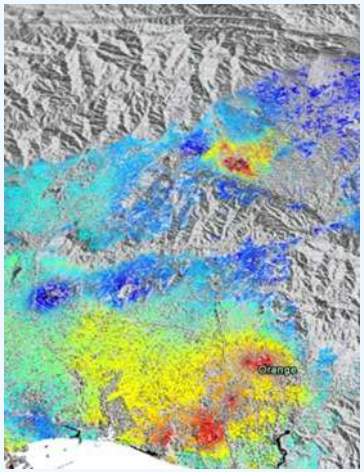

Multiple Approaches to Time Series Analysis

A key distinction is the type of target that is analyzed

Point-like scatterers

One scatter dominates the signal from a SAR resolution cell

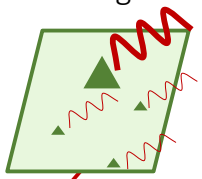

Point Target InSAR

+ high quality for selected points
+ retains full resolution
– only few coherent points
– does not work well for short stacks

Persistent Scatterer Interferometry (PSI)

Distributed targets

Many scatterers contribute to signal
Extended targets

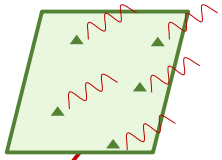

Distributed Target InSAR

+ higher point density
+ flexible, easily applicable to large areas
– usually higher noise level
– averaging reduces resolution

Small Baseline Subset (SBAS)

Two Philosophies on How to Form Interferograms from Multiple Images

- **PSI uses single reference image**

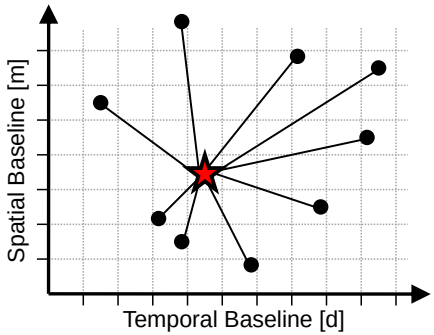

  - Ifgrms formed relative to one unique reference image

- **SBAS uses multiple reference images**

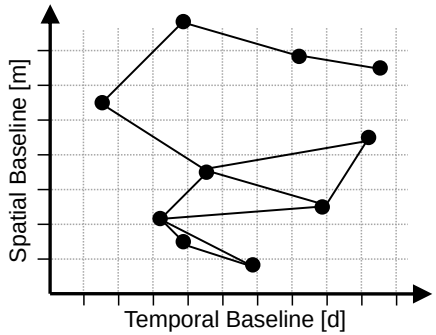

  - Igrms formed between all image pairs that fulfill user defined baseline requirements (min – max allowed baselines)

Used in Persistent Scatterer InSAR (PSI) [Lecture 15]

+ solving of equation system “simple”
+ very low noise level of selected points
– **Only few coherent points**
– Long time lag to reach critical number of images in stack

Used in Short Baseline Subset InSAR [Lecture 16]

+ **higher density of coherent point**
+ quicker stack buildup
– equation system underdetermined
– higher phase noise → lower absolute accuracy or filtering required

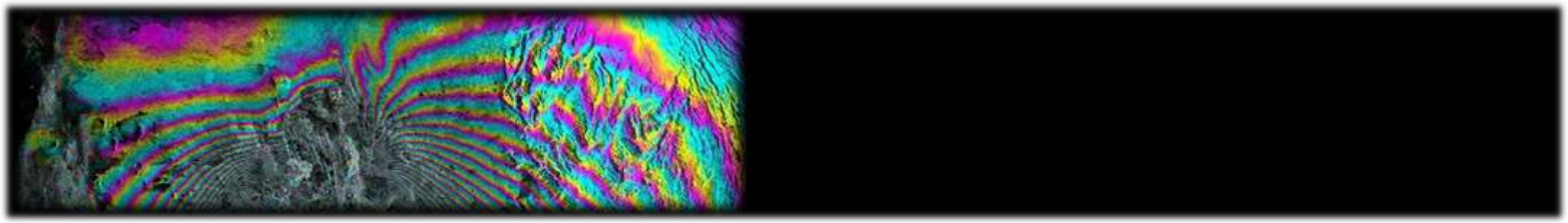

POINT TARGET-BASED INSAR TIME SERIES ANALYSIS

Persistent Scatterer Interferometry (PSI)

- Developed by A. Ferretti, F. Rocca, and, C. Prati, Politecnica di Milano, Italy
- **Idea:** Every Interferogram ***always*** contains ***a few coherent pixels*** whose phase can be exploited for deformation analysis

incoherent average of 70 ERS SAR images

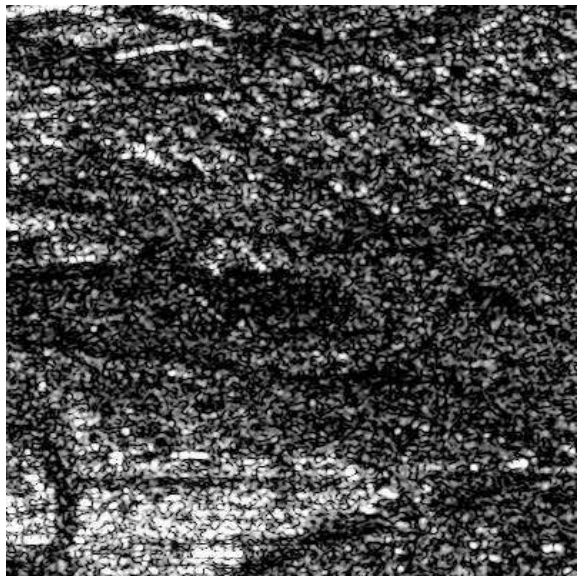

individual images (9 years)

Persistent Scatterer Interferometry (PSI)

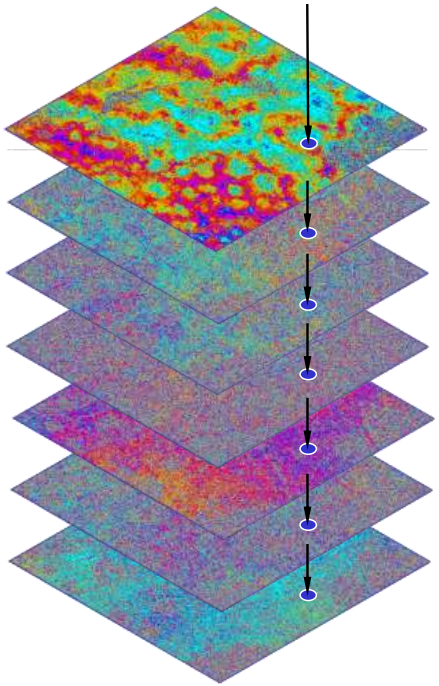

- Many interferograms all referenced to ***single reference image***
- Identification of isolated stable points
- Analyze ***phase difference*** between pixels both in time and space
- Phase difference analysis is a powerful means for noise suppression
- Detectable velocities from cm/day to mm/year

General Scatterer Types in SAR Images

- **Distributed targets:**
  - Many scatterers contributing to the signal from a resolution cell with about equal importance
  - **Examples include**: vegetated surfaces; bare soil; general natural terrain

- **Point-like scatterers:**
  - One scatter dominates the signal from a SAR resolution cell
  - **Examples include**: Corner reflectors; man-made features such as buildings

Characteristics of Distributed and Point Targets

Goal: Understand Nature of Persistent Scatterers

Distributed Targets

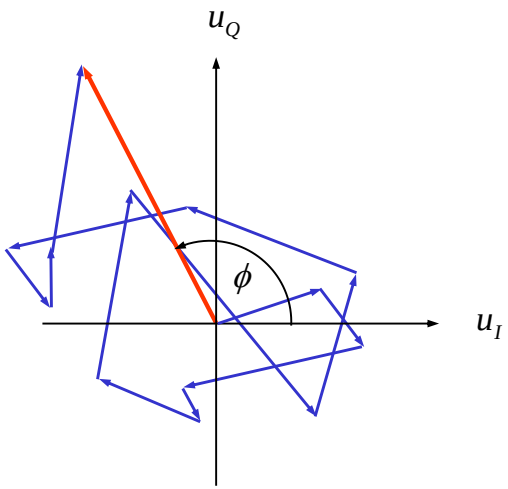

Point Targets

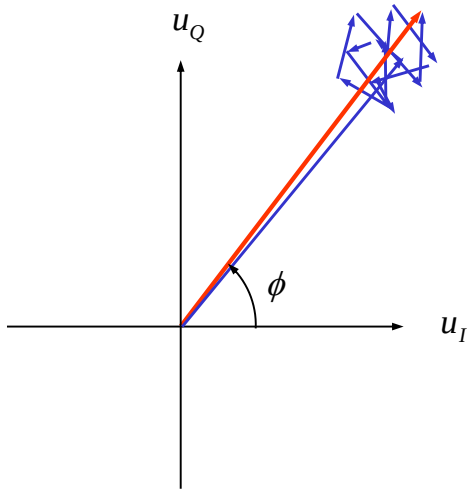

Point Targets are likely to show consistent phase and amplitude over time → **most persistent scatterers are point-like targets (rocks, manmade structures, …)**

Characteristics of Distributed and Point Targets

Distributed Targets Decorrelate Quickly

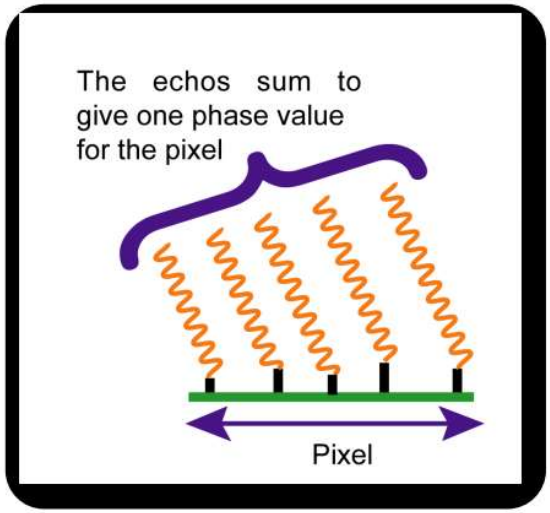

Distributed scatterer pixel

If scatterers move with respect to each other, the phase sum changes

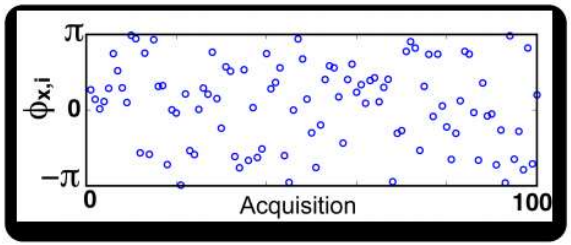

(similar effect if incidence angle changes)

Source: A. Hooper, University of Leeds; UNAVCO InSAR Training

Characteristics of Distributed and Point Targets

Point-Like Targets keep Coherent For Long Times

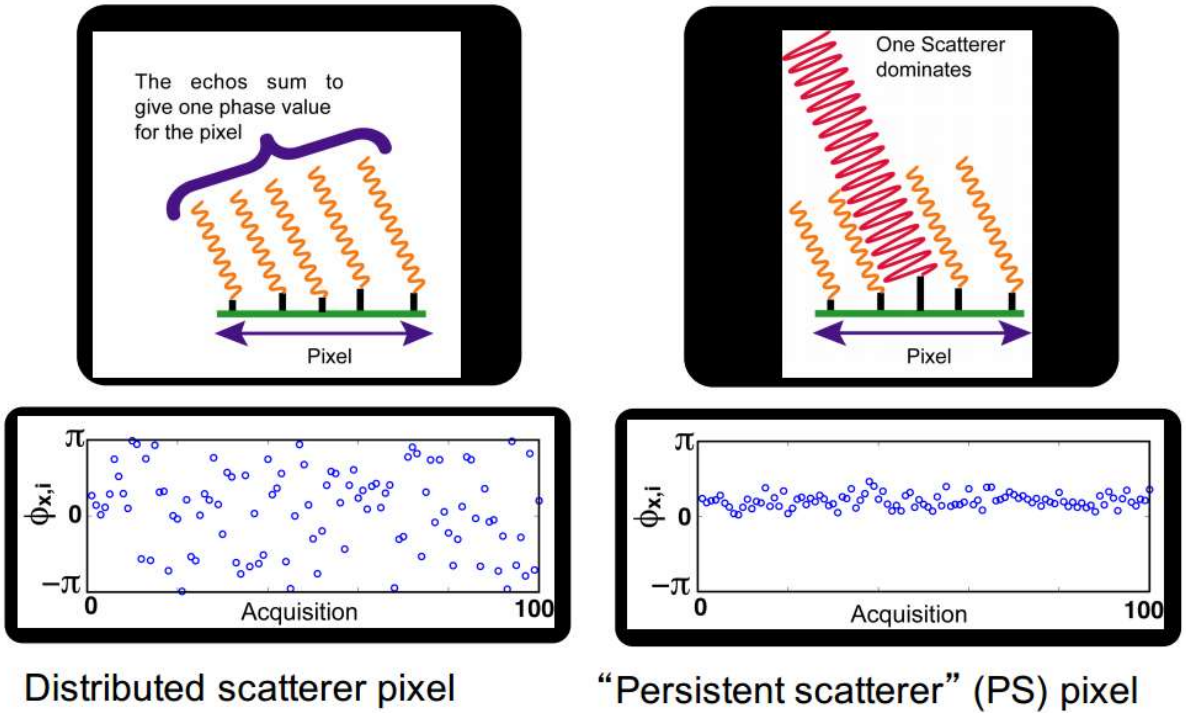

Distributed scatterer pixel

"Persistent scatterer" (PS) pixel

Source: A. Hooper, University of Leeds; UNAVCO InSAR Training

Persistent Scatterer Interferometry (PSI)

- **Phase of an interferogram:**

$$\phi = W\{\phi_{topo} + \phi_{defo} + \phi_{atmo} + \phi_{orbit} + \phi_{noise}\}$$

$$= W\left\{\frac{4\pi}{\lambda}\frac{B_{\perp}}{R \cdot sin(\theta)}h + \frac{4\pi}{\lambda}v \cdot \Delta t + \phi_{atmo} + \phi_{orbit} + \phi_{noise}\right\}$$

(W: wrapping operator $\rightarrow \phi$: $[-\pi, \pi[$)

- **Form several interferograms referenced to a unique "reference" image**
  - i*th* image = reference
  - j*th* image = secondary

N+1 scenes

N interferograms

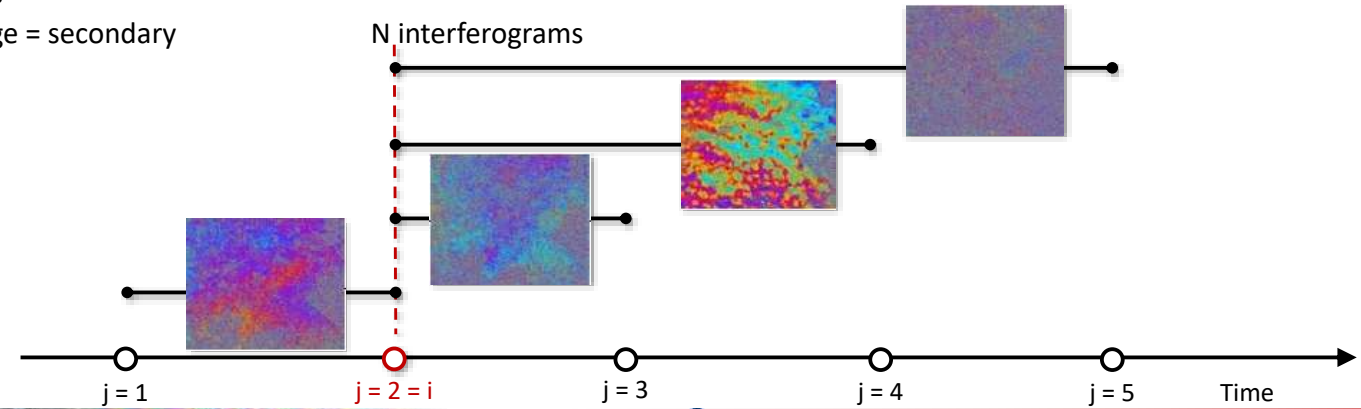

PSI Processing Chain

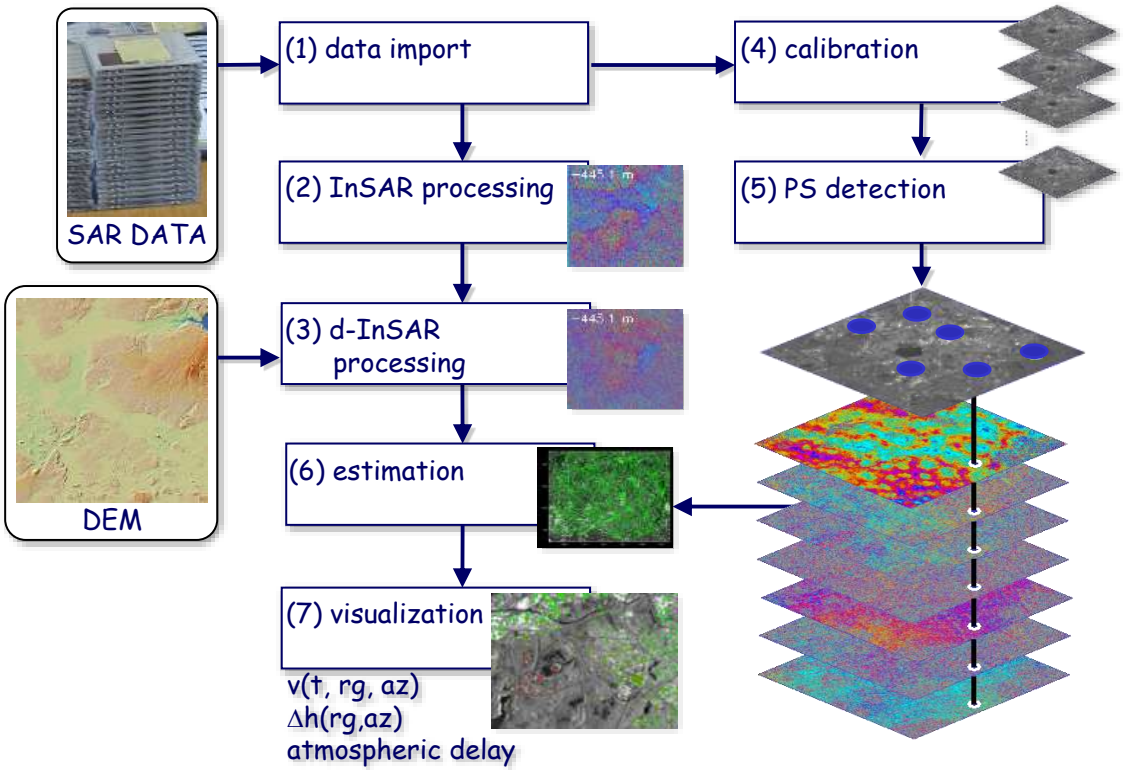

PSI Processing Chain

Steps (1) – (3): InSAR and D-InSAR Processing

1. **Interferogram generation:**

$$\phi_x^k = W\left\{\frac{4\pi}{\lambda}\frac{B_\perp^k}{R \cdot sin(\theta)}h_x + \frac{4\pi}{\lambda}v_x\Delta t^k + \phi_{x,atmo}^k + \phi_{x,orbit}^k + \phi_{x,noise}^k\right\}$$

$$h = h_{DEM} + h_{ERR}$$

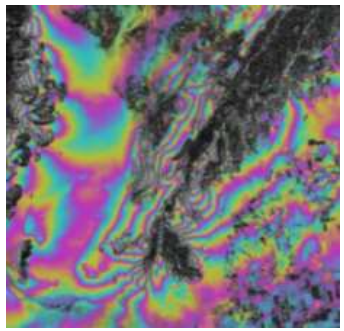

2. **Remove DEM via D-InSAR processing:**

$$\Delta\phi_x^k = W\left\{\frac{4\pi}{\lambda}\frac{B_\perp^k}{R \cdot sin(\theta)}h_{x,err} + \frac{4\pi}{\lambda}v_x\Delta t^k + \phi_{x,atmo}^k + \phi_{x,orbit}^k + \phi_{x,noise}^k\right\}$$

- $h_{x,err}$ remains due to
  - Imperfect interferometric baseline
  - Imperfect DEM

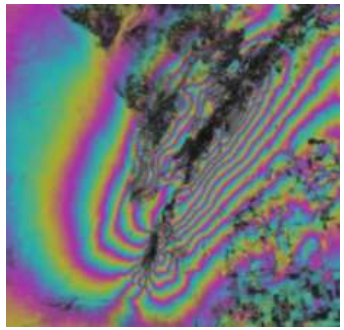

Example of Single-Reference d-InSAR Stack

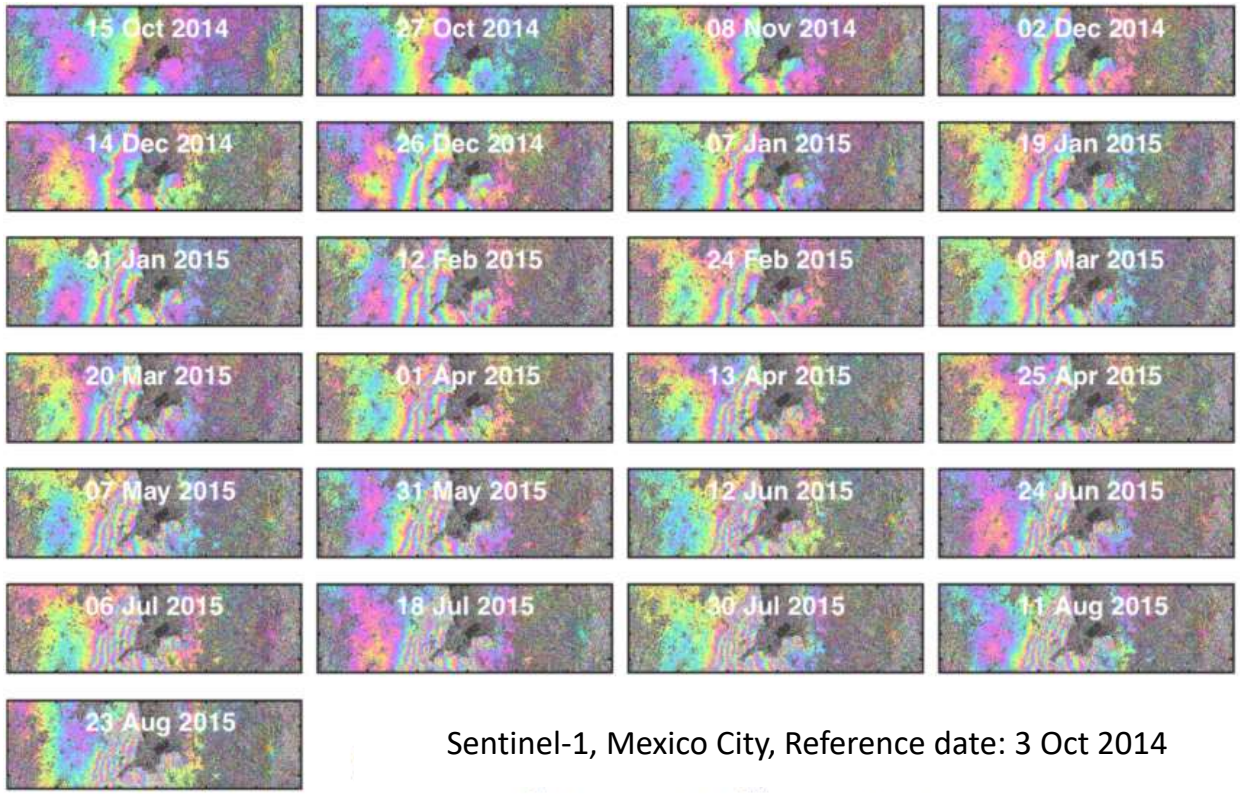

Sentinel-1, Mexico City, Reference date: 3 Oct 2014

Source: A. Hooper, University of Leeds; UNAVCO InSAR Training

PSI Processing Chain

Steps (4) & (5): Selection of Persistent Scatterer (PS) Candidates

- **Various ways for detecting PS:**
  - **Amplitude dispersion index:** $D_A = \frac{\sigma_A}{\mu_A} \rightarrow$ points with stable amplitude A over time
  - **Points with high signal-to-clutter ratio**
  - …
- **Features of Persistent Scatterers**:
  - No temporal decorrelation
  - Very low phase noise
- **Goal: Dense spatial distribution of high quality PS**
  - ⇨ Favorable description of spatial deformation signal
  - ⇨ Easier phase unwrapping

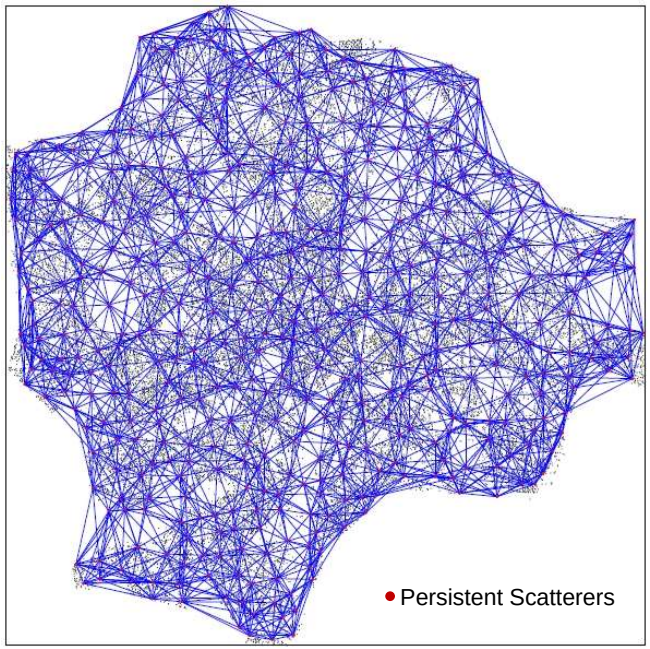

PSI Processing Chain

A Few Words on the Amplitude Dispersion Index

- Amplitude Dispersion Index initially published in (Ferretti et al., 2001)

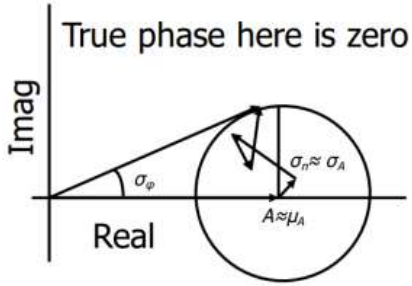

$$\sigma_\varphi \approx \frac{\sigma_n}{A} \approx \frac{\sigma_A}{\mu_A} = D_A$$

Phase noise

- **Approach**: Calculate D_A per pixel and use points with $D_A <$ threshold

- Data analysis has shown that D_A is a good approximation for σ_φ for low values of D_A

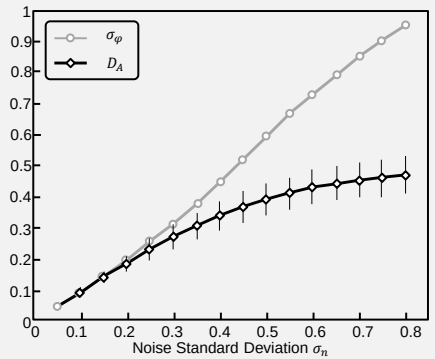

PSI Processing Chain

Step (6a): Spatio-Temporal Modeling

- **Linear deformation model:** phase $\phi^k_{x,defo}$ of pixel x of ifgrm k

$$\phi^k_{x,defo} = \frac{4\pi}{\lambda} v_x \Delta t^k$$

- **Linear dependence of DEM error on interferometric baseline →**

$$\phi^k_{x,topo} = \frac{4\pi}{\lambda} \frac{B^k_\perp}{R \cdot sin(\theta)} h_{x,err}$$

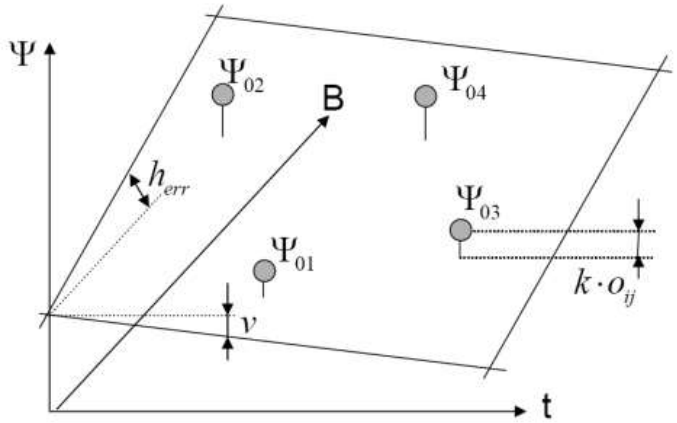

- **Estimation of DEM error and deformation using spatio-temporal model**:
  - **Fitting of a 2-d plane into the phase observations in the spatio-temporal baseline plot (see above)**

PSI Processing Chain

Step (6b): Persistent Scatterer Estimation I

- **Goal:**
  Estimation of
  - DEM error
  - Surface deformation

  at the position of the Persistent Scatterers

- **Problem:**
  - Noise contributions at the PS positions may mask desired signal
  - Some phase components are random in time and prevent successful estimation

Step (6b): Persistent Scatterer Estimation II

Calculation of Phase Differences between Nearby Points

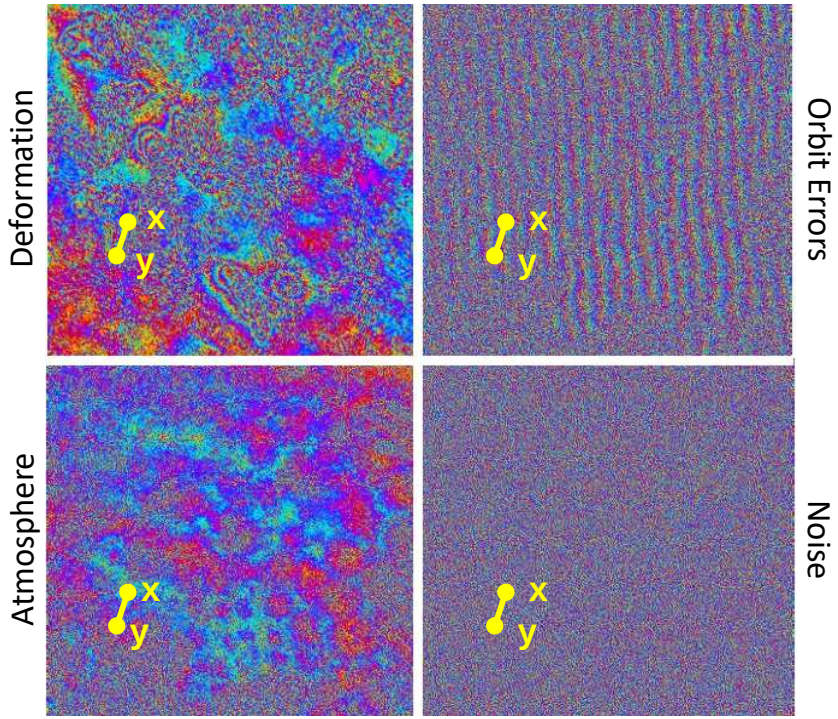

$$\Delta\phi^k_{x-y} = \frac{4\pi}{\lambda}\frac{B^k_\perp}{R\cdot sin(\theta)}\Delta h_{x-y,err} + \frac{4\pi}{\lambda}\Delta v_{x-y}\Delta t^k + \phi^k_{x-y,atmo} + \phi^k_{x-y,orbit} + \phi^k_{x-y,noise}$$

small

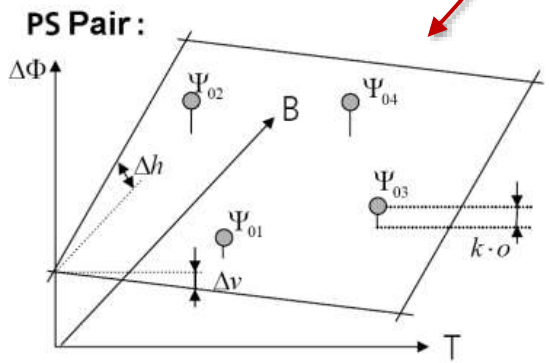

PSI Processing Chain

Step (7c): Integration Step

- We now have estimated $\Delta h_{x-y,err}$ and Δv_{x-y} corresponding to the height-error and deformation velocity **differences between pairs of PS points**
- To obtain parameters at the PS locations ($h_{x,err}$ and v_x), we **perform a least-squares integration** with respect to a reference point (**X**)

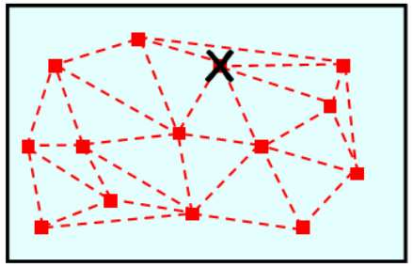

- **Example:**
  - Integration Result for InSAR Stack over Las Vegas

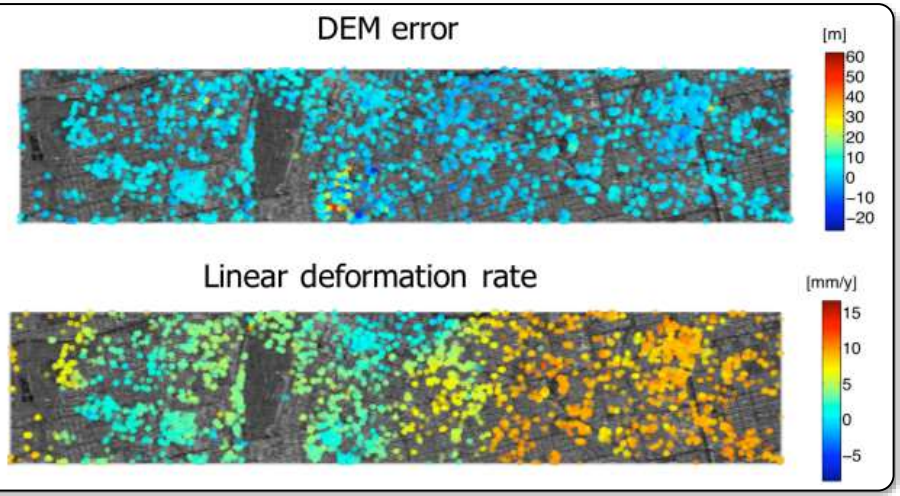

Source: A. Hooper, University of Leeds; UNAVCO InSAR Training

Analysis of Residuals to Separate Atmospheric Delay from Noise

- Residuals:

$$\phi^k_{x,res} = \phi^k_{x,atmo} + \phi^k_{x,noise} + \phi^k_{x,orbit}$$

- **Properties:**
  - Atmosphere correlated in space and uncorrelated in time
  - Noise uncorrelated in both space and time

→ Separation:

– Spatial filtering and subsequent interpolation

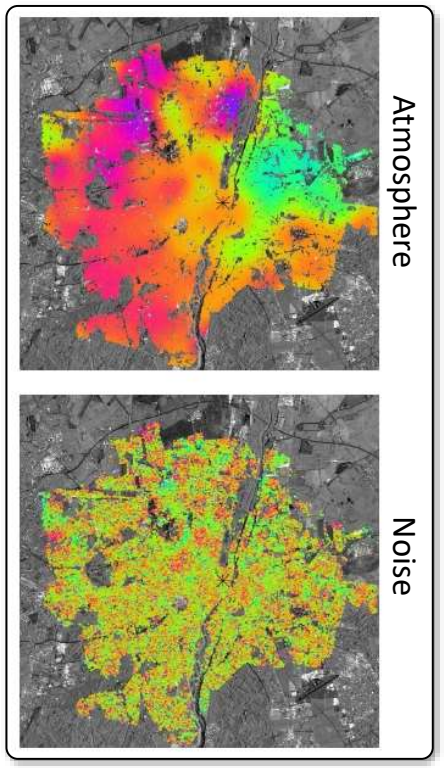

Summary of PSI Results

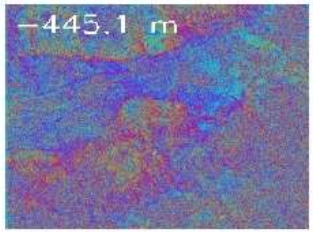

InSAR

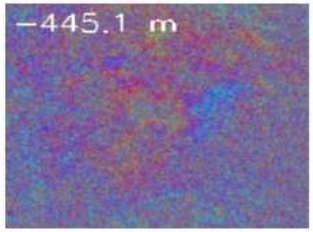

D-InSAR


Coherence

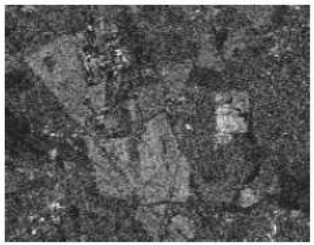
Calibrated Amplitude


multi-look Amplitude

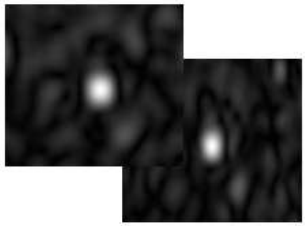
super resolution

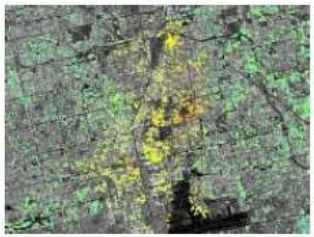
Deformation Map

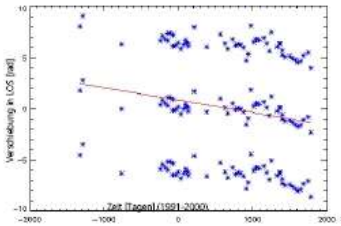
Deformation per PS

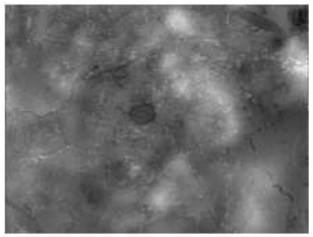
Atmo. Water Vapor

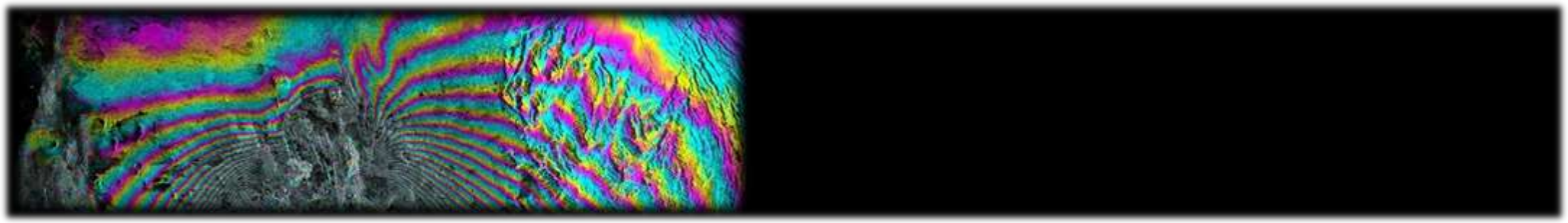

PS-INSAR (PSI): ACCURACY ASSESSMENT AND EXAMPLES

Assessment of Accuracy of PS-InSAR

Corner Reflector Experiment Conducted by Delft University, NL

- **Experiment Setup:**
  - Row of oriented corner reflectors
  - Surveyed using levelling for validation of PSI results

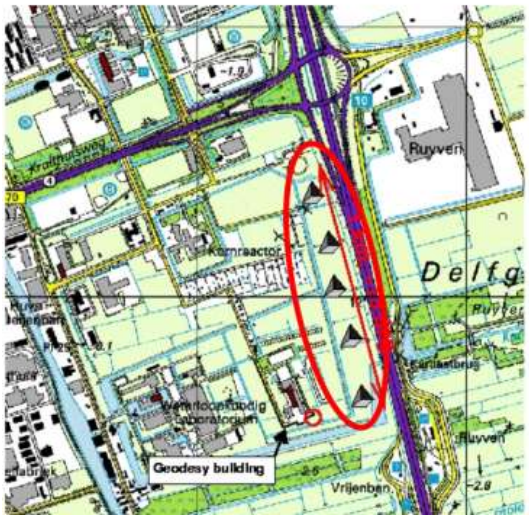

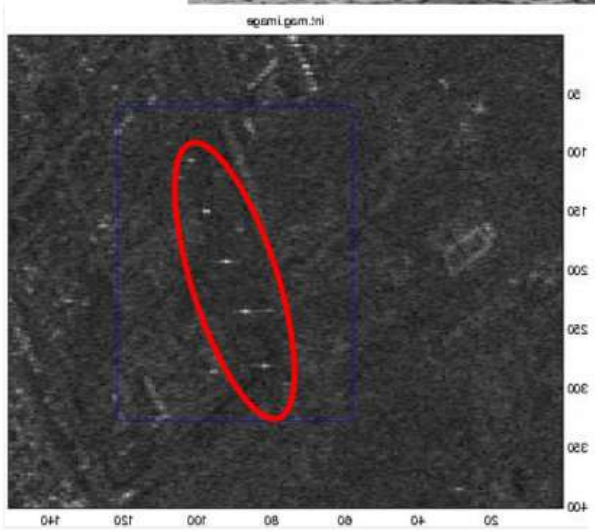

Assessment of Accuracy of PS-InSAR

Corner Reflector Experiment Conducted by Delft University, NL

- **Comparison of leveling and PSI deformation measurements**
  - Excellent match of measurements

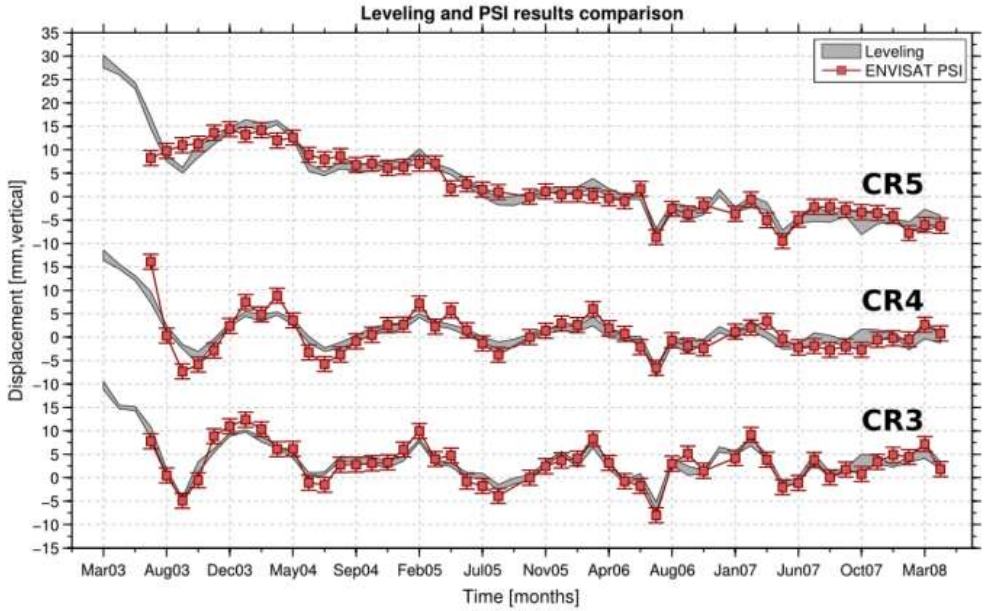

Marinkovic et al, CEOS SAR workshop, 2004

PSI Example: Subsidence in Las Vegas

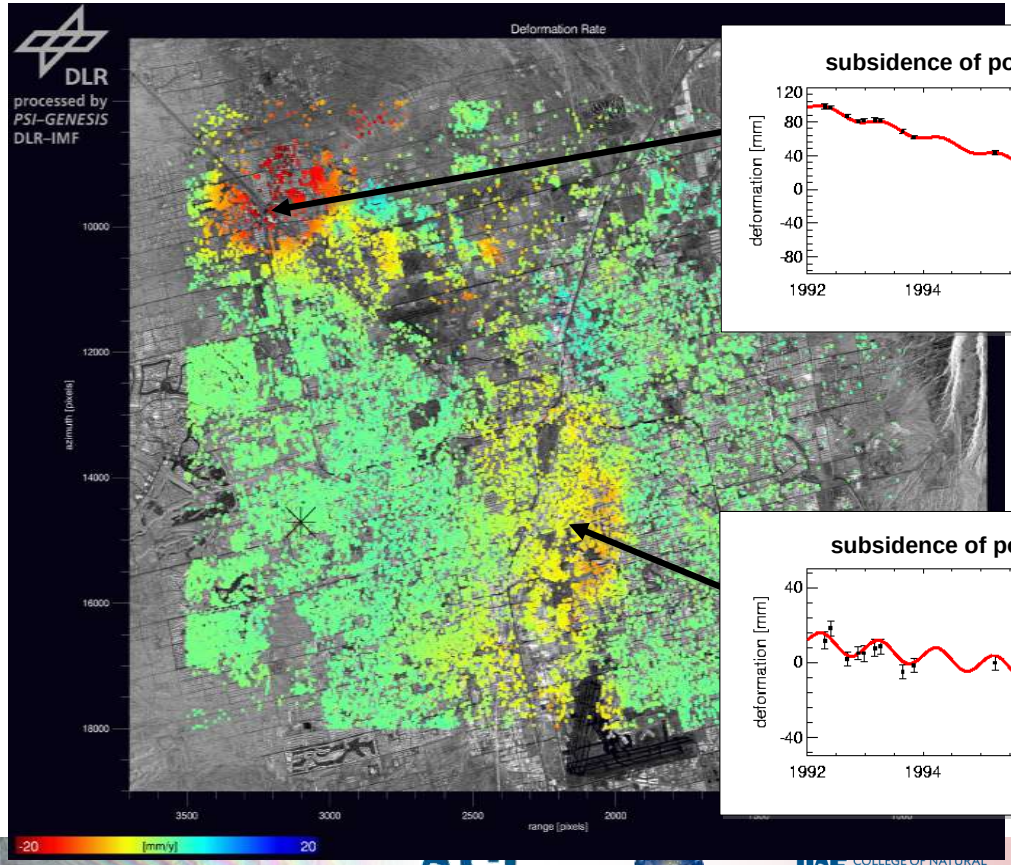

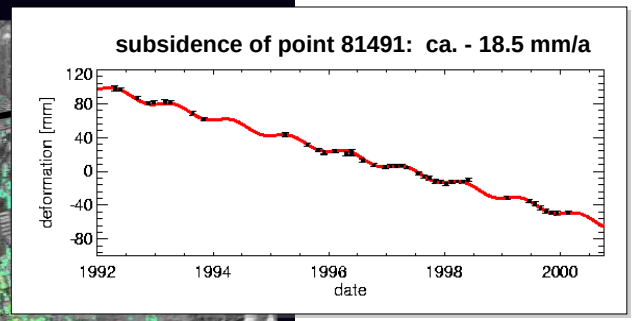

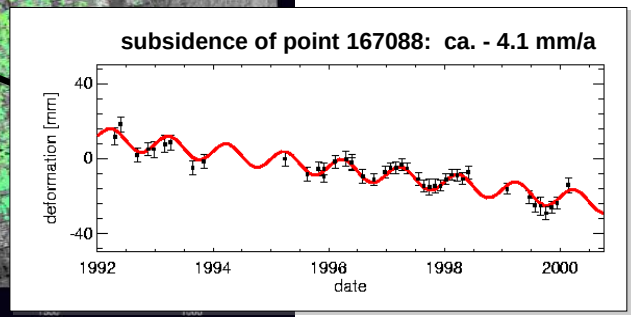

PSI Example: Bay Area, California

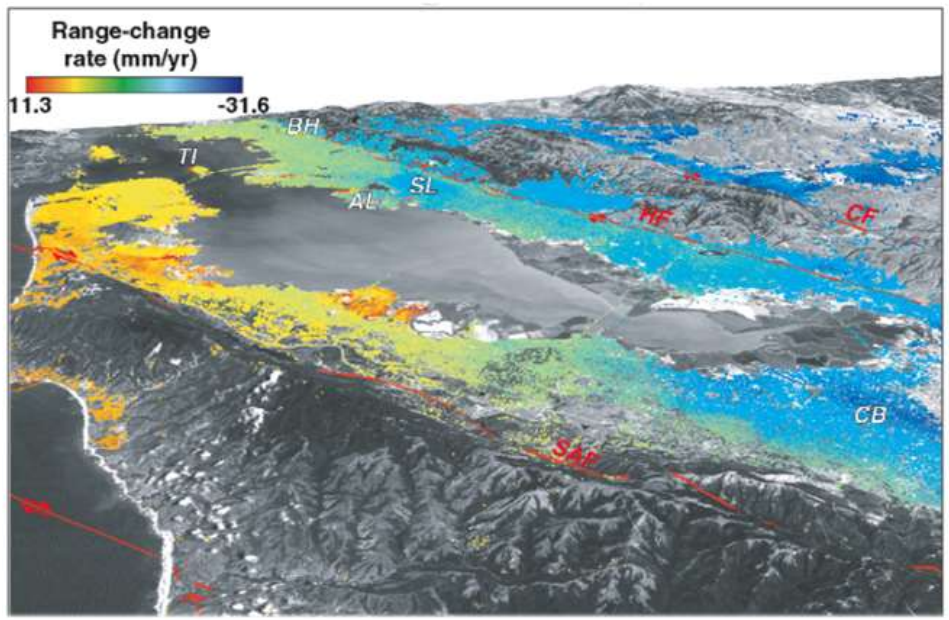

San Francisco Bay Deformation (Ferretti et al., 2004)

- These results indicate that PSI works well in **urban areas**, but not so well in areas without man-made structures. **Why?**

Think – Pair – Share:

Let's look at some PS-InSAR Data: Explore the following deformation site on the InSAR Norway PSI Portal

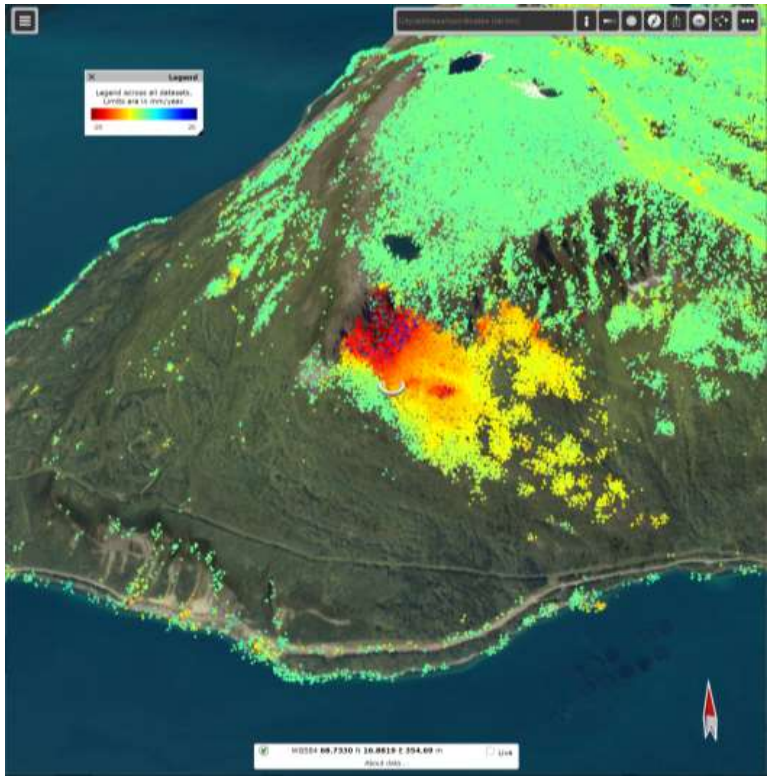

Activity 1: Explore and compare ascending and descending deformation data:

- How do the deformation features for ascending and descending compare.
- What do ascending and descending data tell you about the direction of surface motion?

Activity 2: Analyze data gaps / point density variations:

- The PSI point density varies throughout this site.
- Look at ascending and descending data. You may notice distinct differences in the point coverage between these geometries.
- Formulate two reasons why point densities may vary between these geometries.

High-Resolution PS-InSAR Study in Berlin, Germany

Linear deformation rate (Gernhardt, 2011)

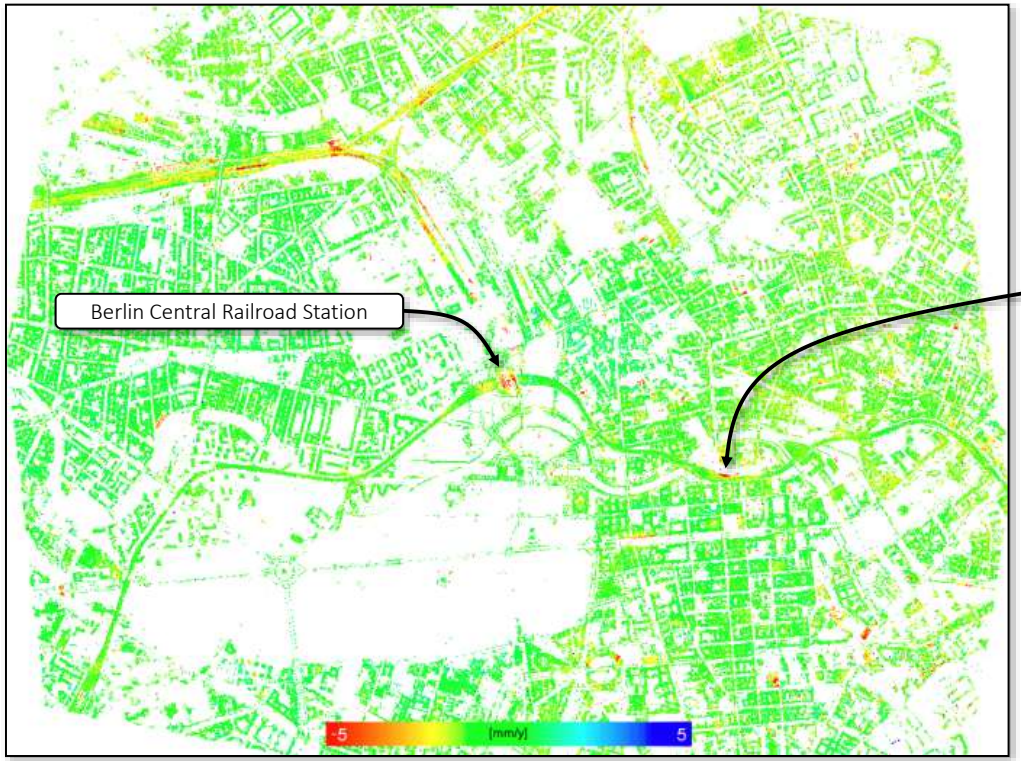

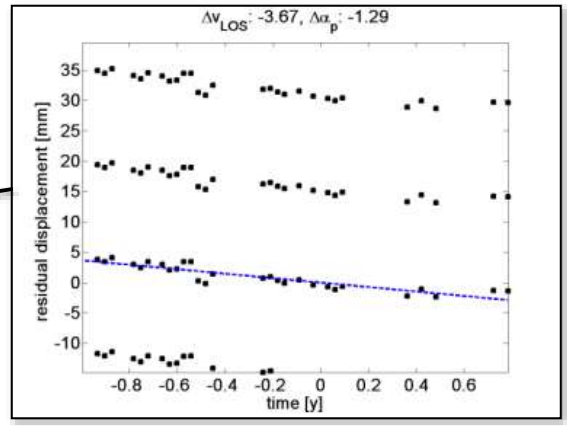

High-Resolution PS-InSAR Study in Berlin, Germany

Linear deformation rate (Gernhardt, 2011)

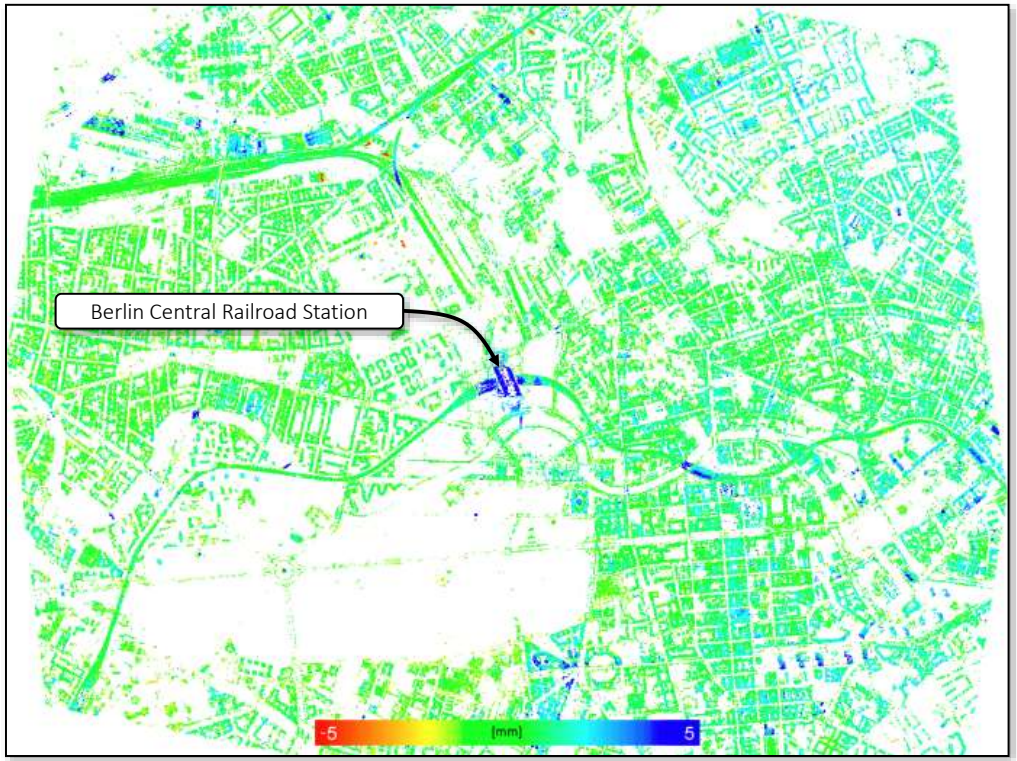

Subtle phenomenon

Seasonal deformation (vertical)

High-Resolution PS-InSAR Study in Berlin, Germany

Point density depends on sensor properties and land cover

Case Study Berlin: ERS-2 Data (resolution ~ 20m)

Case Study Berlin: TerraSAR-X Spotlight data (resolution ~ 1m)

Gerhardt, 2011

Sub-Milimeter Surface Analysis

Building Deformation in Berlin, Germany

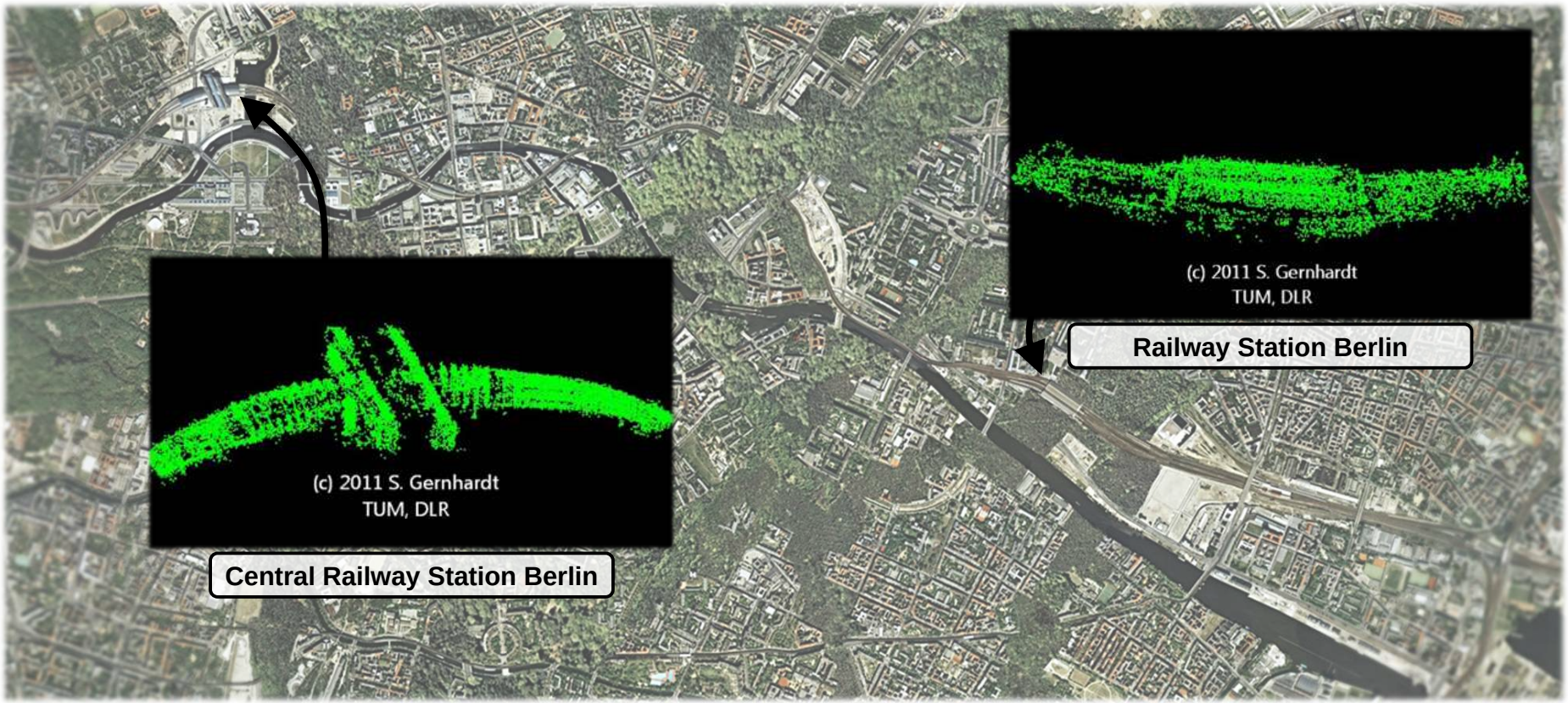

Summary of PSI

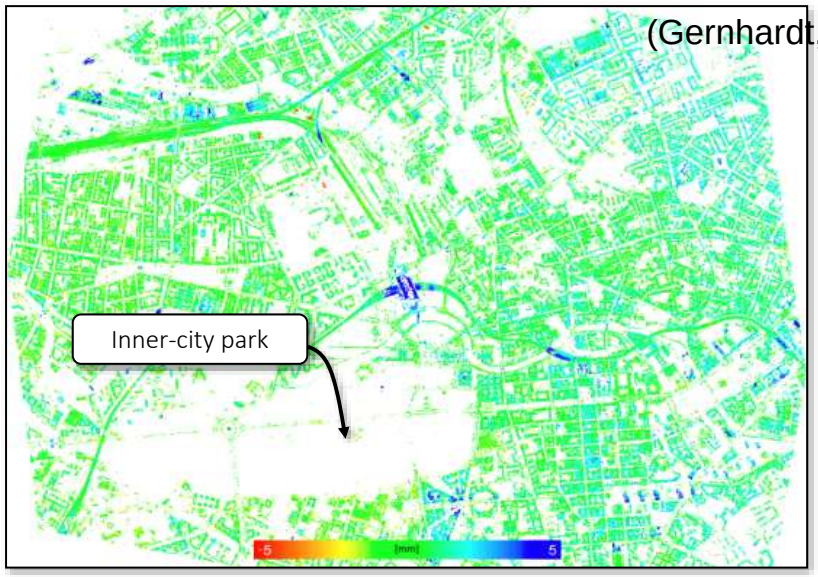

Key features

1. **PSI exploits and requires stable scatterers**
   - Such as buildings, rock outcrops
   - Hence works well in e.g. urban environments
   - High precision at full resolution

2. **Drawbacks**
   - Point density dependent on environment
   - Point density dependent on sensor
   - Computational cost

Most large-scale geohazard applications focus on distributed targets, using medium-resolution SAR imagery.